Optimum coordination of directional overcurrent relays in a distribution network with distributed generation

SM Mapapanyane

20469276

Dissertation submitted in fulfilment of the requirements for the degree *Master of Engineering* in Electrical and Electronic Engineering at the Potchefstroom Campus of the North-West University

Supervisor: Prof. PA van Vuuren

May 2017

Abstract

The conventional relay protection coordination method is mainly used in the industry to calculate the protective overcurrent relay settings. The conventional method requires many inputs and does not produce the best relay coordination results. When there are multiple sources, the calculation process becomes even more complicated and cumbersome. In order to optimize the coordination results of the interconnected network with multiple sources, the particle swarm optimization algorithm is proposed in this research. Optimization algorithms have been applied to many engineering problems. However, few researchers have applied particle swarm optimization to the coordination problem especially in power systems with distributed generation sources. The objective of this research is to propose a particle swarm optimization algorithm to improve on the protection settings for a distribution network with distributed generation sources as calculated by the conventional method.

The proposed particle swarm intelligence algorithm is compared with the conventional method by making use of two case studies. The IEEE[1] 8-bus test case consisting of a total of 14 primary relays and 20 relay pairs is used. Relay pairs are identified and set, determining the primary and back-up relays in each pair. Three-phase faults are simulated at 5% of the protected line. The operating time of the primary relays is calculated by randomly selecting the time multiplier settings, fixed pick-up currents and simulated three-phase fault currents. The coordination time interval of 0.3 seconds is used.

Based on the coordination results obtained in this research, the proposed particle swarm optimization algorithm can be used to calculate the settings of the directional overcurrent relays in a distribution network with distributed generation. The proposed algorithm has shown to have the ability to maintain selectivity between the relays being coordinated and minimize the operating times of the primary relays for close-in three-phase faults.

Keywords: distributed generation, distribution network, protection, coordination, optimization

[1] IEEE is an abbreviation for Institute of electrical and electronics engineers

Acknowledgements

First and foremost, I would like to thank God for keeping me till the end of this research, and for the strength, courage and wisdom. *“For from Him and through Him and to Him are all things. To Him be the glory forever. Amen.”* (The Holy Bible, ESV, Romans 11:36).

I would like to extend my sincere gratitude to my supervisors Prof. P. A. van Vuuren and Prof. J. A. de Kock for their academic support and supervision. I thank you so much for being patient with me and always encouraging me to do my best.

To Motlatsi, I would not have made it this far without your support, understanding and kindness. Your love gave me the courage and strength to carry on. Thank you so much.

Thanks to my colleagues Ndabeni Stenane and Martin Slabbert for your undoubted support and countless advice.

To my extended family and friends, thank you so much for your prayers and support. I could not have done this without your support and words of encouragement from all of you!

Table of contents

List of figures

List of tables

Abbreviations

AC	Alternating Current
ACO	Ant Colony Optimization
B/U	Back-up
CSP	Concentrated Solar Power
CTI	Coordination Time Interval
CB	Circuit Breaker
DC	Direct Current
DG	Distributed Generation
DER	Distributed Energy Resources
DFIG	Doubly Fed Induction Generator
DoE	Department of Energy
DP	Dynamic Programming
DT	Discrimination Time
EA	Evolutionary Algorithm
E/F	Earth Fault
EHV	Extra-High Voltage
ERRC	External Rotor Resistance Controller
IED	Intelligent Electronic Device
EI	Extremely Inverse
EOL	End of Line
FC	Fault Current
IG	Induction Generator
EMT	Electromagnetic Transient
IDMT	Inverse Definite Minimum Time
LP	Linear Programming
LV	Low Voltage
MCCB	Moulded Case Circuit Breaker

MBS	Model-Based Search
MINLP	Mixed Integer Nonlinear Programming
MTA	Maximum Torque Angle
MV	Medium Voltage
MVA	Mega Volt-Ampere
NI	Normal Inverse
NP	Nonlinear Programming
O/C	Overcurrent
PCC	Point of Common Coupling
PLL	Phase Locked Loop
PI	Proportional Integral
PSM	Plug Setting Multiplier
PSO	Particle Swarm Optimization
PU	Per Unit
PV	Photovoltaic
SE/F	Sensitive Earth Fault
SCIG	Squirrel Cage Induction Generator
TMS	Time Multiplier Setting
VA	Volt-Ampere
VI	Very Inverse
WTG	Wind Turbine Generator
WPP	Wind Power Plant

List of symbols

Symbol	Description
c_i	*weighting coefficient*
E_{gen}	*DG source voltage*
E_{grid}	*Distribution grid source voltage*
$f(\bar{x})$	*Objective function*
G_i	*Constraint factor*
$g_j(x)$	*Inequality constraint*
$gene\ [m]$	*Binary version of* P_n
$h_j(x)$	*Inequality constraint*
I	*Measured fault current*
I_A	*Phase current*
$I_{CB\ 1}$	*Fault current through circuit breaker 1*
$I_{PU,Max}$	*Maximum pick-up current*
$I_{PU,Min}$	*Minimum pick-up current*
I_r	*Relay current*
k	*Iteration number*
L_{fault}	*Feeder length to the fault*
L_{gen}	*Feeder length to the DG source*
L_i	*Constraint factor*
M	*Mutation factor*
N_{bits}	*Number of bits in the chromosome*
N_{gene}	*Number of bits in the gene*
N_{keep}	*Number of chromosomes in the mutation pool*
N_{par}	*Number of parameter variables*
N_{pop}	*Number of chromosomes in the population*
P_{hi}	*Highest variable value*
P_{lo}	*Lowest variable value*
P_{nom}	*Normalized variable*
P_n	*n^{th} variable*
P_{quant}	*Quantized variable of* P_n
PSM	*Plug setting multiplier*
PU_{max}	*Maximum value of the pick-up current*

PU_{min}	*Minimum value of the pick-up current*
q_n	*Quantized version of* P_n
$rand$	*Random number between 0 and 1*
S_{gen}	*Generator apparent power rating (DG)*
s_i^k	*Particle position* i *at iteration number* k
S_t	*Transformer apparent power rating*
t_i	*Operating time of the primary relay*
$t_{i,max}$	*Maximum operating time of the primary relay*
$t_{i,min}$	*Minimum operating time of the primary relay*
t_{ii}	*Operating time of the primary relay* i *for a fault location at* i
t_{ij}	*Operating time of the back-up relay* j *for a fault location at* i
TMS_{max}	*Maximum time multiplier setting*
TMS_{min}	*Minimum time multiplier setting*
U_{nom}	*Nominal bus voltage*
V_{BC}	*Phase-phase voltage (quadrature voltage)*
v_i^k	*Velocity of the particle* i *at iteration number* k
w	*Weighting factor*
x	*Constriction weight*
$\bar{x}$	*Design vector*
X_{rate}	*Crossover rate*
w_{max}	*Initial weight*
w_{min}	*Final weight*
Z_{fault}	*Fault impedance*
Z_{gen}	*Generator impedance (DG)*
α_i	*Constant variable*
δ	*Constant (equal to 0 or 1)*
μ	*Mutation rate*
ω	*Rotational rotor speed*

1 Introduction

1.1 Background

Producing energy should not threaten the environment. It should benefit the environment in one way or the other. Over the last five years South Africa has become a leading renewable energy investment destination [1]. The South African government has incentivized initiatives aimed at addressing the challenges of energy demand, economic growth, the country's carbon footprint and climate changes. This is the reason why there are now an increased number of renewable energy resources being connected to the Eskom distribution network [1].

The two flowcharts in Figure 1-1 show the old and the new power system design. The arrows in the diagram show the direction of the electrical power flow and current. In the old design, as depicted on the left of Figure 1-1, conventional power stations are the main sources. During power system faults the main fault current contributors are synchronous machines used in the conventional power stations.

The new paradigm in power system design is shown on the right of Figure 1-1. The flow of power and current is bi-directional. With this new design, during power system faults the distributed generation source (DG) has the capability to contribute to the fault. However, the main contributors to faults are synchronous machines in the conventional power stations.

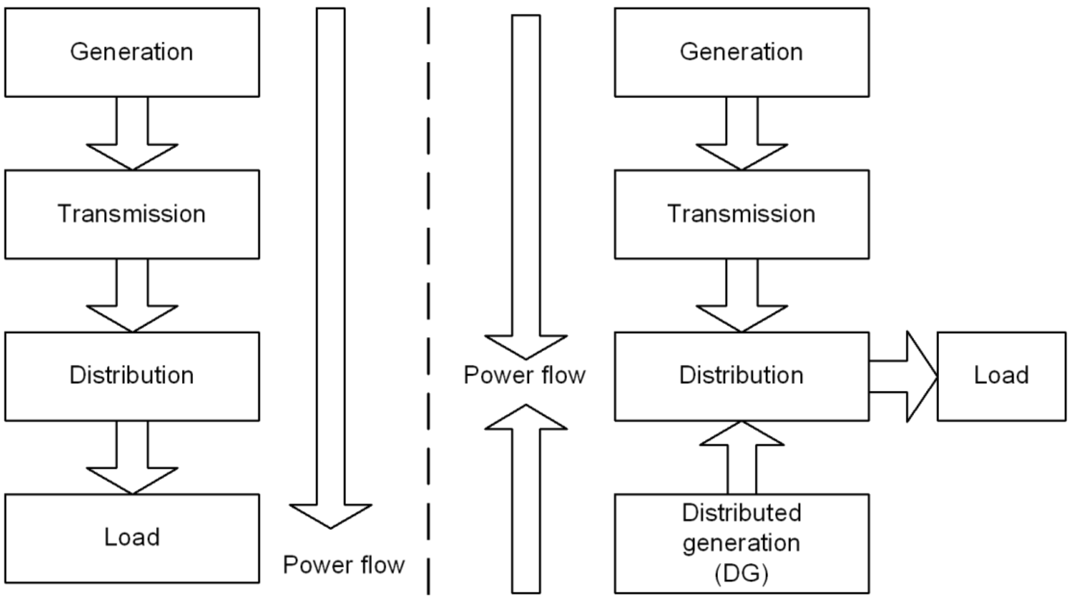

Figure 1-1: Radial (classical) and new design power system

The benefits of connecting more DGs to the distribution network are threefold. Firstly, it increases the existing power system capacity, thereby ensuring a higher probability that demand for electrical energy will be met even during peak periods. Secondly, construction of a single conventional coal power station takes longer than constructing a single DG substation. Thirdly, most of the DG sources are connected at the distribution side, therefore only a few additional transmission lines are needed in the transmission network. Thus, the source is brought closer to the load centre. As a result, technical losses and capital expenditure are reduced, while reliability and integrity of the network are enhanced [2],[3]. The impact of the DG depends mainly on the location, capacity and the technology of the DG used.

However, connection of DG sources to the distribution network introduces network conditions which were not encountered before. The new conditions include a change in the magnitude and direction of the power flow and the short circuit current [4],[5]. Secondly, during a transient fault in the power system, DGs (when connected) will continue operating, thereby sustaining the power system voltage and feeding the fault current. Consequently, this prevents the arc of a transient fault from being extinguished, and results in an unsuccessful auto-reclose operation of the device clearing the fault. Lastly, transient overvoltages may be experienced, which could damage the power system equipment and customers' equipment [4],[5]. These conditions have a significant impact on the operation and integrity of the power system [4],[5],[6]. Therefore, proper resolution of these challenges, and others as outlined in Chapter 4, determines whether the benefits of connecting more DG sources to the distribution network described above will be achieved.

When the number and capacity of the DG sources increases in the distribution network, the coordination of protective relays becomes more complex and challenging [6]. Coordination of overcurrent relays is the ability of the relay to discriminate and operate sequentially for faults in the protected zone in order to avoid unnecessary trips. There are various methods which can be used to calculate the settings of the overcurrent relays. The conventional method is used to calculate the overcurrent protection relay settings. The particle swarm optimization (PSO) algorithm is proposed to improve on the calculated overcurrent protection relay settings. The PSO algorithm is a relatively new stochastic search algorithm. PSO emulates the behaviour of swarms such as birds, fish and social insects.

The conventional method of calculating the protective overcurrent relay settings requires many inputs and does not produce the best coordination results. When there are multiple sources, the calculation process becomes even more complicated and cumbersome. Deterministic methods have been used to solve the directional overcurrent relay coordination problem and the results were not optimal [8]. The disadvantage of using deterministic methods is that the results are based on an initial guess of the primary relays, the method is computationally expensive and ineffective [8].

Particle swarm optimization (PSO) has been used by other researchers to solve the directional overcurrent coordination problem optimally [12]. Due to PSO's ease of implementation, better computational efficiency and high quality of results, the PSO algorithm is proposed in this research to calculate the optimum settings of the protective directional overcurrent relays.

1.2 Problem statement

The conventional relay protection coordination method is mainly used in the industry to calculate the protective overcurrent relay settings. Calculating the protective overcurrent relay settings using the conventional method is a tedious and long process. The conventional method requires many inputs and the coordination results are not always optimal, since the final results are based on the initial guess of the initial relays' operating times [8]. When there are multiple sources (e.g. DGs), the calculation process becomes even more complicated and cumbersome.

In order to optimize the coordination results of the interconnected network with multiple sources, the particle swarm optimization (PSO) algorithm is proposed in this research. The PSO algorithm has been applied to many engineering problems. However, only few researchers have applied PSO to the coordination problem especially in power systems with distributed generation sources.

The objective of this research is to propose an optimization algorithm, which can be used to improve on the settings of the directional overcurrent relays in a distribution network with DGs as calculated by the conventional method.

1.3 Issues to be addressed

The hypothesis to be tested in this research is: A particle swarm optimization algorithm can be used to improve on the protection settings for a distribution network with DGs as calculated by the conventional method.

The following sub-section describes research questions formulated in this research and the objectives guiding research questions. The scope and limitations of this research are discussed in sub-section 1.3.2 below.

1.3.1 Research questions

The research objectives are guided by the following research questions:

a) What is the impact of the DGs in the existing distribution network?

b) What is the impact of the DG in the protective coordination?
c) How do different technologies differ in operation and response during power system abnormal conditions?
d) How does the PSO algorithm perform in comparison with the conventional coordination method?

The proposed PSO algorithm should meet the following objectives:

a) Minimize the operating times of the primary relays for close-in three-phase faults in the IEEE 8-bus test case in both study cases.
b) Maintain a coordination time interval of 0.3 seconds between the primary and backup relays in the IEEE 8-bus test case in both study cases.

1.3.2 Scope and limitations of this research

The scope of this research is limited to a comparison between the proposed PSO algorithm and conventional coordination method. The two methods are used to calculate the protection settings for a distribution network with DGs connected to the high voltage (HV) side of the distribution system. The main focus is placed on wind and solar power – other technologies are not discussed. The distance and differential relays are not considered in this research, only the directional overcurrent relays. The standard inverse (also known as normal inverse) relay characteristic is considered and other characteristics such as very inverse, extremely inverse and definite time are not considered, however they are discussed briefly in Chapter 2.

Due to lack of benchmark power systems for relay overcurrent coordination studies, the IEEE 8-bus is used in this research as a test case to calculate the power system fault currents under two network configurations (i.e. the standard distribution network and active distribution network).

There are various standard IEEE test cases, which are used mainly for power flow studies. The reasons for using the IEEE 8-bus test case are as follows:

a) Firstly, it is used because it is widely applicable and has been used in the coordination research problem recently [7],[9],[65].
b) Secondly, the selected test case is used due to lack of the standard protective relay coordination test cases.
c) Thirdly, in the IEEE 8-bus test case there are at least 20 relays to be coordinated. Using the 14-bus or 30-bus test case will increase the number of the relays to be modelled and coordinated. As the test case expands the problem dimension increases, resulting in longer execution times and a high dimension problem.

d) Lastly, the IEEE 8-bus test case is used to show that it can be used in other research on distributed generation [9].

1.4 Research methodology

Protective relay coordination is the process of calculating and selecting optimal relay settings, which ensures that the directional overcurrent relays trip selectively. Two case studies are used in this research to prove the formulated hypothesis. In the first case study, is the IEEE 8-bus test case operating in normal network conditions, i.e. prior to the interconnection of DGs. In the second case study is the modified IEEE 8-bus test case. In the modified test case, a single DG source developed by the IEEE power and energy society is connected to bus 4 [42].

Two methods used to calculate the protection settings are compared in this research to validate the performance of the proposed PSO algorithm. The first method is the conventional coordination. In this method, the initial operating times of the primary relays are set to operate in 0.2 seconds for close-in faults and the backup relays in 0.2 seconds plus the coordination time interval (CTI) of 0.3 seconds. The time multiplier settings are then calculated based on the initial calculated times. The second method is the proposed PSO algorithm. In this method, the initial operating times of the primary relays are randomly generated. The time multiplier settings of the primary relays in the modified IEEE 8-bus test case are calculated based on the initial randomly generated operating times before they are optimized.

1.5 Chapter layout

Chapter 2: This chapter introduces the power system protection background and objectives. Different types and applications of overcurrent relays, coordination fundamentals and methods are discussed. Lastly, the chapter discusses the directional and non-directional system coordination.

Chapter 3: This chapter introduces the concept of the distributed generation sources. Secondly, it classifies DG sources according to different technologies and classes based on their unit rating. Lastly, the contributions of different technologies of different DG types are simulated in PowerFactory, discussed and results are provided at the end of the chapter.

Chapter 4: This chapter presents an overview of the impact of DG and the implications thereof on protection. These impacts are broken down into three sub-sections where the first discusses the impact of extreme fault currents. Secondly, the impact of reduced short circuit currents on protection coordination is outlined and lastly, auto-reclosing and re-synchronism are discussed. The implications of different transformer vector groups and the type of different technologies of DG used are discussed at the end of the chapter.

Chapter 5: This chapter gives an introduction to optimization and classification of optimization problems. The second part of the chapter provides an overview of artificial intelligence optimization algorithms, makes a comparison between particle swarm optimization and genetic algorithms.

Chapter 6: This chapter presents the mathematical modelling of the directional overcurrent relay coordination problem. The first section models the problem for the conventional coordination method. The second part of this chapter models the problem as a linear and constrained optimization problem for particle swarm optimization algorithm.

Chapter 7: This chapter provides the fault responses of the DG sources as well as coordination results obtained from both coordination methods. The first part of the chapter details how the test and calculation models are set up in PowerFactory simulation tool. Secondly, the verification process and the performance comparison of both methods are discussed. The last section validates the PSO algorithm by comparing the applied overcurrent settings with the new settings obtained when calculating the settings using the PSO algorithm. One of the problematic HV ring network (Makalu 88 kV) in the border of Free-State and Gauteng is selected for additional validation process.

Chapter 8: This chapter concludes the research by discussing the results of the research, experienced drawbacks and recommendations for future work.

2 Power system protection and coordination

This chapter introduces the power system protection background and objectives. Different types and applications of overcurrent relays, coordination fundamentals and methods are discussed. Lastly, the chapter discusses the directional and non-directional system coordination philosophies.

2.1 Power system protection

Faults can occur anytime and anywhere in the electrical power system. Often very high current levels in the electrical power system are caused by faults. These currents are used to determine the presence of faults in the power system and operate protection devices, which vary in designs depending on the complexity and accuracy required [22].

The most commonly used types of protection are, amongst others: thermo-magnetic switches, moulded-case circuit breakers (MCCBs), fuses and overcurrent relays. The first two have a simple operating principle and are often used in the low voltage (LV) level. Fuses are used to protect the distribution transformers and feeders in the LV network. The overcurrent relay, which forms the basis of this chapter, is the most popular relay used to protect equipment against high fault currents [18],[20],[23]. Overcurrent relays are primarily installed to protect against fault conditions and not overload. However, the selected settings are often selected to protect the equipment against fault conditions and overloading, which is associated with thermal capacity of the equipment [22].

2.2 Basic objectives of protection

To make certain that the network is adequately protected, it is vital to ensure that each system protection component meets the following design criteria [20],[21].

2.2.1 Selectivity

Selectivity refers to the ability of the relays to trip sequentially for faults within the protected zone and remain stable for through faults or external faults in order to avoid unnecessary trips. The property of selective tripping is also called discrimination. There are two methods which discrimination can be achieved, namely: time grading and unit protection [26].

When a fault occurs in the electrical power system, it is required that selective circuit breakers operate to clear the fault and isolate the faulted portion from the healthy part of the electrical power system [26].

2.2.2 Speed

The main objective of protection is to isolate faults as fast as possible in the power system. Furthermore, to safeguard continuity of supply by ensuring that disturbances are quickly removed from the system before they lead to a widespread loss of synchronism and a consequent collapse of the system. As the load increases in the system, the phase shift between the voltages at different substations increases. Therefore, this increases the probability of loss of synchronism during fault conditions. Figure 2-1 below shows the relationship between the load power and the duration of the fault in the system. As seen from the graph, the longer the fault is uncleared, the more the chances of the power system being unstable. Three-phase faults have more impact on the power system stability than the single-phase-to-ground faults [26].

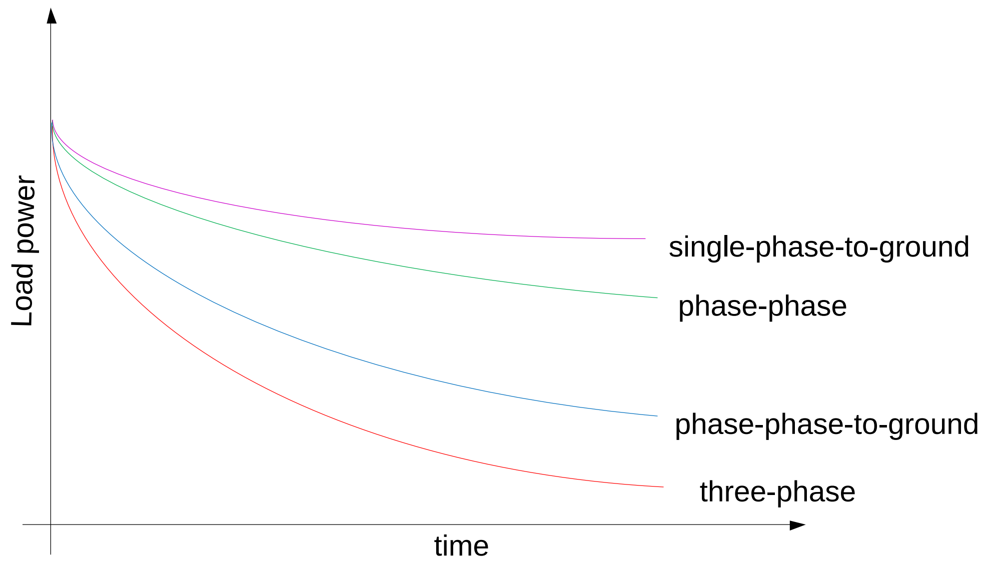

Figure 2-1: Typical power/time relationship for various faults [26]

The other aspect of rapid operation is minimization of the damage to the equipment caused by the fault. The damaging energy during fault conditions is proportional to the time the fault is present. Distribution networks, which do not require fast fault clearance, are normally protected by time-graded protection. Generation and extra-high voltage (EHV) systems require protection with fault clearance capability. Therefore, unit protection systems are normal practice with back-up time graded protection [26].

2.2.3 Sensitivity

The sensitivity of the protection system is associated with the minimum operating level (current, voltage, power etc.) of the relay or protection scheme. When the relay parameters are set too low, the protection scheme is said to be too sensitive [26]. The older electromechanical relay's sensitivity was measured in terms of the volt-ampere (VA) consumption to cause an operation. Modern relays such as digital and numerical relay's sensitivity are limited by the relay's application and the parameters of the current and voltage transformers [26].

2.2.4 Stability

The term "stability" refers to ability of the protection system to remain stable, unaffected by external faults to the protected zone, power system unbalances and changing network conditions, especially when there are no fault conditions [26].

2.2.5 Reliability

Reliability of the protection systems is associated with the ability of protection system to operate whenever a trip command is received. Reliability depends on the following conditions [26]:

a) Incorrect design / settings
b) Incorrect installation / testing
c) Deterioration in service

Protection settings parameters are often selected to take into account parameters of the primary plant, system loading, fault levels and dynamic performance of the system. The characteristics of the system change with time due to changes in loads, location and generation type. It is important to ensure that relay settings are checked to ensure that they are still appropriate. This will avoid unnecessary protection system trips [26].

2.3 Overcurrent protection

An overcurrent protection system consists of three main components where each component has different functions within the system. The first component comprises the instrument transformers, which includes both the current and voltage transformers (i.e. CTs and VTs). The instrument transformers convert high magnitudes of voltage and current into small and safe measurable values. The second component is a relay recently being called the intelligent electronic device (IED). An IED performs advanced local control intelligence calculations. The IED gets the network information from CTs and VTs and compares it with its own settings [21].

When the IED settings are exceeded, the IED makes a decision and sends a trip command to the circuit breaker. Circuit breaker (CB) is the last component which, when a trip or block command has been received from the IED, executes the instructions by either extinguishing the fault (i.e. opening the circuit breaker contact to isolate the circuit) or remaining in the closed position [21]. Due to the unreliability of AC power supply during fault conditions, batteries are used to power the protective relay circuit. Figure 2-2 below shows the protection system components discussed above briefly.

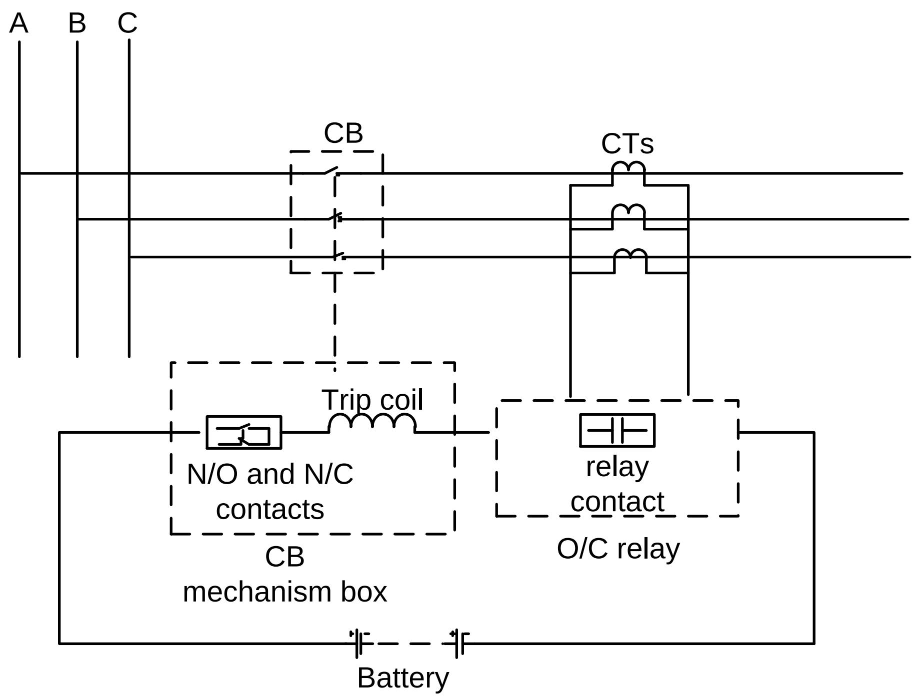

Figure 2-2: Protection system components

The three important parameters which need to be set in the overcurrent relays are the pick-up current, the time multiplier (TM) and the time-current relay curve characteristic. More details on these parameters follow in the next section.

2.3.1 Overcurrent relay pick-up setting

The pick-up (PU) setting of the overcurrent relay is set in such a way that the maximum load current is less than the pick-up setting [21],[22]. This ensures that the relay will not trip under normal load conditions. The pick-up current setting is used to define the minimum operating level of the relay and fault currents are usually defined as multiples of the pick-up current. The ratio of the fault current in secondary amps to the relay is referred to as the plug setting multiplier (PSM) and is mathematically formulated as follows [22]:

$$PU = \frac{OLF \times I_{nom}}{CTR} \tag{2.1}$$

where,

PU The pick-up setting (A)

OLF Overload factor depends on the circuit being protected

I_{nom} Nominal current (A)

CTR CT ratio

The recommended OLF is typically 1.05 for lines and 1.25 – 2 for transformers. A CT ratio close to the nominal current is usually recommended to ensure that the secondary current does not exceed the relay rated current [22]. It is common practice to use an OLF of 1.1 and 1.2 for lines in the distribution network.

2.3.2 Overcurrent relay time multiplier setting

The time multiplier setting determines the operating time of the relay whenever the fault current reaches a value equal to, or greater than the pick-up setting. The purpose of this setting is to enable time-delayed overcurrent relays to be coordinated. In electromechanical relays, the time multiplier is selected by physically adjusting the distance between the moving and stationed contacts [22],[54].

The smaller the time multiplier setting, the faster will the relays operate. There are other timing mechanisms such as clock movements, bellows and diagraphs in the old electromechanical relays. These devices are either inverse or fixed timing devices. In solid state relays, timing is achieved by means of R-L-C circuits. In digital relays, timing is established by means of algorithms using internal clocks or external clocks can be accessed [54].

2.3.3 Overcurrent relay characteristics

There is more than one overcurrent relay characteristic, which can be selected when setting the relay. The most commonly used characteristic is the standard inverse (SI) also known as normal inverse (NI) and extremely inverse (EI). An extremely inverse overcurrent relay characteristic is normally used where the fuses are used on the T-offs and load centres. The extremely inverse characteristic operates faster than the other characteristics and is typically used in fuse saving schemes [17].

The third characteristic used is the definite time. DT characteristics are mostly used at the end of the MV feeders where fault currents are low compared to the fault currents at the substation. The second application of this characteristic is when fast protection operation is required and does not need to coordinate with any other protection. The instantaneous overcurrent protection is usually used for fast operation and it is used with no intentional time delay (instantaneously) [17].

The NI characteristic is normally said to be between the two extremes [17]. As the name implies, the normal inverse operates on the inverse characteristic principle, that is, it operates faster for high fault currents and slower for low fault current magnitude. The standard equation for the overcurrent relay characteristics is given below in equation (2.2).

$$t = \left(\frac{\beta}{I^{\alpha} - 1} + L\right) \times TMS \tag{2.2}$$

where,

$$I = \frac{I_{sc}}{I_r} \tag{2.3}$$

and

I_{sc}	- short circuit current (A)
I_r	- pick-up current (A)
t	- relay operating time (s)
TMS	- time multiplier setting
L	- Constant factor

The IEC 60255 standard values for α, β and L used in equation (2.2) are given in table 2-1 below.

Table 2-1: Overcurrent relay characteristics

Curve type	Coefficient value		
	α	β	L
Normal Inverse (SI)	0.02	0.14	0
Very Inverse (VI)	1	13.5	0
Extremely Inverse (EI)	2	80	0

In Table 2-2 the operating times of the overcurrent relay characteristics given in Table 2-1 above is calculated at different fault currents with a constant TMS.

Table 2-2: Operating times of different relay characteristics

Plug Setting Multiplier (PSM)	Operating time in seconds (For TMS = 1)		
	SI	VI	EI
2	10.0	13.5	26.7
5	4.3	3.4	3.3
10	3.0	1.5	0.8
20	2.2	0.7	0.2
30	2.0	0.5	0.2

The time-current overcurrent curves for different characteristics are shown in Figure 2-3. The three characteristics are plotted based on common settings and TMS of 1.

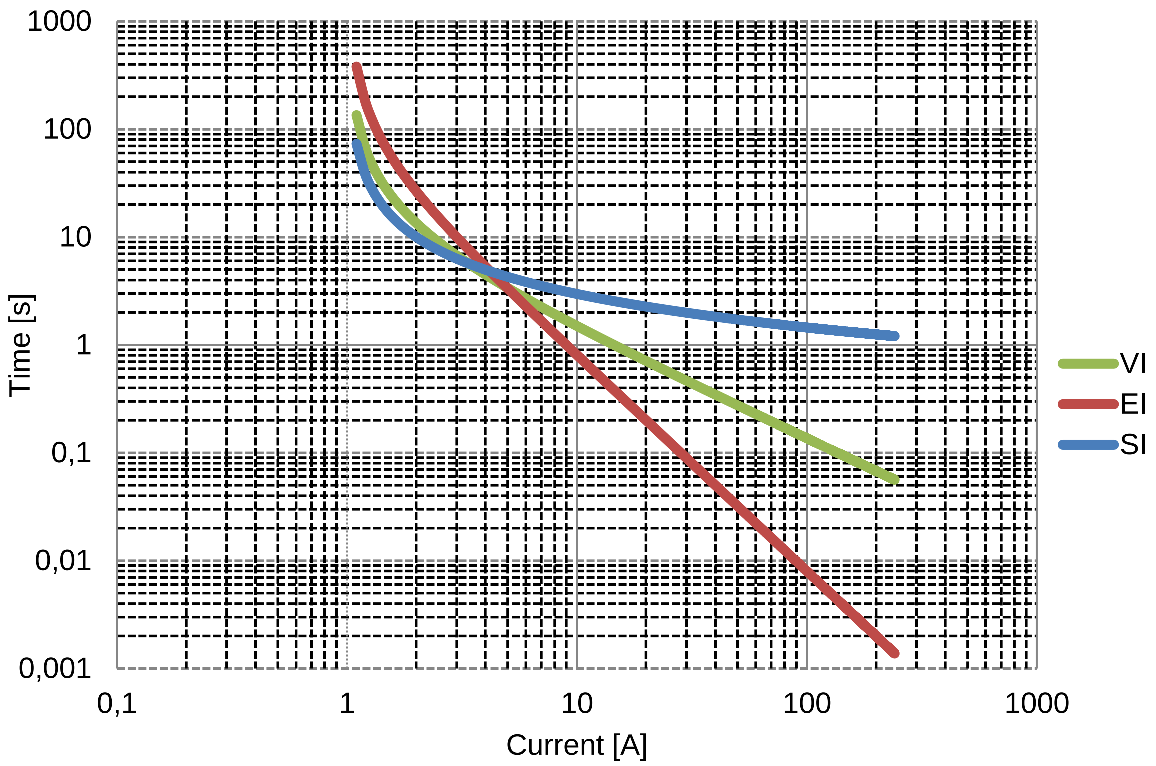

Figure 2-3: Overcurrent relay characteristics

From the calculations in Table 2-2 the EI characteristic is faster than both the NI and VI characteristics. It is apparent that at lower fault currents the NI characteristic clears the fault faster than the VI and EI. As the fault current increases, all three characteristics operate faster, though the EI outperforms the other two characteristics.

2.4 Application of non-directional overcurrent relays

2.4.1 Radial power system

The non-directional overcurrent relays are mainly used in radial systems where the fault current flows away from the main source and towards the load centres. Radial systems are single-source arrangement with multiple loads as shown in Figure 2-4. This type of a system is generally associated with distribution systems. Distribution systems are very economical to build, however, from a reliability point of view, they are not reliable. Because a loss of a single source results in a total loss of supply to the consumers connected downstream. From a protection perspective, a radial system presents a less complex problem [54].

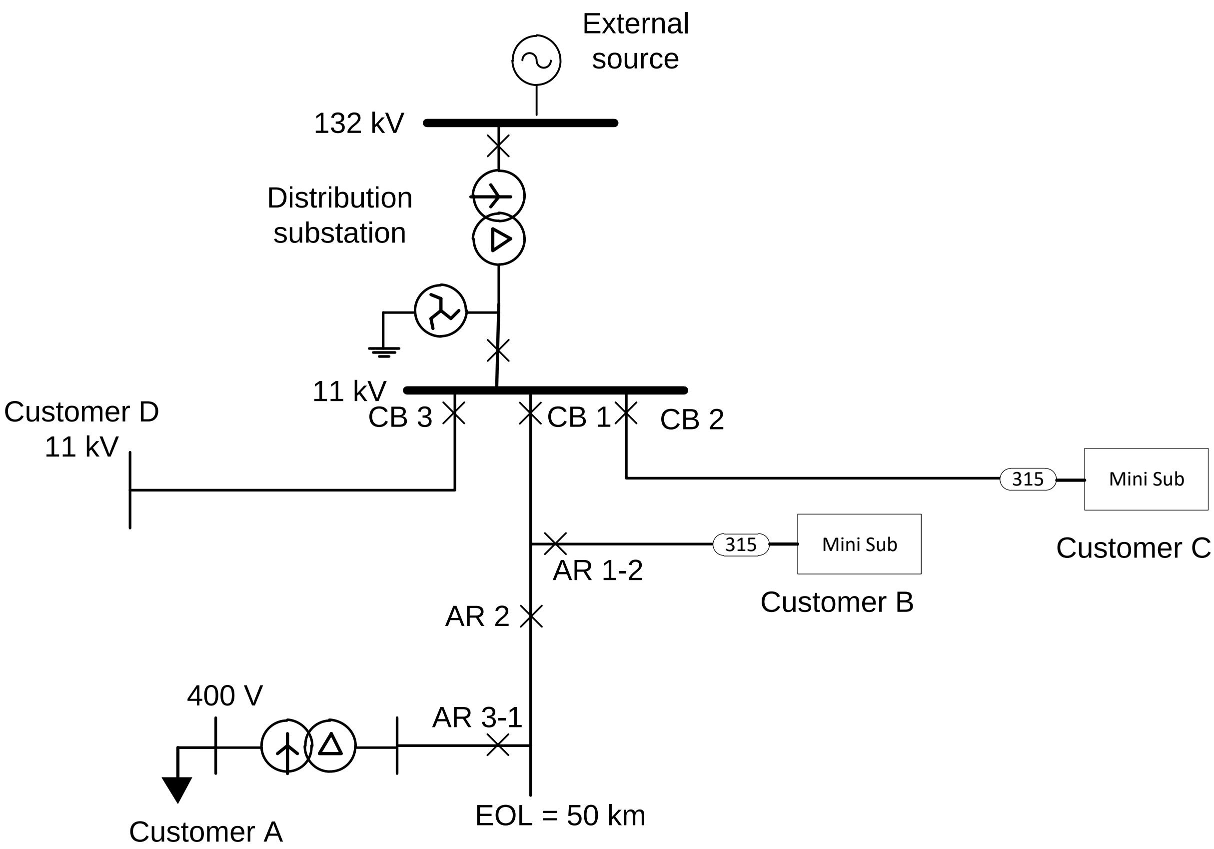

Figure 2-4: Radial distribution system

Fault current can flow in one direction, i.e. from the main sources toward the fault [54]. Since radial systems are generally electrically remote from the generation point, the fault current does not vary much with the changes in generation capacity [54].

2.5 Directional overcurrent protection

The directional overcurrent protection is extensively used in interconnected distribution networks. This is done to avoid the overcurrent relay operating for faults external to the protected zone. The directional overcurrent protection can also be used in parallel feeders, where there is a fault on the feeder and the fault is reverse fed (from the feeder side) from the unfaulted feeder [21].

Due to the changing distribution network, future distribution networks will have multiple sources connected at the load side of the power system. In the active distribution network, fault currents can be fed both from the DG source and the power system side. This presents more challenges when coordinating the non-directional overcurrent relays in the active distribution network. However, the directional overcurrent relay is used to resolve this challenge. The contribution of different DG technologies is thoroughly investigated and discussed in Chapter 3.

The classical directional overcurrent protection employs the phase relationship between the power system phase-to-neutral voltage and phase current (I_p and V_{pn}) to determine the fault location. The directional overcurrent relay is required to operate for faults in the forward direction only. Since the feeder impedance is mostly inductive, the forward direction is when the fault current is lagging the voltage by almost 90°. When the fault current leads the voltage by almost 90°, the fault is said to be in the reverse direction [18],[22].

The directional overcurrent protection would have been simpler if the watt flow was used to determine the direction of the fault current. In the watt flow method, the phase current (I_p) and phase-to-neutral voltage (V_{pn}) are compared. If the phase-to-neutral voltage and the phase current are in phase, the power flow is considered to be in the forward or reverse direction depending on the defined convention. However, the drawback with this method is that during a single-phase-to-ground fault, the phase voltage may collapse to zero and there will be no phase voltage for use in calculations. Hence, the quadrature voltages (i.e.$V_{BC}\ vs.\ I_A$) are used to determine the direction of the current to the fault [18],[22].

The directional sensing unit requires a reference quantity, which should remain constant when compared to the protected circuit [20]. The circuit in Figure 2-5 shows the connection of the classical directional overcurrent relay. In this circuit diagram, only the *phase A* current and its corresponding quadrature voltage are shown.

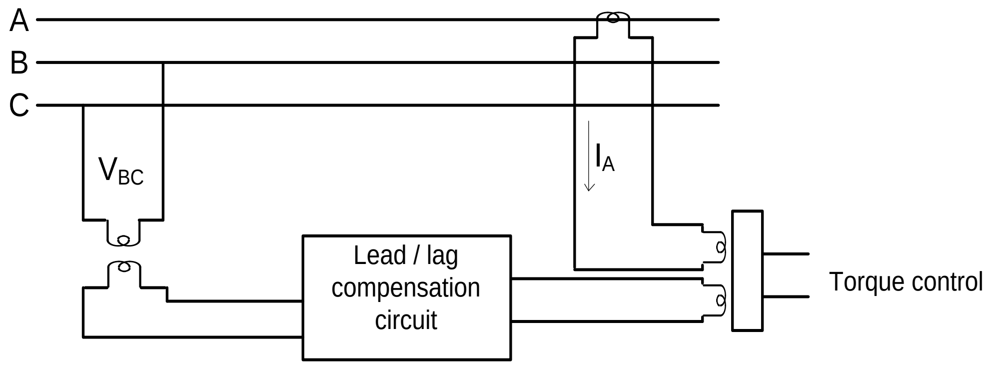

Figure 2-5: Classical directional overcurrent relay circuit

There are three commonly used direction sensing units, namely the 30°, 60° and 0° types [20]. The next section provides more details on how the application of the directional overcurrent relays.

2.6 Application of directional overcurrent relays

In South Africa, the directional overcurrent protection is commonly used in the sub-transmission network. The reason for directionalized overcurrent protection is twofold. Firstly, the directional overcurrent protection is used in a ring and interconnected network, where the current can flow in both directions at the relay location. Secondly, the directional overcurrent protection is used to establish the direction characteristics for distance protection and all directionalized protection functions [26]. The next sections discuss three different applications where directional overcurrent protection is commonly used.

2.6.1 Parallel feeders

When non-directional overcurrent relays are used in a sub-transmission network with parallel feeders and a single source as shown in Figure 2-6 below, a fault can occur on any feeder, regardless of the relay settings used, to clear a fault on either line A-B or C-D, it will require both lines to be isolated. Thus, the power supply (source) is completely disconnected. To achieve a proper coordination, the remote end relays B and D are directionalized and coordinated with both non-directional relays A and C [26]. The arrows associated with the relays shown in the diagram below in Figure 2-6 indicate the direction of flow of current, which will cause the relay to operate [26]. Double headed arrow indicates a non-directional relay such as those at the sending end and a single headed arrow indicates a directional relay such as those in the receiving end in Figure 2-6 below.

For a fault on line A-B, relay D will not operate, since the fault current (I_2) is flowing in the non-operate direction and relay B will be set to operate slower than relays A. The usual practice is to set relays B and D to 50% of the normal full load current, a time multiplier setting of 0.1 and an IDMT curve is used instead of a definite time (DT) curve [26].

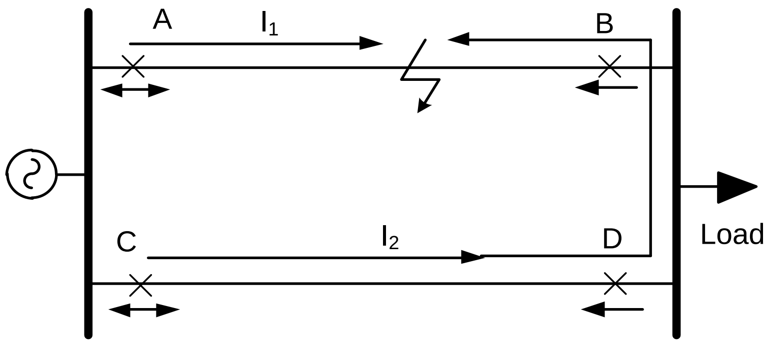

Figure 2-6: Distribution network with parallel feeders

In this case, relays A and B are required to clear the fault and relay C will only operate if both relays fail to clear the fault. Therefore, the supply is maintained to consumers by only isolating one faulted feeder at a time. Ring mains are the most common arrangement in the distribution network [26]. In the next section the second application of the directional overcurrent relays in the distribution network is discussed.

2.6.2 Ring main networks

Ring networks are the most common arrangement in the distribution network. The main reason for its use is to maintain supply to consumers in the case of a fault in one of the interconnected feeders. In this setup, current can flow in either direction through various relay locations, and hence the need for directional overcurrent relays [26]. A typical ring main network is given in Figure 2-7 below.

In the case of a ring main network with only one source as depicted in Figure 2-7, the settings at the mid-point substation are the same (i.e. bus 4) for both directions. Thus, the relays at the sending end and mid-point substation can be made non-directional. In the case where the number of feeders is even, it is often noted that the two relays with the same operating times are at the same substations. They will therefore have to be directional. Whereas, when the number of feeders is odd, the two relays with the same operating times will be at different substations. Therefore, the relays can be non-directional [26].

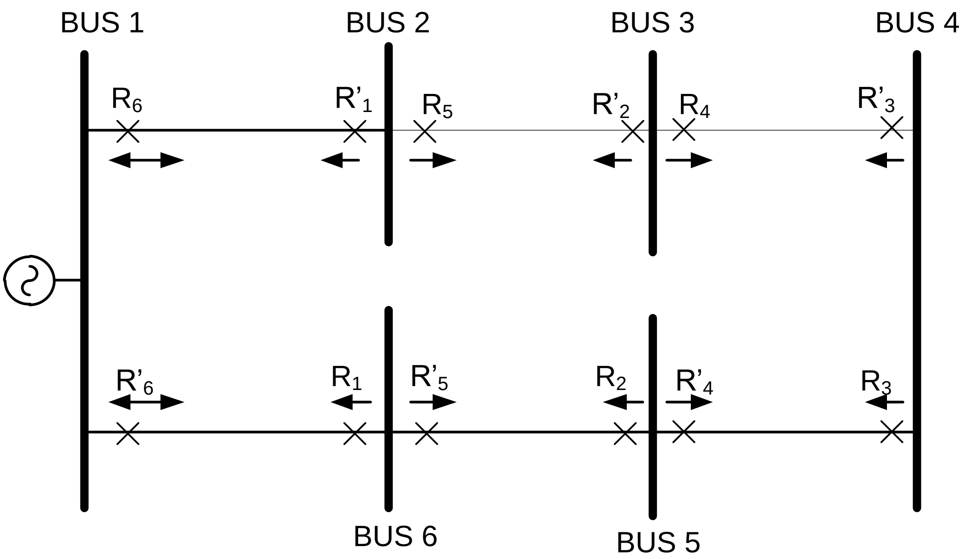

Figure 2-7: Ring main network

At intermediate substations, the operating times of the relays are different and their difference is always not less than the grading margin of 0.4 seconds [26].

2.6.3 Directional control

The third application of the directional overcurrent protection is to establish direction for the quadrilateral characteristic of the distance protection [26]. Figure 2-8 shows the protected feeder and its directional overcurrent relay characteristics. The following sections discuss the characteristics of the directional overcurrent relay.

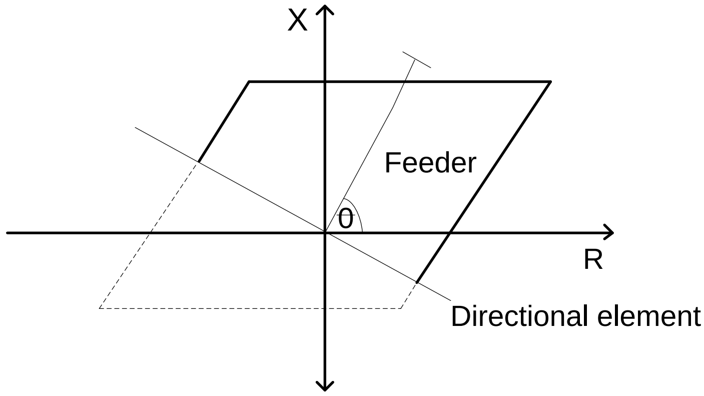

Figure 2-8: Directional overcurrent characteristics

The other application of the directional element is in impedance protection where the relay zones are set either to be forward or reverse looking zones. There are typically three forward looking zones, namely; zone 1, zone 2 and zone 4 and one reverse looking zone 3. The first forward looking zone (i.e. zone 1) is an underreaching zone set to 80% reach of the protected line and is set to clear faults instantaneously. The second and the fourth forward looking zones (i.e. zone 2 and zone 4) are overreaching zones set to 120% and 150% reach of the protected line. [21]. Figure 2-9 shows the time-distance graph of an impedance relay set at point A. Typical time settings for zone 2 and zone 4 are set to clear the fault in at least 0.4 seconds and 1.5 seconds respectively.

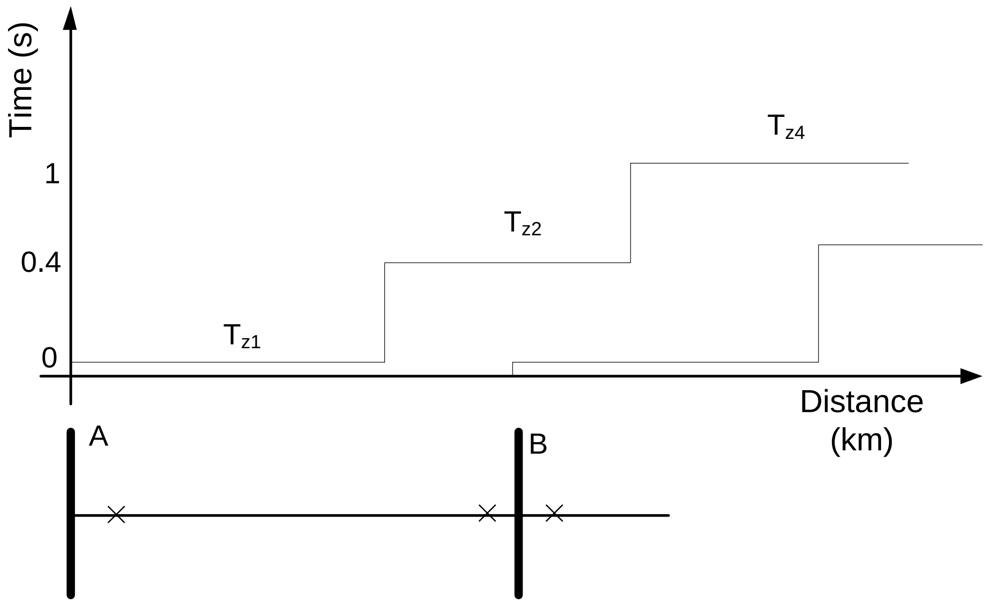

Figure 2-9: Impedance relay time-distance characteristic [21]

Details on how the directional element of the overcurrent relay is established are discussed in the next sections.

2.6.3.1 A 30° relay characteristic

For phase faults, a single-phase voltage is used as a reference quantity. The reference voltage is referred to as a 'polarizing' voltage. The reason for using phase voltage instead of phase current as a reference is that during fault conditions voltage does not change its phase position as compared to current. The phasor representation of the current changes and is mainly affected by the fault location [20].

The inputs of the phase "A" into the relay are supplied by a phase current I_a and a phase voltage V_{BC} displaced by 30° phase shift in the phasor diagram below in Figure 2-10. In the solid-state type relays, the maximum torque and zero torque line are the minimum operating lines for the directional overcurrent relays. The maximum torque in electromechanical relays is obtained when the angle between two fluxes is 90° apart. The phasor representation of the voltage, which forms a 90° phase shift to the reference is V_{BC} as shown in Figure 2-9 [20].

The maximum torque angle (MTA) is the angle difference between the phase current and displaced polarizing voltage (V'_{BC}) at unity power factor. When the phase current lags the system phase-to-neutral voltage (V_{pn}) by 60° the relay becomes more sensitive. For all faults within the tripping zone (i.e. operate area as shown in Figure 2-10) the relay is more sensitive and will operate for such faults [20].

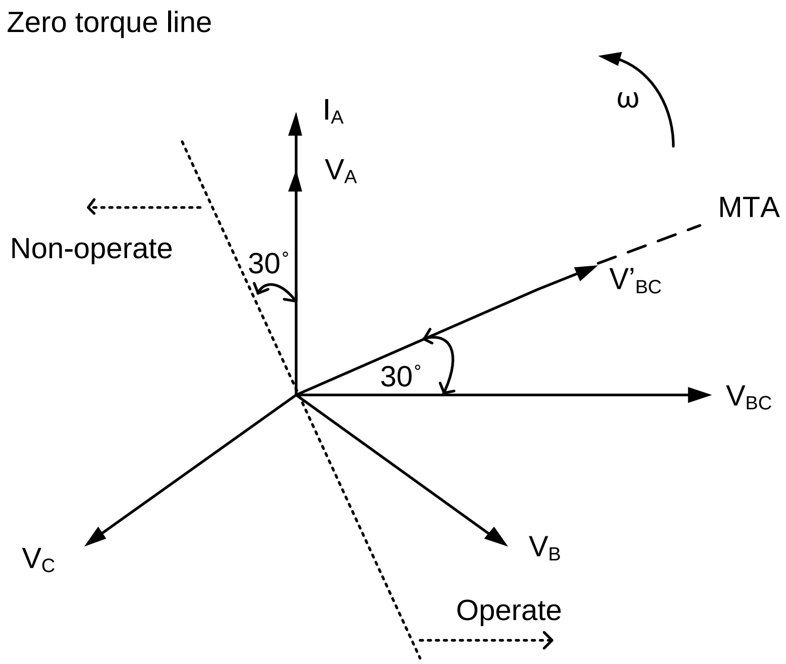

Figure 2-10: A 30° relay connection

The second characteristic discussed is a 45° phase shift between the phase angle and its quadrature voltage. The next section briefly gives an overview of this characteristic type.

2.6.3.2 A 45° relay characteristic

Using phase A as an example, the phasor representation of the phase current I_a and voltage V_{BC} are now displaced by 45° phase shift in an anti-clockwise direction. In this case, the maximum sensitivity of the relay is reached when the phase current lags the phase-neutral voltage (V_{pn}) by 45°. The relay operates correctly for all faults in the tripping zone (operate) [20]. The 45° characteristic is shown in figure 2-11. The MTA occurs when the phasor representation of the phase-phase voltage (V_{BC}) is displaced 45° away from the polarizing voltage (V'_{BC}).

When comparing the two characteristics at unity power factor, the 45° characteristic is more sensitive than the 30° characteristic. Whereas at zero power factor the 30° characteristic is more sensitive that the 45°characteristic [20],[26].

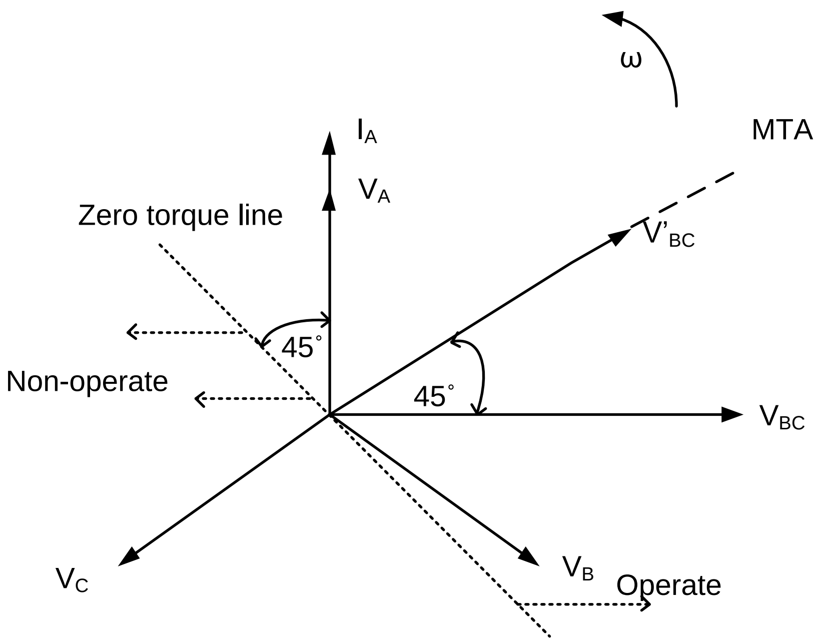

Figure 2-11: A 45° relay connection

The table below shows the phase currents and their corresponding quadrature voltages used in the directional overcurrent relays.

Table 2-3: Directional overcurrent quadrature voltages and currents

Current	Quadrature voltage
I_A	V_{BC}
I_B	V_{CA}
I_C	V_{AB}

2.7 Coordination fundamentals

The significance of relay coordination is to ensure selectivity of the concerned relays in the power system. This ensures that correct relays operate for the correct fault and avoids nuisance tripping of relays.

The objective of protective relay coordination is to calculate the relay settings, which provide the shortest operating time at maximum fault levels and ensure that relays trip selectively. The calculated overcurrent relay settings are checked for minimum fault current operation. This implies checking coordination for maximum and minimum conditions [17]. Maximum fault levels are attained in cases where all feeders and the transformers at the local station are in service while minimum conditions refer to the sources being weakened i.e. when maximum contributing circuits are taken out of service and transformer impedance is increased by taking one of the parallel transformers out of service.

2.7.1 Coordination time interval (CTI)

The time difference between the two coordinated relays for the same fault current is known as the coordination time interval (CTI). The commonly used CTI is between 0.25 seconds to 0.40 seconds. However, this depends on various factors and the relay technology used. For electromechanical relays the recommended coordination time interval in the South African electricity utility is 0.40 seconds and for numerical relays a minimum of 0.25 seconds to 0.30 seconds is recommended.

The CTI is set to ensure that the following are accounted for [16],[17],[18]:

a) the circuit breaker operating time (i.e. interrupting and clearing the fault), which is typically between 2 cycles and 8 cycles,
b) relay overshoot time, typically not more than 0.03 seconds to 0.06 seconds,
c) relay timing errors,
d) CT and VT errors, and
e) the safety margin for errors and differences in equipment operating times.

Overcurrent protection coordination can be achieved in the power system by means of three different methods. Details on each method are given in the next sections.

2.7.2 Protective relay coordination methods

There are at least three ways protective relay coordination can be achieved to provide proper selectivity. The protective relay coordination methods are given below:

a) time graded protection only,

b) current graded protection, and

c) time and current graded protection.

In the time graded protection method coordination of relays is by time only. In the current graded protection method coordination of relays is achieved by taking into account pick-up current only, and the last method incorporates both methods. In time and current graded protection coordination of relays is achieved by taking into account both time and current. Depending on the network, any of these methods may be employed to satisfy the protection requirements. The last section of this chapter explains three ways in which coordination can be implemented.

2.7.2.1 Time graded protection

Definite time relays are typically coordinated by time only. The operating time of the DT relays is constant for all fault currents. It is usually used in the feeder T-offs or applied on the last recloser where fault current is very low. It is further used in sensitive earth-fault (SEF) and instantaneous overcurrent protection applications. This method is seldom used at the substation or feeder breakers as the fault current is high and will clear the fault at a fixed time unless it is used in the first cycle. This implies that the clearing time cannot be set to lower values, because there are downstream auto-recloser devices, which should be coordinated with this relay. Thus, using DT relays and coordinating them with downstream the auto-recloser devices will cause the relays at the substation to take long to clear fault currents closer to the substation [26].

In the radial network, the locations of the relays and auto-reclosers are such that they protect a certain number of customers in order to minimize the number of customers affected during system faults [17],[26]. The auto-recloser devices are used on the T-offs protects all customers connected in the T-off and some are used on the feeder backbone.

Each relay is assigned an appropriate time to clear the fault, and relays close to the fault are set to operate faster than the immediate upstream relay. Selectivity is provided by the time delay between two consecutive relays, which is typically 0.5 seconds and 1.0 second for earth fault protection. When two DT relays are coordinated, only time is taken into account for coordination and the pick-up current is not used, but the upstream recloser pick-up must be less sensitive compared to the downstream pick-up.

2.7.2.2 Current graded protection

The current graded method is different from the method discussed in the previous section. In this method, pick-up currents are selected based on the fault currents, which change proportionally with the line impedance. The pick-up current for an upstream auto-recloser is set to be less sensitive than the pick-up current of the downstream auto-recloser [17]. The auto-reclosers are set to operate at different magnitudes of fault currents along the feeder. This means that the auto-recloser closest to the fault will operate first, then an immediate upstream auto-recloser.

The challenge in this method is that in instances where fault currents are too low, it becomes difficult to discriminate between load current and fault current, especially when relays are too close to each other. This makes it difficult to coordinate auto-recloser devices, which are a few kilometres apart as the impedance would not have changed significantly.

2.7.2.3 Current and time graded protection

The last and commonly used method is the time and current graded protective method. The two methods discussed in the previous sections, both have disadvantages. When the time graded method is used, the highest fault currents will be cleared in longer constant times, especially when there are other relays to coordinate with downstream. At the same time the current graded method is very difficult to use, especially when the impedance between the two circuit breakers concerned has not changed significantly. Therefore, it is difficult to maintain good selectivity between the two CBs involved. The inverse-time overcurrent coordination method originates from the limitations of the two methods [26].

The overcurrent relays are coordinated at maximum fault levels and should be checked at minimum fault levels to ensure that coordination is satisfied for all network conditions. The protection settings of feeder circuit breaker should be set to detect faults beyond the next immediate circuit breaker in order to provide back-up protection to the next immediate circuit breaker. Therefore, the operating time of the feeder circuit breaker for a far-bus three-phase fault is set such that it will operate longer than the sum of the next immediate circuit breaker's operating time and the CTI.

2.8 Non-directional overcurrent relay coordination

The principle of non-directional overcurrent relay coordination is explained with reference to Figure 2-12, which shows a radial feeder with series of normal inverse relays characteristics plotted in the time-distance graph.

For a fault at F_1, which is at the farthest end of the source, the circuit breaker at C should operate first. The initial operating time for circuit breaker at C is set to clear the fault in 0.20 seconds. The immediate upstream circuit breaker (i.e. at B) is set to operate in 0.20 seconds plus the coordination time interval (CTI) of 0.40 seconds, which will result in the quickest time of 0.60 seconds. The third circuit breaker to clear this fault (F_1) is the circuit breaker at A, which is set to operate in 0.60 seconds plus CTI and this will result in an operating time of 1.0 second. This circuit breaker (A) will only clear the fault (F_1) in the case when the other two circuit breakers (B and C) fail to clear this fault [54].

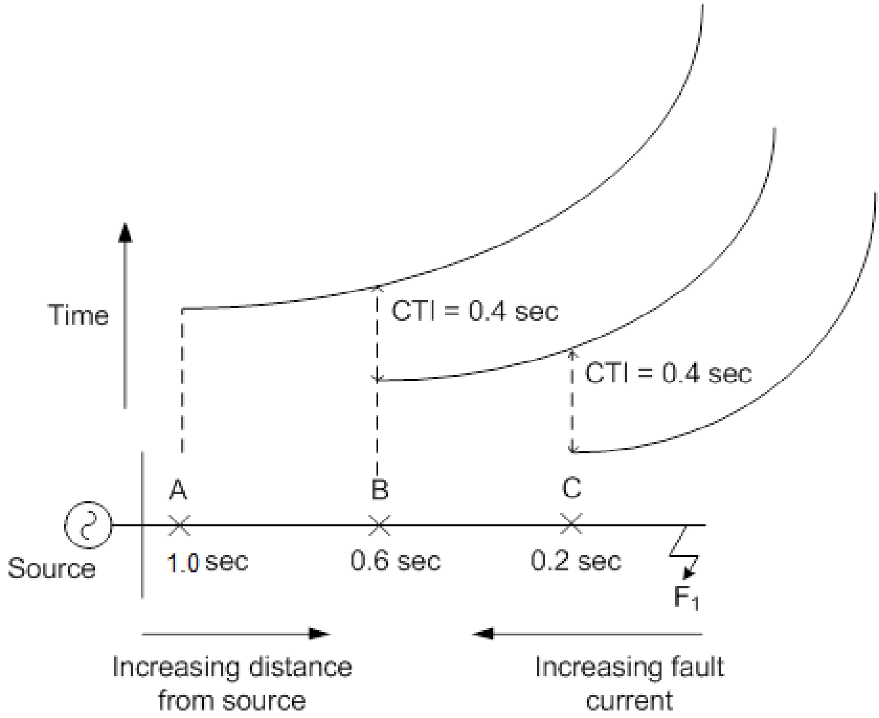

Figure 2-12: A simple radial feeder [54]

In a case where the fault is between B and C, the relay at C will not have current and therefore it will not operate. In this case, the circuit breaker B is expected to clear this fault as fast as possible and circuit breaker A will have a longer operating time, which is the sum of the operating time of the relay at B plus CTI of 0.40 seconds [54].

2.9 Directional overcurrent relay coordination

The principle of grading relays in a ring network is referenced in Figure 2-13, which shows a series of directional relays to be connected. The usual procedure for grading relays in the ring main network is to open the ring at the supply end and grade relays in a clockwise direction first and then anti-clockwise. Considering the same ring network shown in Figure 2-13, relays looking in a clockwise direction are arranged to operate in the following tripping sequence R_1-R_2-R_3-R_4-R_5-R_6 and relays looking in the anti-clockwise are arranged in the same tripping sequence R_1'-R_2'-R_3'-R_4'-R_5'-R_6' respectively [26].

The ring is opened at the supply end and an initial operating time for the first relay R_1 and R'_1 is set to be 0.20 seconds for close-in three-phase fault. A back-up relay's operating time is set to operate in 0.60 seconds. That is, the operating time of the primary relay plus the grading margin of at least 0.40 seconds. The grading margin is added to every relay's operating time till the last relay [26].

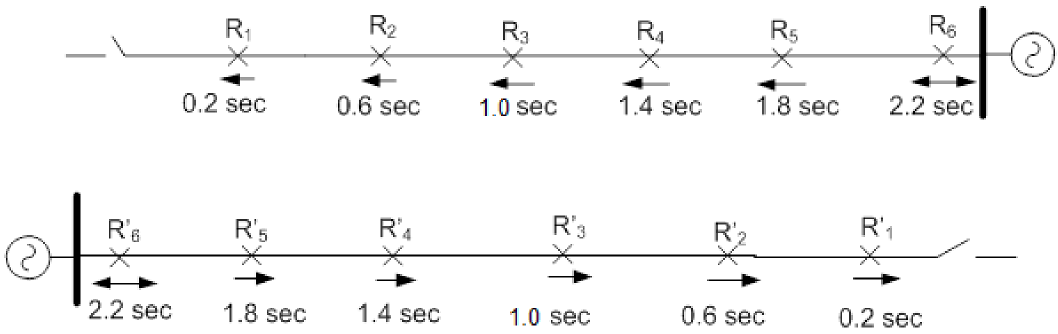

Figure 2-13: Simplified ring main network for grading

The following relays R_3 and R'_3 are both at the midpoint substation and it can be seen above that there is no need for a directional overcurrent relay, since the operating times of both relays are the same. A non-directional relay can be used and set to operate in 1.0 second for faults either in the forward or reverse of the relay.

2.10 Concluding remarks

This chapter has presented an overview of the basic power system protection background. The basic design objectives of protection are discussed and used in chapter 6 to analyse the performance of the proposed method against the conventional method. A distinction between the non-directional and directional overcurrent relays is made by discussing different applications and grading approach for both the directional and non-directional overcurrent relays.

The following chapter investigates different types of distributed generation connected to the distribution network. This chapter will provide an understanding of the protection behaviour when DG is present in the distribution network.

3 Distributed generation concept and technology

This chapter introduces the concept of the distributed generation sources. Secondly, it classifies DG sources according to different technologies and classes based on their unit rating. Lastly, the contributions of different technologies of different DG types are simulated in PowerFactory, discussed and results are provided at the end of the chapter.

3.1 Introduction

3.1.1 Distributed generation definition

The present renewable sources of energy (i.e. wind, solar and hydro), which in today's world are non-conventional sources, were conventional sources of energy until James Watt invented a steam engine in the 18th century [1]. The benefits of these renewable energy sources are: free of cost, pollution free and inexhaustible. Through the years, the use of the non-conventional energy declined due to the technological challenges, difficulty in transporting and the uncertainty of its availability [1]. The growth of the renewable energy resources commenced after the oil crisis in the early 1970s. It was only after the oil embargo that people started to realize that fossil fuel is not reliable and has a greater impact on the global climate [1].

Distributed generation (DG) has attracted a lot of attention recently and has become more important for future power generation system. According to a recent study, more than 2 457 gigawatts (GW) of power will be installed worldwide over the next 25 years, while total energy capacity will grow to 3 930 GW by 2035 [59].

The recent common technologies used or under development in the developing countries are: solar, wind and bioenergy devices. Wind energy production is gradually growing in South Africa. Since 2009 the total amount of generated power from renewable energy sources (RES) in Germany has reached 16% and the growth continues unabated. Denmark has generated about 2.5% of its total energy usage and has seen a growth of 25% rate per annum. The use of concentrated solar power (CSP) is increasing rapidly and its market has seen about 740 MW of generated capacity installed since 2007. Spain and United States (US) have taken the lead by 632 MW and 503 MW respectively [59].

The graph below in Figure 3-1 shows the total world installed capacity per technology. It is evident from the graph below that the most prevalent DG technology in the future will be hydro, wind and solar photovoltaic (PV) [59].

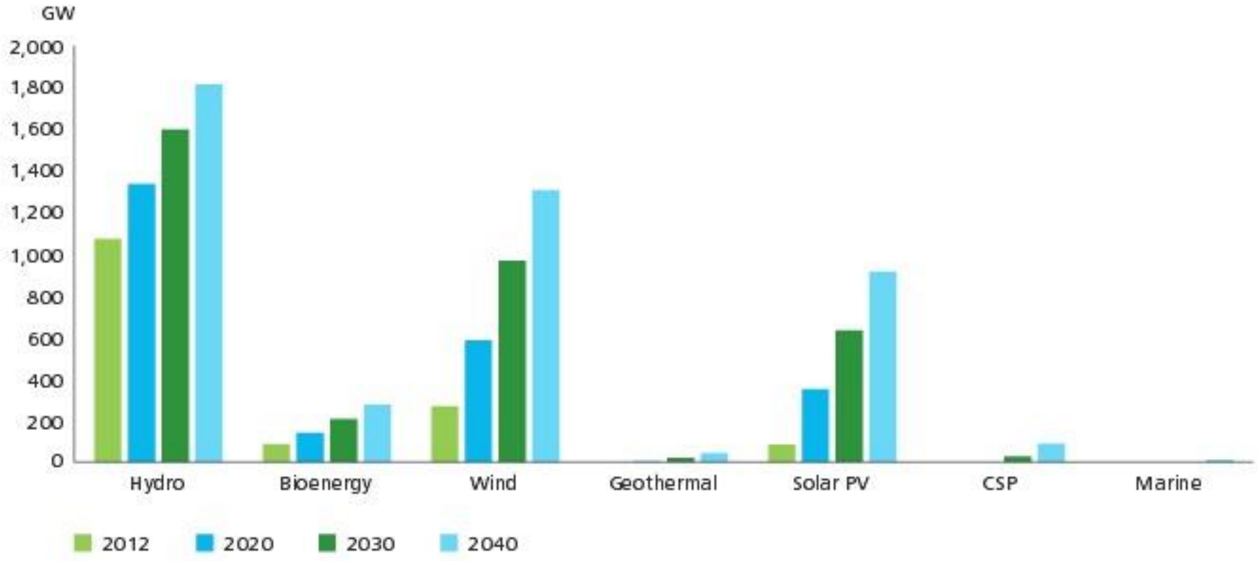

Figure 3-1: World installed capacity [59]

There are many definitions of the distributed generation due to various government regulations in different countries. Distributed generation (DG) as it is generally called is a new approach of generating electricity from natural resources such as water, wind and the sun. It is usually connected to the distribution network or near the load centre. Furthermore, DG refers to any type of the electricity generation, which has the ability to operate in parallel with the utility. DG sometimes can be used interchangeably with the term distributed resources (DR). However, DR is intended to encompass non-generating technologies such as power storage devices like batteries and flywheels in addition to generators [27],[60]. The diagram below in Figure 3-2 shows an interconnected distribution network with distributed generation unit. The interconnection block simply shows the point of common coupling (PCC) between the DG and the utility of which in the diagram a distribution network is used as an example.

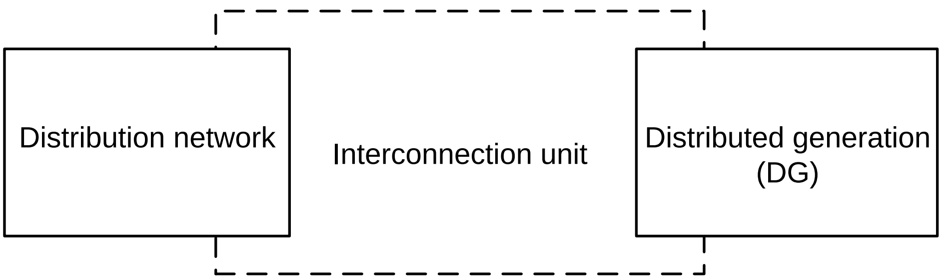

Figure 3-2: Representation of an interconnected system

3.1.2 Different substation bus configurations and voltage levels at PCC[2]

There are various configurations, which can be selected from when connecting a DG and the electricity utility. Typical configurations include single bus, sectionalized bus, ring bus, breaker-and-a-half and double breaker bus. These are standard configurations as per IEEE 666 TM 2007, IEEE design guide for electrical power systems for generating stations. The most commonly used configurations in the transmission and distribution grids (i.e. single bus and sectionalized bus) are shown in Figure 3-3 below. The choice of the HV bus configuration is generally related to cost versus reliability needs of the DG and the interconnecting utility [42].

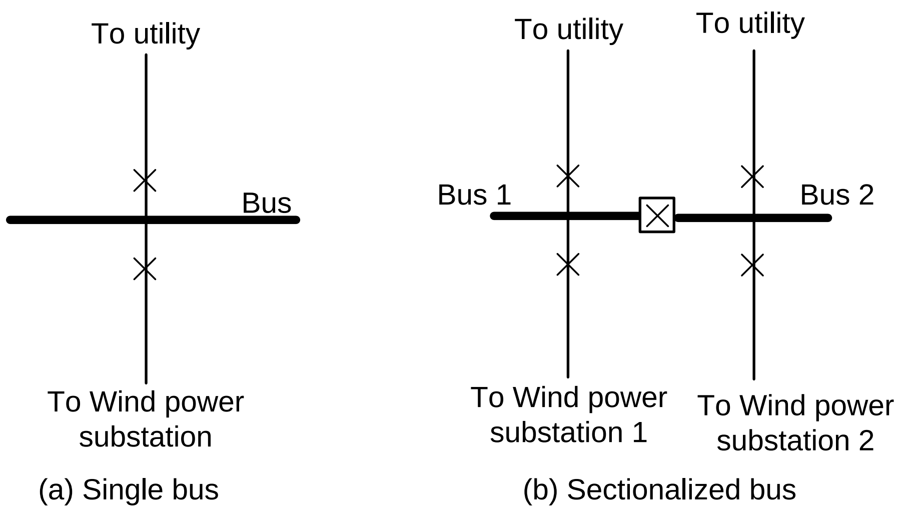

Figure 3-3: Various DG switch-yard configurations [42]

New DG substations are typically connected to the existing infrastructure via radial lines, switchyards and substations. The interconnection decisions are justified based on existing voltage levels, electrical losses, line servitudes and environmental concerns, economics related to conductors as well as reliability and security [42]. The type of the renewable energy resources affects the size of the generation plants and type of grid connection [66].

The European power grid is a three-phase AC system operating at 50 Hz at all voltage levels. The power system has four voltage groups (i.e. EHV, HV, MV and LV), which are established as per International Electrotechnical Commission (IEC) [66]. The European power grid is operated similar to the South African grid except for the defined voltage levels. Table 3-1 and Table 3-2 show the similarities and differences between the two power grids.

[2] PCC refers to point of common coupling

Table 3-1: German grid voltage levels for DG plants at PCC [66]

Rated power generation plant	Voltage abbreviation	Voltage level	Role
Up to 30 kW	LV grid without verification	400 V	Distribution (Dx)
30 kW to 200 kW	LV or MV grid		
0.15 MW to 20 MW	MV grid	30 kV, 20 kV, 15 kV & 10 kV	
15 MW to 80 MW	HV grid	110 kV	
80 MW to 400 MW	EHV grid	220 kV, 380 kV	Transmission (Tx)

Comparing the above in Table 3-1 to the South African grid, the following DG categories have been defined in the South African grid code and follow the schema in Table 3-2.

Table 3-2: South African grid voltage levels for DG plants at PCC [67]

DG category	Rated power	Voltage abbreviation	Voltage level	Role
A	0 – 1 MVA	LV grid	≤1 kV	Distribution (Dx)
B	1 MVA – 20 MVA	MV grid	11 kV, 22 kV 33 kV	
C	20 MVA and higher	HV and EHV grid	33 kV- 220 kV	
			220 kV and higher	Transmission (Tx)

The substation designs of the DG units and existing substations are not designed and built the same way. Therefore, this creates complexities when designing a DG substation. Some factors which affect the interconnection of DGs and utility substations are: interconnection lines and facilities, grounding, reactive compensation, power quality, harmonics, protection and control devices, surge protection and transformers. All these factors mentioned above have a significant impact on the design of the DGs, which typically are developed over a short period and have to comply with the grid code requirements [42]. Some of these factors such as grounding, protection and control devices as well as transformers are discussed thoroughly in the next chapter.

3.1.3 DG technologies

Given the definition of the distributed generation in the beginning of the chapter, it is also important to classify DG sources according to different technologies. Examples of DG technologies are given below in Table 3-3.

Table 3-3: DG technologies [61]

<table>
<tr><th>Type</th><th>Energy technologies</th><th>Primary energy</th><th>Conversion type</th></tr>
<tr><td rowspan="4">Non-conventional</td><td rowspan="2">Solar radiation</td><td>PV, solar thermal
(direct solar radiation)</td><td rowspan="2">Thermal conversion</td></tr>
<tr><td>Hydro, wind, bio-energy, wave energy
(indirect solar radiation)</td></tr>
<tr><td>Planet movement and gravitation</td><td>Tidal and sea current energy</td><td rowspan="4">Mechanical conversion</td></tr>
<tr><td>Radioactive decay in the earth crust</td><td>Geothermal energy</td></tr>
<tr><td rowspan="2">Conventional</td><td rowspan="2">Non-renewable energy sources</td><td>Nulear energy</td></tr>
<tr><td>Fossil carbon based energy</td></tr>
</table>

Solar radiation is a thermonuclear conversion of elements in the sun. In the non-conventional energy resources, this is the main energy source. This energy technology can be divided into two sub-categories: direct (PV and thermal solar) and indirect (wind, hydro and wave) solar sources. Direct solar radiation uses solar beams of radiation directly during the electricity generation process. The indirect solar radiation sources on the hand use solar beams of radiation indirectly and make use of the transformed energy in the form of wind or water cycle. Bio-energy is through the process of photosynthesis an example of an indirect solar radiation resource [61].

Power plants in the movement and gravitation category in Table 3-3 above is based on the utilization of tide and any other source of energy, which uses water in the ocean. Uranium and potassium are typical examples of the basic and original energies used in radioactive decay of materials in the earth's crust [61].

A breakdown in Figure 3-4 shows the classification of DGs based on their grid interface or connection and fault current contribution to the grid. A distinction is made between the inverter coupled and directly coupled DGs. DG units, which are coupled directly to the grid are mainly wind turbine generators and combined heat and power (CHP), which use synchronous generators. The squirrel cage induction generator and wound rotor induction generator with variable resistor are the two types of wind turbine generators, which are connected directly to the grid.

Due to different technologies, the directly coupled DG units have a significant contribution to fault currents, while the inverted coupled renewable energy devices are capable of controlling the contribution of fault current to the grid and automatically synchronize with the voltage and frequency from the electric grid after a system disturbance [61],[64].

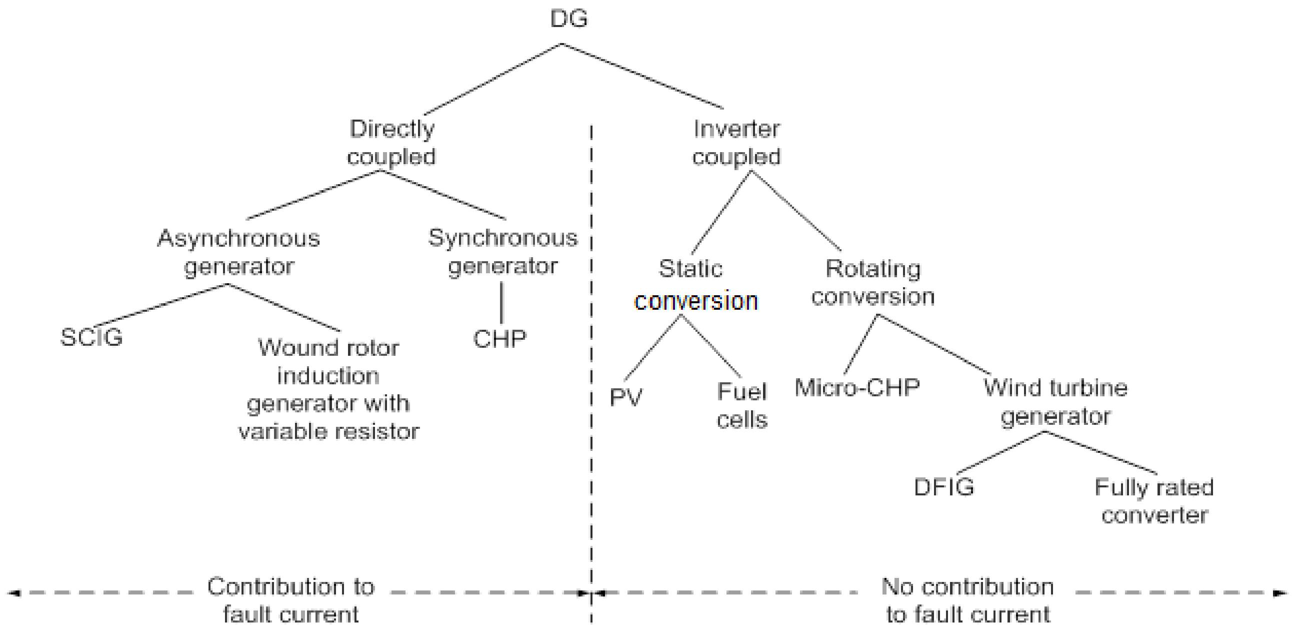

Figure 3-4: Classification of DGs [61]

The next section discusses the control methods employed in renewable energy devices. However, this research scope only focuses on wind and solar power plants. Therefore, in section 3.2 only wind turbine generators (WTG) and solar power systems are studied. This selection is based on the fact that the most prevalent future technologies in South Africa in renewable energy technologies are wind and solar PV as shown in the beginning of this chapter (Figure 3-1). Small scale hydro and hydro power is not considered, since most of hydro power stations are using the synchronous generators, whose contribution and response to fault is known.

3.2 Inverter based DGs

Not all DGs use conventional synchronous machines. Some DGs use energy sources that produce dc voltage, which is used as an input to the inverter, which is ultimately connected to the grid. The control and electronic topology of the inverter determines how the inverter is seen by the grid. Power electronic circuits (inverter based) in wind and PV systems perform the following functions [39]:

a) Convert AC into DC
b) Convert DC into AC
c) Control voltage
d) Control frequency
e) Convert DC into DC

These functions are performed by solid state switches, which switches ON and OFF periodically at desired frequencies. For DG devices, the power electronic systems used are mainly inverters and converters. A detailed behaviour of the inverter based DG's response to faults are often quite complex. However, an approximate response of the inverter based DG in the first few cycles (i.e. 2 to 60 cycles) may be used for fault analysis [39].

The benefits of using inverter coupled DGs over non-inverter coupled DGs are [62]:

a) fast response to system disturbances,
b) improves system harmonics and
c) flexibility to connect with the grid after a system disturbance.

Power electronics interfaces contain some level of metering and control. This is to ensure that the DG can perform as close to accuracy as designed. The diagram below shows a detailed block diagram of the power electronic interface DG system. The inverter coupled DGs consist of a three-level block, which summarizes the connection between the utility grid and the DG source [62]. The power electronics interface block diagram between the grid and the DG source is shown in Figure 3-5 below. The distinction between the engine or turbine driven and static DG sources is made and how each is connected to the grid.

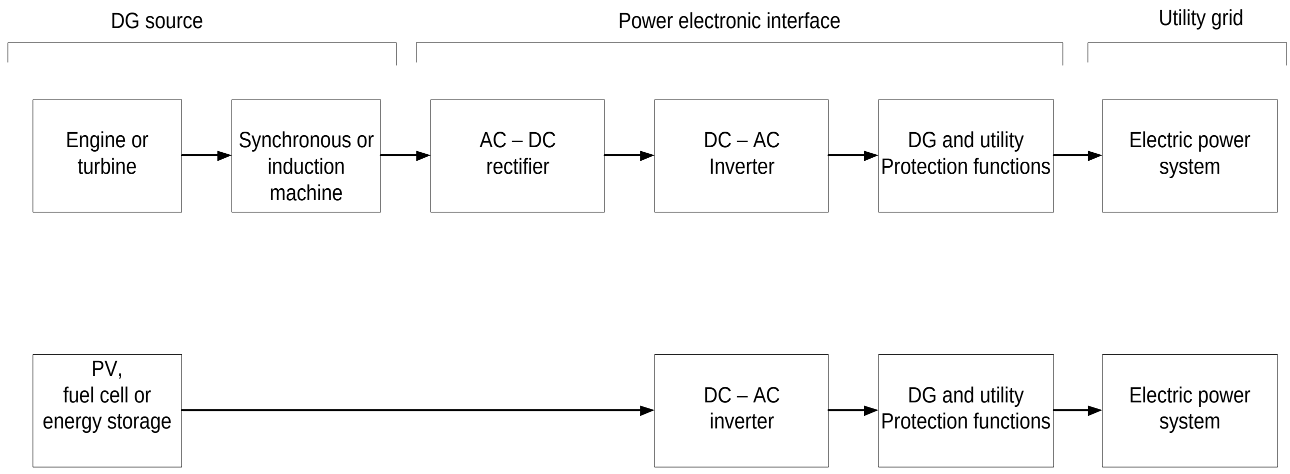

Figure 3-5: The power electronic interface DG system [62]

The model of the inverter based DG is accomplished by assumption that the input voltage from a dc source to a pulse width modulation (PWM) inverter is regulated and fixed. Thus, the inverter based DG operates as a controlled voltage source connected to the grid through a step-up transformer. The step-up transformer is usually a delta/star (the star being on the HV side) connection to ensure that the zero sequence components from the inverter to the grid are eliminated. Figure 3-6 below shows the generalized controller model of the inverter based DGs. The controller consists of two loops, namely: amplitude controller and the angle difference controller [63].

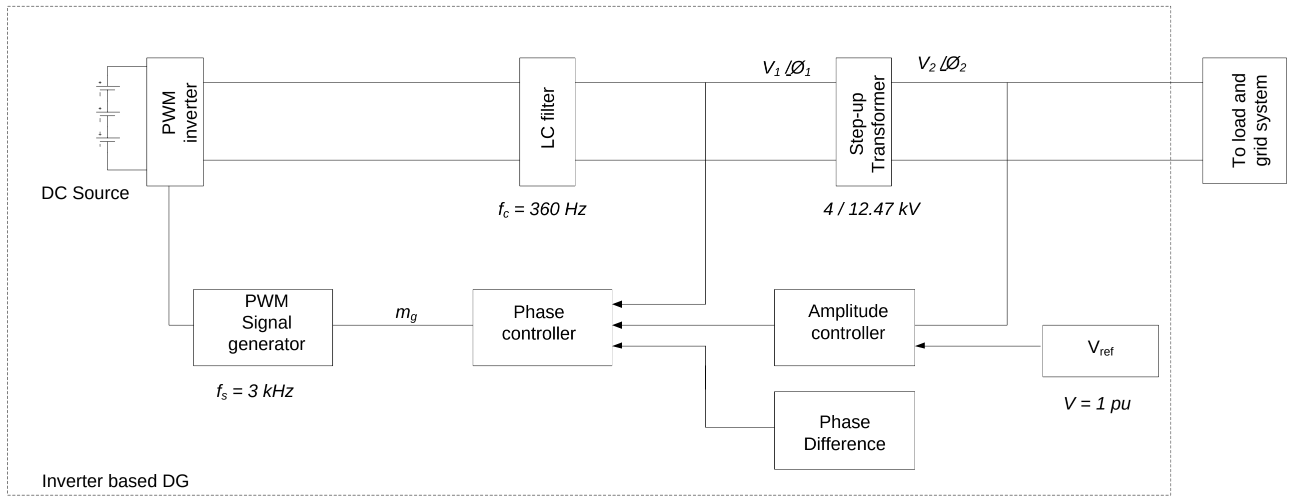

Figure 3-6: Control model for an inverter based DG [63]

The amplitude controller and phase difference (δ) controller provide the modulating signal to the PWM signal generator. A low pass LC filter is used to filter the harmonics from the PWM inverter. The cut-off frequency is set in such a way that the LC filter allows the fundamental power signal to pass through and ensure that the harmonics of the inverter voltage are attenuated [40],[63]. Details of the amplitude and phase difference controller are discussed in the next subsections.

3.2.1 Amplitude controller

The output voltage from the DG (V_2) as shown in Figure 3-7 is transformed through a time dependent transformation. The direct-quadrature-zero (dq0) transformation is used.

The phase locked loop (PLL) is used to detect the power frequency of the grid system at the point of common coupling (PCC), which is used as an input to the transformation block. The time domain phase variables ($V_{pn}(t)$) consist of the power frequency components and the dq0 transformation is time varying with dc and power frequency components. When designing and modelling the above controller, the root mean square (rms) voltages of the phase voltages are used and are denoted as all three-phase-to-neutral voltages (V_{pn}) and direct-quadrature-zero voltages (V_{dq0}) [40],[63].

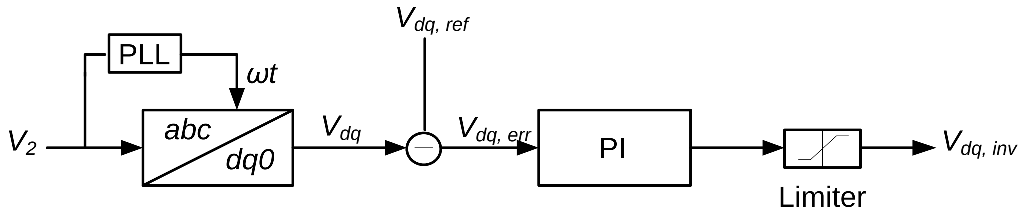

Figure 3-7: Amplitude controller of an inverter based DG [63]

The error signal ($V_{dq0,err}$), which is the difference between the reference signal ($V_{dq,ref}$) and the transformed signal $v_{dq}(t)$, is passed through the proportional-integral (PI) controller to be minimized [40],[63].

3.2.2 Phase controller

The phase controller (δ_{diff}), provides the angle difference between V_1 and V_2 as shown in Figure 3-5. The model of the phase controller of the inverter based DG is shown in Figure 3-8. In the phase controller, the operation of the phase controller is summarized below in four steps.

Firstly, the voltages V_1 and V_2 are used as inputs to the phase controller and are transformed to the dq0 reference frame. The following equation (3.1) below is used to calculate the phase difference between the primary (V_1) and secondary (V_2) voltages [40],[63].

$$\emptyset = tan^{-1} \frac{v_d}{v_q} \tag{3.1}$$

The second step is to calculate the average output power (P_{avg}) and compare it with the reference output power ($P_{out,\ ref}$). The error of the specified output power is passed through the PI controller, which is intended to minimize the error. The low-pass filter is used to attenuate the measured noise as well as to provide good transient response of the phase controller. The cut-off frequency of the low-pass filter should be set appropriately to ensure that the above mentioned functionalities of the low pass filter are satisfied [40],[63].

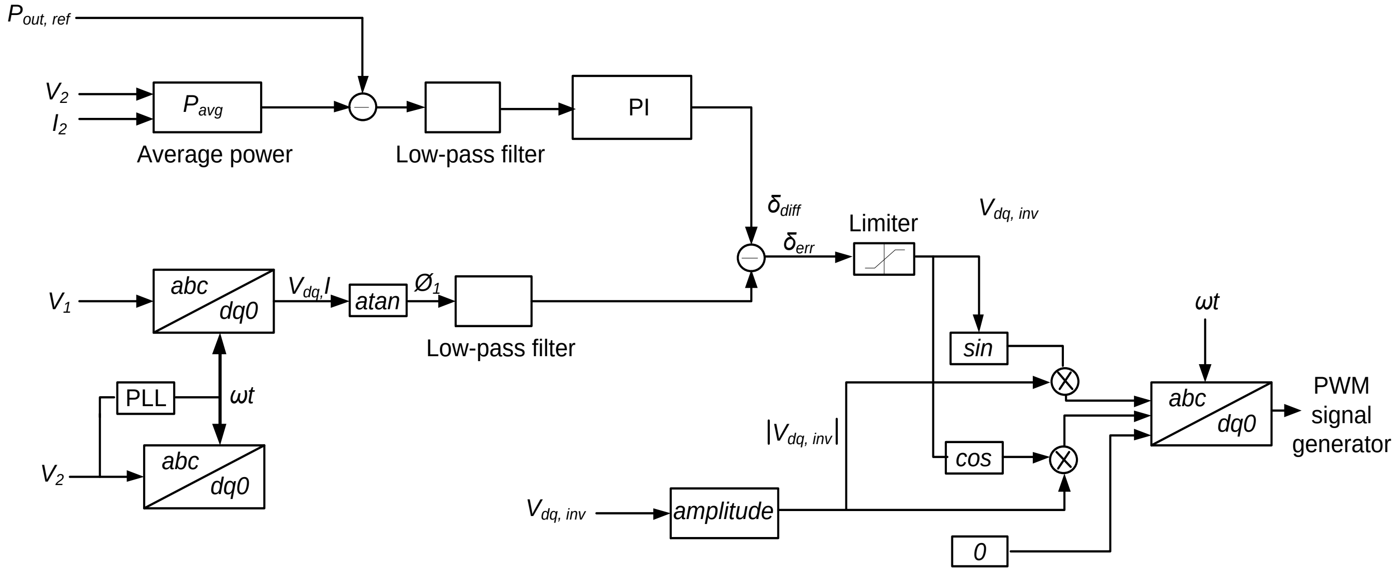

Figure 3-8: Inverter based phase controller [63]

The third step, the output of the PI controller (δ_{diff}) is added to the phase angle of V_1(i.e. $\emptyset_1$) and is used to calculate the required amplitude and phase angle of the modulating signal. In the last step, the modulating signal is transformed back to the abc reference frame. Therefore, the transformed modulating signal is used to control the PWM signal generator [40],[63].

3.3 Inverter based DG contribution to fault currents

3.3.1 Photovoltaic solar power (PV)

The photovoltaic solar power plant consists of various components that convert DC power produced by the PV array to a form that is usable to the load. If the load is AC, DC power should be converted to AC electrical power. The most critical component of a PV plant is the inverter, which converts DC to AC power [41].

The following diagram in Figure 3-9 shows the grid connected PV model. This network is modelled in PowerFactory to investigate the contribution of a PV system during fault conditions. The information of the PV model used can be found in Appendix A.

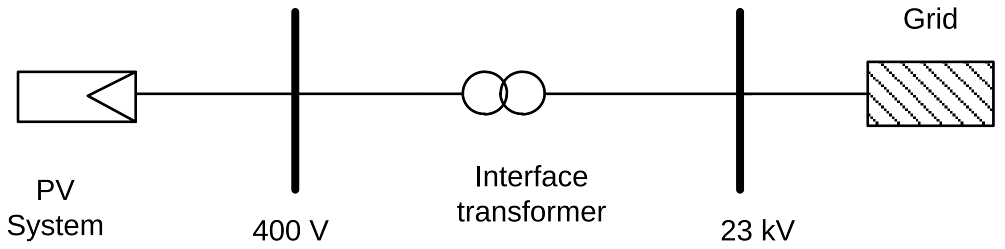

Figure 3-9: The grid connected PV model

Figure 3-10 shows the fault current contribution of a PV system. The electromagnetic transient fault study is simulated for 0.3 seconds, three-phase fault is initiated at t = 0.1 seconds and cleared at t = 0.2 seconds. It is shown from the diagram that during a three-phase fault at the 23 kV bus in Figure 3-10, the PV system does not contribute anything to the grid.

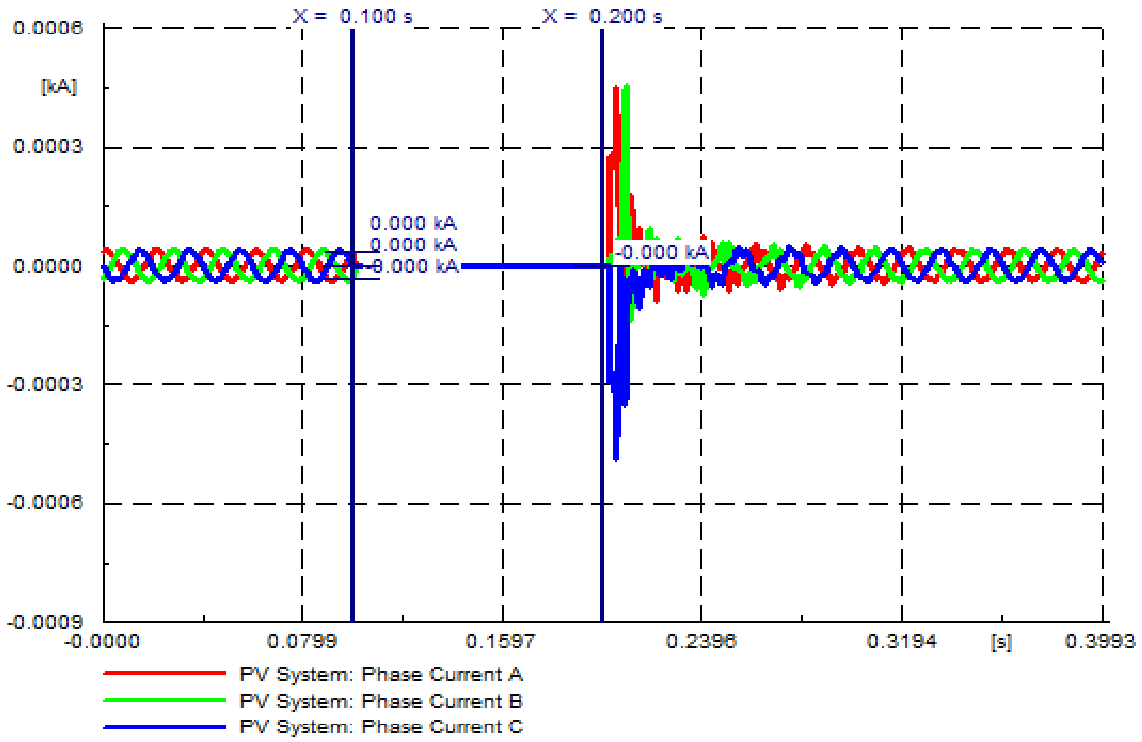

Figure 3-10: PV model contribution to fault

From Figure 3-4, the inverter coupled DGs are divided into two classes, namely: static and rotating conversion. PV systems are static conversion inverter coupled DGs. Rotating conversion inverter coupled DGs are discussed in the following section. Doubly-fed and fully-rated converter induction generators are the examples of the rotating conversion inverter coupled DGs. These generators are known to operate at a variable speed. The variable speed generators are connected to the grid via a power converter, which controls generator speed, thereby controlling power fluctuations caused by wind fluctuations [60].

3.3.2 Doubly fed induction generator (DFIG)

The principle of operation of the DFIG is fairly simple compared to the wound rotor induction generator with a variable resistor and the squirrel cage induction generators respectively. The electronic power converter is interposed between the rotor of the induction generator and the grid in order to supply the power dissipated as heat in the external resistor to the grid at rated frequency. The AC/DC and DC/AC converter, converts an excess amount of AC power in the rotor to DC power by a controlled rectifier. DC is converted to AC power at rated 50 Hertz frequency through an inverter [46]. The circuit shown in Figure 3-11 is modelled in PowerFactory to investigate the contribution of a DFIG during power system fault conditions. A transient fault study is simulated for 0.4 seconds and the fault is cleared in 0.2 seconds.

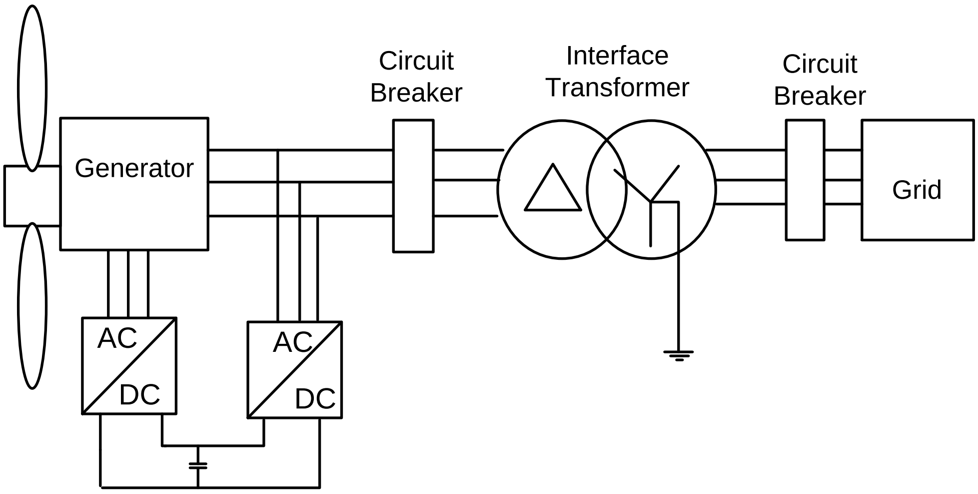

Figure 3-11: Doubly-Fed induction generator (DFIG)

The fault current contribution of this type of a generator is different for different faults. A higher peak is realized with a shorter decay for a three-phase fault. The fault current will decay longer for single-phase-to-ground and double-phase-to-ground faults, and the peak will be lower than the one in the three-phase fault.

The magnitude of the fault current in a three-phase fault is approximated to be 3 times the rated current [44]. The advantage of using this type of the generator is the flexible integration, best power quality and voltage ride through that can be realized [44].

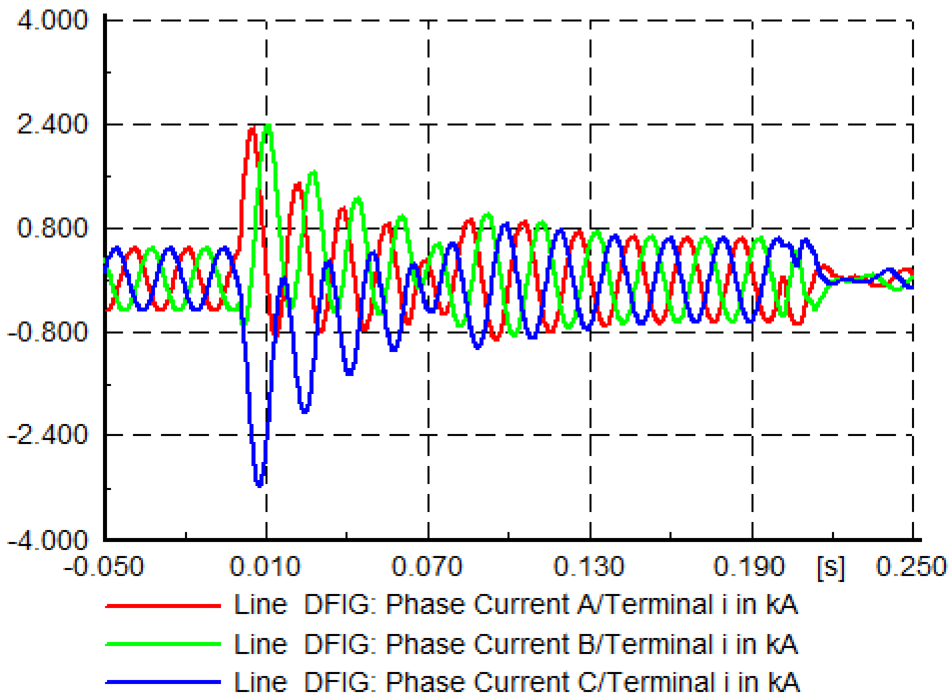

Figure 3-12: DFIG fault current contribution results

3.3.3 Fully-rated converter generator

The second inverter-coupled wind generator is the fully-rated converter generator. The fully-rated converter generator is connected directly into the power system through the power converter. The operation is similar to the doubly fed induction generator (DFIG). The generator is allowed to operate at variable speed. A wind generator is operated at optimum power coefficient below rated wind speed and at rated power above the wind speed [43].

The circuit shown in Figure 3-13 is modelled in PowerFactory to investigate the contribution of a fully-rated converter generator during power system fault conditions. A transient fault study is simulated for 0.4 seconds and the fault is cleared in 0.2 seconds.

A fully rated converter generator allows for the generator to electrically isolate from the grid during abnormal conditions. Thus, the contribution of fault current is minimal or limited to its rated current. The pitch control is used to control a temporary imbalance between the aerodynamic power and generated power during a power system transient [44].

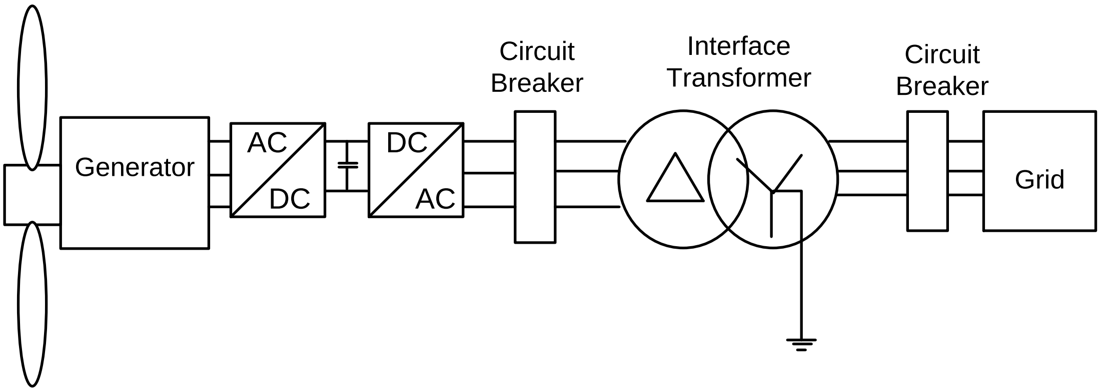

Figure 3-13: Fully rated converter induction generator

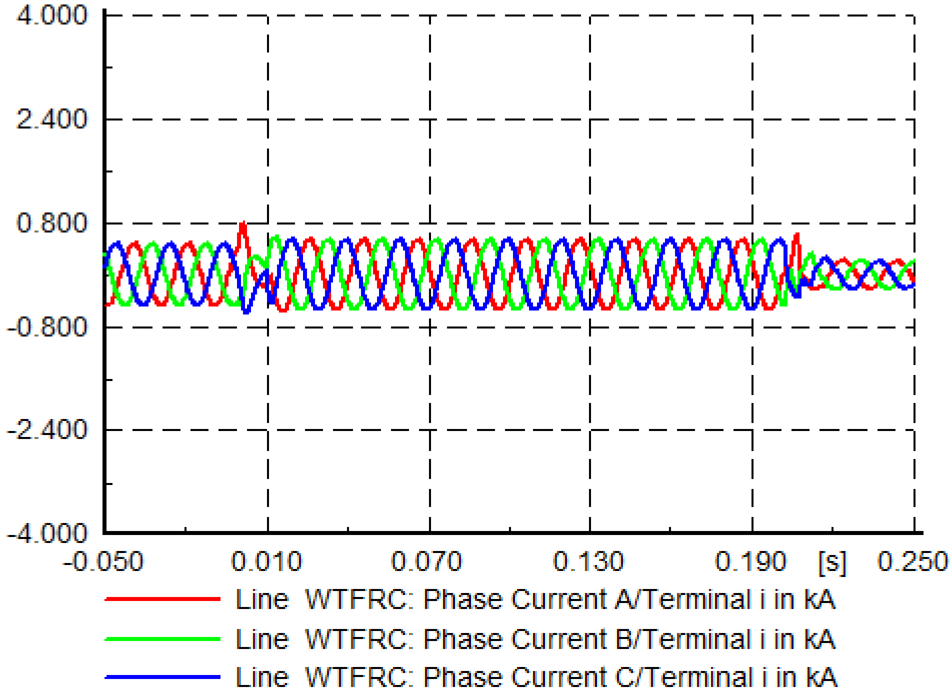

Figure 3-14: Fully rated converter fault current contribution

The next section provides the contribution of the non-inverter based DGs. These DG sources are generally connected directly to the grid and do not employ any power electronic system to control the current during system fault.

3.4 Non-inverter based DG contribution to fault currents

3.4.1 Concentrated solar power (CSP)

Concentrated solar power (CSP) operates differently from the photovoltaic solar power. CSP collects heat energy from the sun radiation and uses it at different temperatures i.e. low and high temperatures. In low temperatures, it is used to heat water and in high temperatures it is used to generate steam, which runs the steam turbine to turn the synchronous generator [39].

Since the CSP plants use the synchronous machines, their contribution to the system fault does not differ appreciable from the conventional power plants. Figure 3-15 shows the grid-interconnected CSP plant.

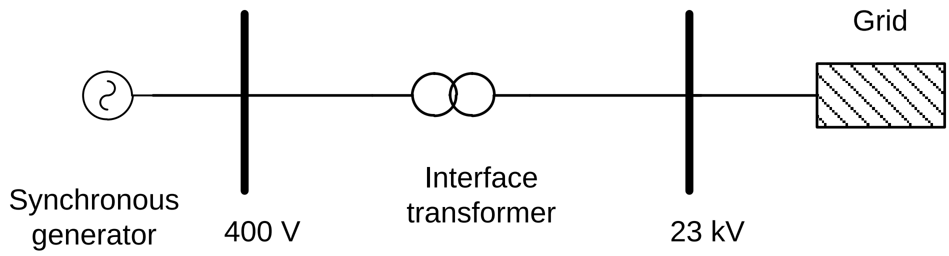

Figure 3-15: Grid-connected CSP plant

The fault current results of a CSP plant are shown in Figure 3-16. The synchronous generator currents in all three-phases for a three-phase fault in the power system initiated at time t=0 and the fault is cleared after 150 milliseconds. The currents in all three-phases are offset from the zero-axis showing the presence of both AC and DC components. During the first cycle (i.e. sub-transient period) all three-phase fault currents are more than the steady state fault current and the sub-transient current can be approximated to 3 to 6 times the steady state fault current.

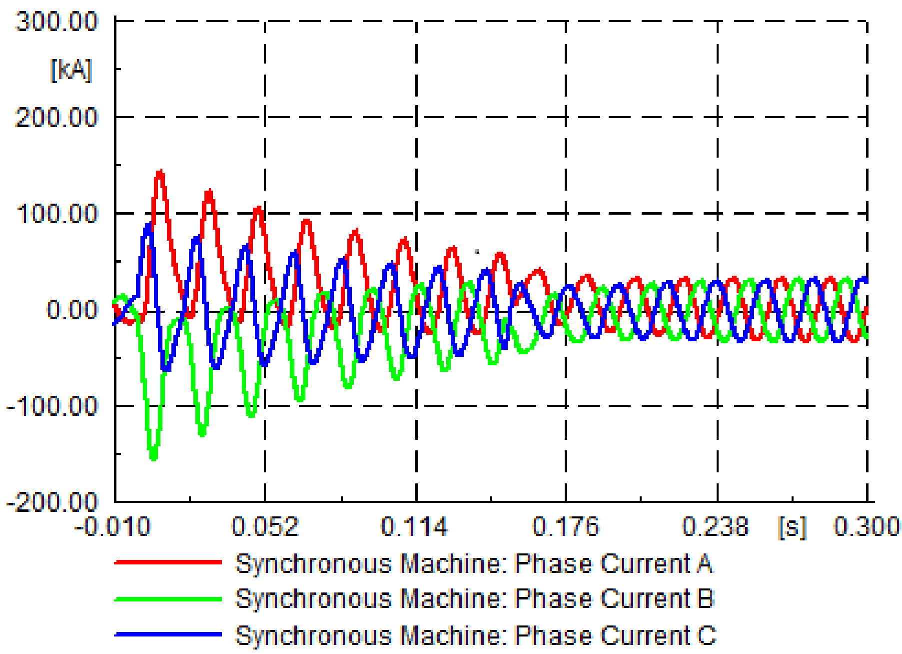

Figure 3-16: The synchronous generator fault current contribution

The next section discusses operation and response of the first generation of the induction generators (squirrel cage induction generators) and a wound rotor induction generator with a variable resistor during fault conditions.

3.4.2 Squirrel cage induction generator (SCIG)

Fixed speed induction generators were popular in the early 1990s and most standard installed generators operated at fixed speed, i.e. regardless of wind speed the rotor speed is fixed and determined by the frequency of the grid, gear ratio and generator design. Typically, fixed speed generators are connected directly to the grid, with a soft starter and a capacitor bank for reducing reactive power compensation [64]. When the induction generator is driven above the synchronous speed, it is said to be in generating mode. The torque of an induction generator increases linearly with speed. Both the induction generator and induction motor consume reactive power and therefore require a given quantity of reactive power to function [42].

Squirrel cage induction generators are configured with shunt capacitors as shown in Figure 3-17 below. The capacitors are used to compensate the induction generator at unity power factor [42],[43],[44]. The machine data used for modelling is given in Appendix A. This type of the wind turbine generator is connected directly to the grid and is a non-inverter based wind turbine generator.

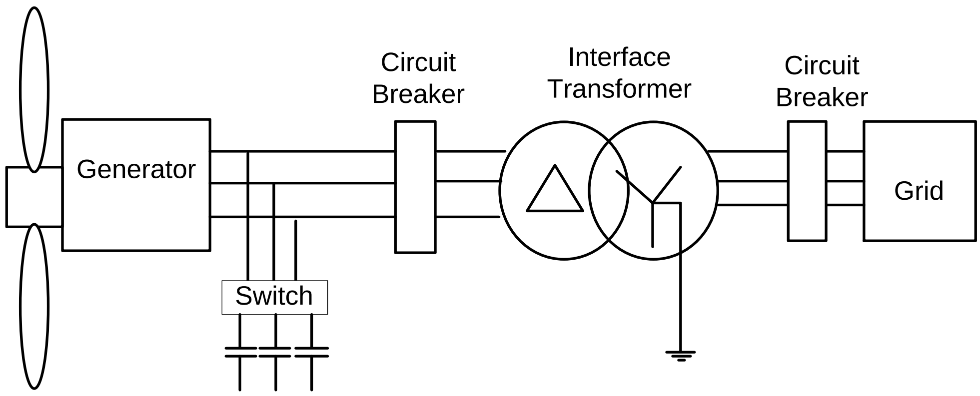

Figure 3-17: Squirrel cage induction generator

A transient fault study is simulated for 0.4 seconds and the results are provided in Figure 3-18. When a single-phase or a multi-phase fault occurs in the power system, the voltage on the affected phase(s) drops to zero at the point of fault. In the case of a fault near the generator terminals, the voltage will drop, however the inertia of the rotor will drive the generator causing the current to flow into the fault until the rotor flux decreases to zero. This is due to the fact that the rotor flux will not change instantaneously and voltage will continue to be produced thereby causing the current to flow.

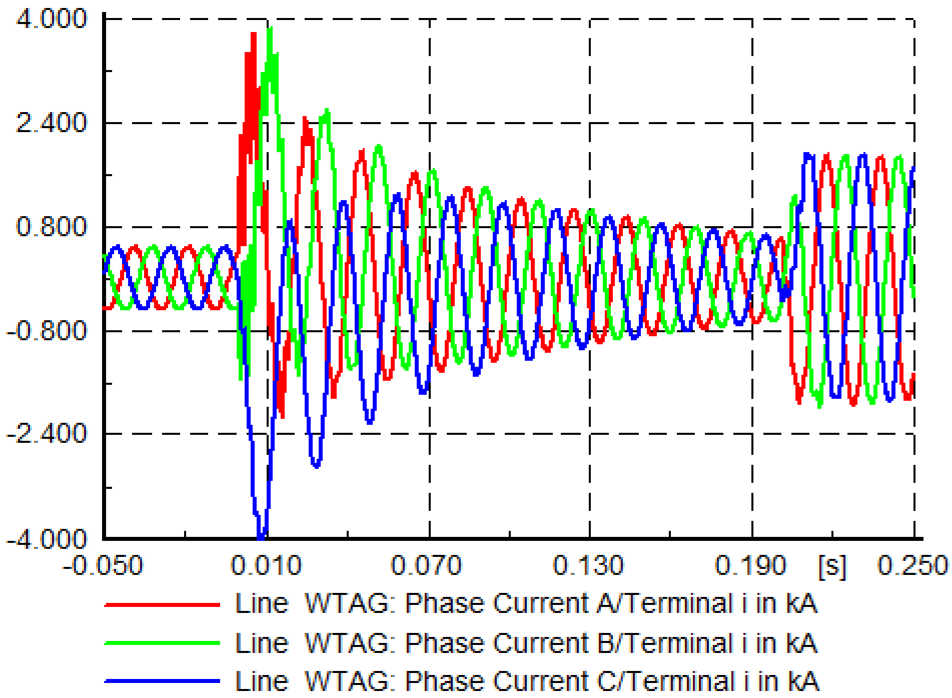

Figure 3-18: The SCIG fault current contribution during fault conditions

A three-phase fault is cleared after 0.2 seconds. During the fault, the SCIG is approximated to contribute between 4 – 6 times steady-state fault current and the contribution is significant during the first cycle. However, this high magnitude of current will last for at least one cycle [44]. The SCIG transient current is used when selecting the circuit breaker rating, because the CB should be able to withstand and break higher fault current magnitudes.

3.4.3 Wound rotor induction generator with variable rotor resistance

The wound rotor induction generators have a variable resistor connected in the rotor circuit. The switching of shunt capacitors is done on the generator terminals as in the SCIG wind turbine generator [42],[45].

As shown in Figure 3-19, when the external rotor resistance is shorted, the circuit becomes similar to that of a type I wind turbine generator. This implies that the short circuit contribution is similar to that of a SCIG. The contribution is significant and in the first cycle the fault current can be as high as 6 times the rated current. However, for a sustained fault, the fault current will decrease. The higher the external resistance the lower will be the fault current contribution from this generator [42],[45].

The circuit shown in Figure 3-19 is modelled in PowerFactory to investigate the contribution of a wound rotor with a variable resistor induction generator during power system fault conditions. A transient fault study is simulated for 0.4 seconds and the fault is cleared in 0.2 seconds. The information of the machines used in circuit below is provided in appendix A.

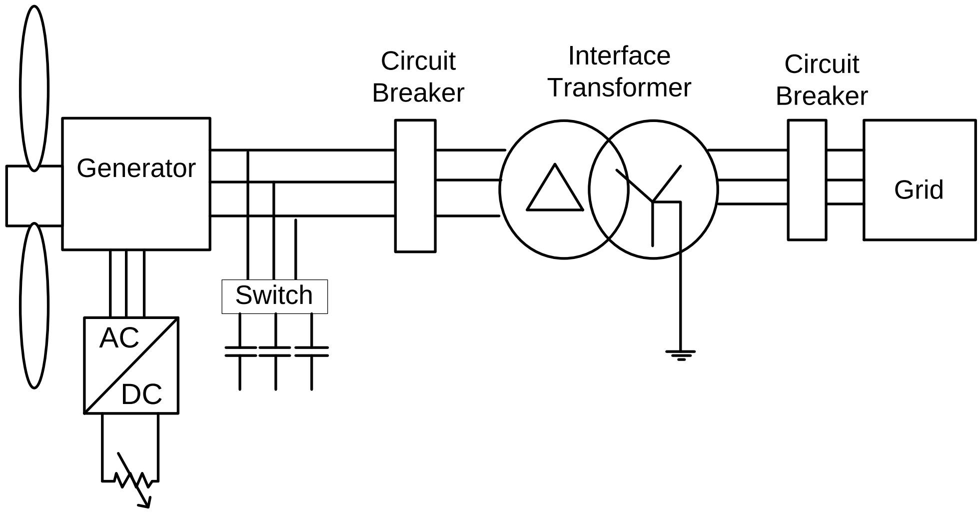

Figure 3-19: A wound rotor induction generator

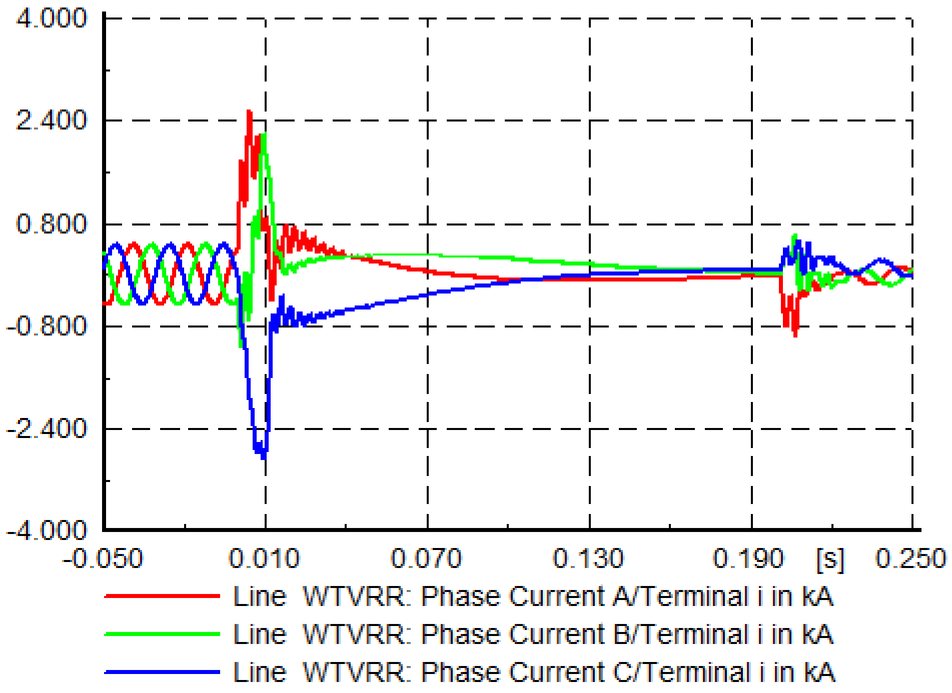

Figure 3-20: Wound rotor induction generator with variable resistor

Figure 3-20 shows the fault current contribution from the variable rotor resistance induction generator. During the first few cycles the contribution is significant, but decays faster than the SCIG generator. The problem with this type of generator is that during the first cycle, the fault current does not cross through zero axis. During this period the circuit breaker will try to clear the fault without success and this can cause the circuit breaker to explode.

3.5 Closing remarks

A general definition of a DG system is provided in the beginning of the chapter. Different DG technologies are presented in the second section of the chapter although only attention is given to solar and wind generation due to the forecasted positive growth of these two main sources of energy for the next 25 years.

In the last section of this chapter, it is shown that CSP, SCIG and wound rotor induction generator with variable resistance (non-inverter coupled) contribute significantly to the grid during the first few cycles of the fault. This is due to the fact that these machines do not use any power electronic control system, which has shown to have fast fault clearance response.

The next chapter discusses the impacts of DGs on distribution network protection. Main focus is placed on the impact of the interface transformer vector groups and grounding methods as well as how DGs impact protection when auto-reclosing and re-synchronising.

4 Impact of distributed generation on network protection

This chapter presents an overview of the impact of DG and the implications thereof on protection. These impacts are broken down into three sub-sections where the first discusses the impact of extreme fault currents. Secondly, the impact of reduced short circuit currents on protection coordination is outlined and lastly, auto-reclosing and re-synchronism are discussed. The implications of different transformer vector groups and the type of different technologies of DG used are discussed at the end of the chapter.

4.1 Introduction

The interconnection of the DG in the existing distribution network has challenges, which were not encountered before and present potential risks to the existing power system. The impact of the DG depends on its location in the network, capacity and the type of DG used. It is therefore important to locate the DG at an optimal location and know the network's hosting capacity in order to connect the DG source in such a way that it will not impact the power system negatively [6]. The location of the DG should be taken into account since it has a severe impact on protection coordination.

The previous chapter has characterized different DG sources according to different technologies used to interconnect with the utility grid and contribution during system faults. It is important for protection engineers to understand how each DG source responds to faults in the power system. In this chapter, the effects of high and reduced fault currents contributions from different DG sources are discussed in detail. With regards to the location where the DG source is connected, plays a significant role since equipment in the HV and MV systems are grounded differently and will impact protection in different ways.

4.2 Effects of high fault currents

Most generators will contribute a certain magnitude of current to the fault. The important part is to distinguish between the make-current and break-current. The transient peak current that occurs in the first cycle during a fault is used to determine the rating of most of the equipment such as switchgears, busbar and isolators. The current decays at an exponential rate to a steady state value. The current can be interrupted from 25 milliseconds onwards and may still have a significant DC offset and decaying component. The DG has a significant impact on the transient current and with time the current decays [30]. The consequence of increased make-current is that it can cause damage to equipment.

Consider the circuit in Figure 4-1 below, which shows two adjacent distribution feeders with a DG sources connected to one feeder. The diagram is used to illustrate the impact of a DG source in the existing distribution network. A distribution network connects into the grid through the interconnection transformer with a rating of S_t and impedance Z_t per unit. The DG is connected to the distribution network and has a rating of S_{gen} and impedance of Z_{gen} per unit. The length of the line from the substation to the DG is denoted by L_{line} and the impedance of the line is Z_{line} per unit [30]. In the second feeder, the length from the substation to the fault is L_{fault} and the impedance is Z_{fault} per unit [30].

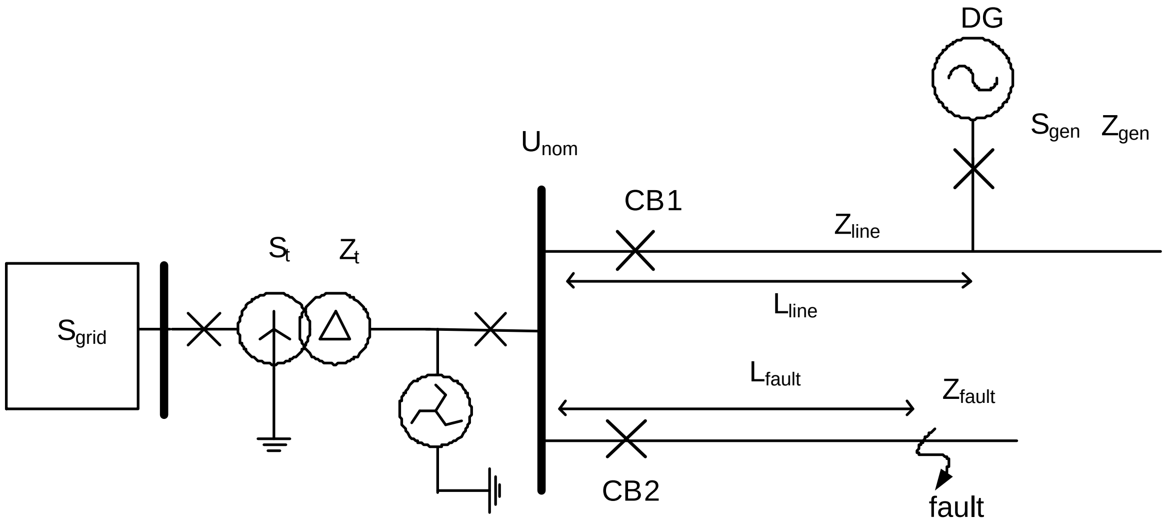

Figure 4-1: Fault current contribution from the DG

For a fault on the second feeder, the fault current flows from the main source (*grid*) to the fault. The circuit breaker (CB2) measures the sum of the fault current from the grid and the DG. This fault current is more than the maximum fault current expected from the grid due to the contribution of the DG connected [30]. Depending on the amount of the fault current contribution, the circuit breaker (CB1) can operate for the fault on the adjacent feeder and circuit breaker (CB2) can operate faster than the predicted operation time. However, the fast operation of CB2 is not a problem as it is the right circuit breaker to clear the fault. The problem arises when CB1 operates for a fault on the adjacent feeder.

With reference to Figure 4-2 below, for a three-phase fault at the fault location shown, CB1 is not expected to trip. In this case, CB4 is supposed to clear the fault and CB3 should be time delayed. Because CB1 detects the fault as a result of the DG, the fault current can be higher than CB1 settings, therefore it is time delayed and should be slower than CB3 [30].

For small DG sizes coordinating the CBs in the above network is feasible until the CB1 limits are exceeded. Once these limits are exceeded, CB1 will have to be graded with CB3 and CB2, which makes coordination more difficult. This causes CB3 to operate slower than its normal operation time, which is the same as not protecting any equipment in the network.

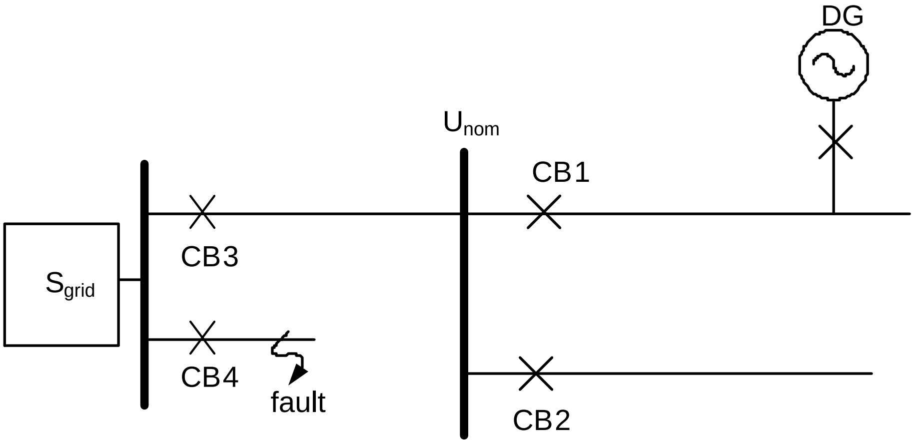

Figure 4-2: Distribution network showing an upstream fault and DG contribution

The use of directional overcurrent relays, differential relay or distance protection relays are possible solutions to this problem [30]. The following section discusses the opposite of what has been discussed in this section, which is the reduced fault current where DG is contributing low fault currents or where there is no contribution at all.

4.3 Effects of reduced fault currents

The preceding sections discussed the contribution of DGs to the fault. The contribution is significant in synchronous and induction generators. The opposite occurs when DG is connected through an electronic inverter interface as shown in Chapter 3.

When an electronic inverter is utilized the contribution is so small that it is possible for an overcurrent protection relay not to detect the fault, especially in a network where fault currents are too small [30]. Typical examples of this type of DGs are photovoltaic (PVs), wound rotor induction generator with variable resistor (with control system), DFIG and fully-rated converter wind turbine generators.

A problem, which could be encountered when DG is connected to the network, is when the fault is downstream as shown in Figure 4-3. When the fault occurs downstream and the fault current from the grid is too small, the relay controlling CB1 will not be able to detect the fault current at the end of the line [30]. However, as long as the minimum fault current is higher than the maximum load current this becomes less challenging [30].

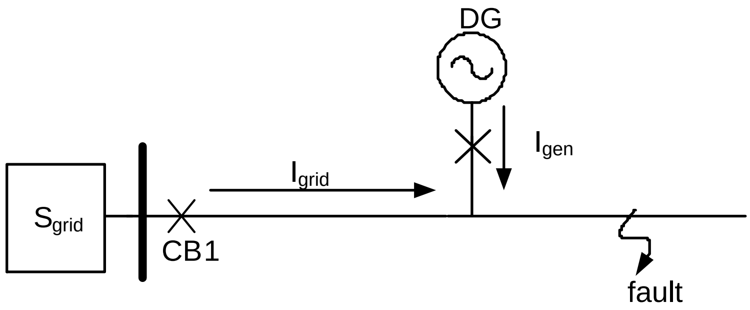

Figure 4-3: A downstream fault in the distribution feeder

In Figure 4-3 DG feeds to the fault and has the potential to operate faster than the protection at CB 1. When DG's overcurrent protection clears the fault the generator will go into an uncontrolled island operation [30].

Secondly, when the relay controlling CB1 auto-recloses, the circuit breaker CB1 will close onto a system with an unknown frequency, voltage and phase angles. This presents the risk of damage to the DG generator and other equipment on the power system due to lack of synchronism [30]. During this period, depending on the power system earthing method, the fault may remain in the system and cause the voltage on the unfaulted phases to rise up to 1.73 times the nominal phase voltage ($V_{pp} = \sqrt{3}V_{pn}$). The frequency depends on the generator. However, it will deviate from the system nominal frequency. This can cause the voltage over the circuit breaker to rise up to 2.7 times of the system nominal voltage [30]. Auto-reclosing and re-synchronizing are discussed in detail in the next section.

4.4 Auto-reclosing and re-synchronization

An automatic recloser is a self-controlled device, which automatically re-closes after opening for a fault. An auto-recloser has its own control system and is not controlled by any relay like the circuit breakers [19]. The purpose of using the auto-recloser devices in the distribution network is to minimize long interruptions when faults are transient. Secondly, auto-recloser devices allow for fast clearance of the fault and quick reclose of the circuit breaker (between 3 seconds and 5 seconds) in order to restore the network to normal conditions. The reason for auto-reclosing after the first 5 seconds is that the fault would have cleared when the air insulation has self-restored, if not, then the auto-recloser opens and recloses again after at least 10 seconds. Essentially, this improves the system availability by ensuring that the power system is restored quickly after a transient fault [21].

When an auto-recloser device closes on a permanent fault it will attempt to clear the fault by isolating the fault arc. The second reclosing interval is delayed longer than the first reclosing interval (i.e.

second reclosing interval) in Figure 4-4. The auto-recloser will attempt to close again and if the fault is permanent, the device will open and lock-out [22]. The advantage of reclosing is to reduce the outage time due to manual intervention. Figure 4-4 shows the reclosing cycle of an auto-recloser for a permanent fault in the distribution network.

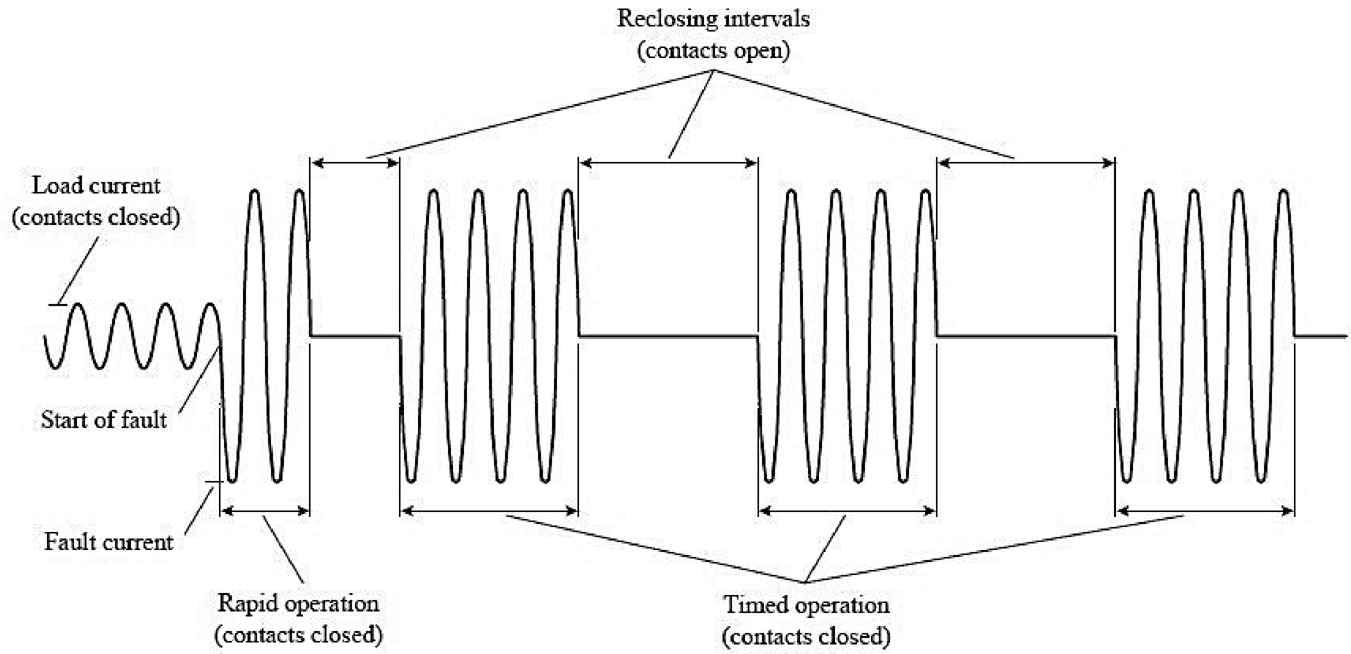

Figure 4-4: Reclosure shots for permanent fault [22]

The time-current characteristic curves usually have three curves incorporated in the reclosure operation. The first attempt is normally fast and then the last two attempts are delayed. Therefore, the downstream device should be coordinated accordingly in order to ensure that the affected part of the network is isolated. When the fast curves are selected for the first attempt zone sequence coordination (ZSC) should be set to active in the downstream recloser device [22].

Single-phase-to-ground faults are less severe compared to three-phase faults, therefore it is always required that the device be sensitive enough to detect low fault currents in the neutral path. Detection of these fault currents is done by connecting the CTs residually. By Kirchhoff's current law, under balanced network conditions the vector sum of phase currents at the node should be zero. During an unbalanced network condition, the vector sum of currents in all three-phases is non-zero. Therefore, the residual current flows through the neutral and the earth fault element will pick-up the unbalance [22].

In the distribution network, most of the faults are transient. According to the IEEE 1547 standard, practically 70% to 95% of the system faults are temporary in nature. This makes the application of auto-reclosing effective when clearing temporary faults resulting from lightning and tree contacts. By de-energizing the power system facility for a short time, the arc will be extinguished and in the case of a temporary fault, the fault would have been cleared from the system after first reclosing cycle [31],[32].

When DG is connected to the distribution network the generator will continue operating during an auto-reclosing open time, sustaining the voltage and feeding the fault current. This prevents extinguishing of the arc of the fault and will result in an unsuccessful auto-reclosing operation. Eventually, a transient fault becomes permanent and the interruption to customers longer than expected. Secondly, the islanded feeder is most likely to be out of synchronism with the power system. In the case where the distribution system breaker recloses and the island, which is energized by the DG, is out of phase severe damage to the system equipment may result [31].

Listed below are the consequences of out-of-phase reclosing [32]:

a) The DG energizing the island may be subjected to severe electromechanical torques, which will cause severe damage to the generator [32].
b) Transient over-voltage will be experienced on the feeder, which is likely to be three times more than the nominal voltage. This situation will result in failure of the power system's surge protection and damage to customers' equipment [32].
c) Transformers and motors connected to the feeder will experience high inrush currents upon closing out of phase. This could result in undesired operation of instantaneous protection or current differential protection and other reclosers in the system [32].

From the South African grid code, all DGs are required to withstand the voltage drop up to zero, measured at the point of common coupling (PCC) for at least 150 milliseconds. This implies that during fault conditions, all DGs are required to remain connected to the grid. However, during the first cycle of the fault condition the fault may be more than what is fed after a few cycles [33]. Therefore, it is important to coordinate the DG tripping, the feeder and auto-reclosing cycles to ensure no out of phase reclosing occurs. It is stated in the IEEE1547 standard that the DG shall cease to energize the power system to which it is connected to before the power system recloses. This requirement is intended to prevent an out of synchronism condition during the power system auto-reclose action [68].

In Germany, DG unit is set shorter than the reclosure time and the independent power producers (DG owners) are required to ensure that their DG units will not be damaged by the auto-reclosure action [68]. In Spain, the DG unit will disconnect and can be reconnected to the grid if the voltage at the PCC is greater than 0.85 pu[3] and $t > 3$ minutes [68].

Distributed generation connects to the grid via an interface transformer. The selection of the interface transformer plays a significant role in the operation of the distribution system neutral grounding and the operation of the protection system. The IEEE standard 142 and SANS 10200 provide engineers with information regarding proper selection and application of different available grounding methods. The next section provides information on how the selection of the interface transformer can affect the distribution system earthing and protection.

4.5 The implications of DGs on the distribution system grounding

Power systems were initially operated unearthed with the assumption that system interruptions due to single-phase-to-ground faults would be low. However, the so-called unearthed systems are capacitive grounded and the system is susceptible to transient overvoltages, which could result in damaged insulation [34]. Therefore, the practice of earthing the power system became the solution to ensure that the following are taken care of:

a) control the voltage within predictable limits,
b) limit transient overvoltages,
c) provide a path for the zero sequence currents and detection of unwanted current flowing through the neutral [34].

Three different grounding methods are compared and discussed in detail. Eskom has adopted these methods in their network following the effects of ungrounded systems encountered in the past. The neutral earthing requirement at the PCC is provided at the end of this section.

4.5.1 Ungrounded system

The system is said to be ungrounded when there is no connection between system conductors and ground. However, there is always a capacitive coupling between one phase and another. There is a capacitive coupling between the phases and ground. The effect of the capacitance between the phases on the system earthing characteristics is insignificant, hence it is often not considered. The distributed capacitive reactance between the phases and ground (X_{CO}) is assumed to be balanced. This type of grounding method is also called capacitive grounding due to the capacitive reactance, which exists between the phase conductors and ground [34],[35].

[3] *pu* refers to per unit

Under balanced network conditions, the phase-to-neutral voltages are equal in magnitude and displaced by 120˚ from each other. The vector sum of the capacitive currents flowing in the neutral is zero and the neutral of the distributed capacitance is at earth potential. Therefore, the neutral of the protected equipment is also at earth potential [34]. During a single-phase-to-ground fault, there is no current flowing through the faulted phase capacitance-to-ground, because there is no potential difference across that capacitance in the faulted phase. The current flowing in the other two unfaulted phases is the $\sqrt{3}$ times the charging capacitance current (I_{CO}). Therefore, the phase-to-neutral voltages in the unfaulted phases will increase to line-to-line voltages [34],[35].

The disadvantages of this grounding characteristic are twofold. Firstly, transient overvoltages may occur throughout the system during restriking ground faults. Secondly, the consequences of system overvoltages may result in a resonant condition, which can be established between the inductive reactance of the system and distributed capacitance-to-ground. To overcome the consequence of transient overvoltages in the network, it is recommended that the system be grounded either solidly or through impedance [34]. The next sections discuss the two grounding characteristics recommended to reduce transient overvoltages.

4.5.2 Solidly grounded system

A solidly grounded system refers to a system where the neutral of the transformer is connected solidly to ground as shown in Figure 4-5 below. For solidly grounded system the healthy phase voltage will remain at phase value [34].

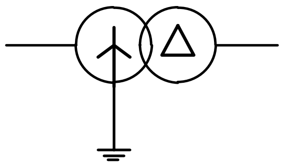

Figure 4-5: Solidly grounded system

A solidly grounded system can be referred to as an effectively grounded system, since an effectively grounded system is grounded through a low ohmic resistance. In an effectively grounded system, during a single-phase-to-ground fault the phase-to-ground voltage on the healthy phases will not exceed 1.4 pu (i.e. *80% of* V_l *= 1.385 pu*) of the line-to-line voltage.

For an effectively grounded system, the ratio of the equivalent zero sequence system reactance to the positive sequence reactance is not greater than 3 and the ratio of the zero-sequence system resistance to positive sequence system reactance is not greater than 1 as shown in equations (4.1) and (4.2) below [34].

$$\frac{X_0}{X_1} \leq 3 \tag{4.1}$$

$$\frac{R_0}{X_1} \leq 1 \tag{4.2}$$

where

X_0	equivalent zero sequence system reactance
R_0	equivalent zero sequence system resistance
X_1	equivalent positive sequence system reactance

The advantages of a solidly grounded system are twofold. Firstly, the system voltages are controlled within the predictable limits. Secondly, the risk of damaging the insulation due to transient overvoltages is minimized. Most of the neutral winding in the HV network are fully graded and some are partially graded, however it is recommended that the neutral be solidly grounded [34].

4.5.3 Impedance grounded system

Impedance grounded systems refer to the neutral of the transformer grounded through a resistor or inductor as shown in Figure 4-6. The values of the resistance used in the resistance grounding characteristic range between 10 Ω to 60 Ω. The function of the resistance is to prevent system resonance [34],[36].

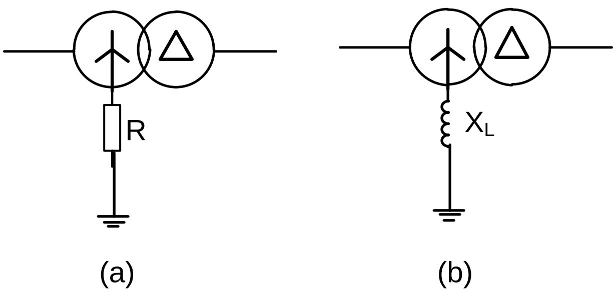

Figure 4-6: Impedance grounding systems

A system is said to be resistively earthed if the following conditions below are met: the ratio of the equivalent zero sequence system reactance to the positive sequence reactance is greater than 1 and the ratio of the zero-sequence system resistance to positive sequence system reactance is greater or equal to 2 [34].

$$\frac{X_0}{X_1} > 1 \tag{4.3}$$

$$\frac{R_0}{X_1} \geq 2 \tag{4.4}$$

There are at least three different grounding systems, which are classified under impedance grounding system, namely: high-resistance, low-resistance and reactance grounding systems. Details on these impedance grounding systems are discussed in the following sections.

4.5.3.1 High-resistance grounded system

A high-resistance grounded system is used where line-to-ground fault current should not exceed a minimum of 10 A to avoid the damage which can be caused by the arcing current in a confined space [34].

As the name implies, the high-resistance grounded system employs a resistor with high ohmic value. The high-resistance system is designed to limit the current to magnitude equal to or greater than the charging current ($3I_{c0}$) [34]. Therefore,

$$R \leq \frac{V_{pn}}{3I_{c0}} \tag{4.5}$$

Where,

R neutral resistor

V_{pn} system phase-to-neutral voltage

I_{c0} charging current

Under normal conditions, the neutral point of the protected equipment such as a transformer is at zero potential. During a single-phase-to-ground fault, the neutral point is raised to the phase-to-neutral voltage. To detect this voltage rise, an overvoltage relay is used as shown in Figure 4-7. A step-down transformer is used to reduce the phase-to-neutral voltages to a small and safe voltage acceptable by the overvoltage relay [34].

Due to low ground faults as a result of high ohmic resistor values used in the high-resistance grounded system, the ground faults are inherently low and therefore, the high-resistance system does not require an immediate clearing of ground faults. The protection used in this grounding system is overvoltage protection, which detects and issues an alarm and not immediate trip out as in low-resistance grounded systems [34].

The advantages of high-resistance grounded system are provided below [34]:

a) The continuity of supply is maintained.
b) Transient overvoltages due to intermittent ground faults are reduced.
c) No ground faults relay coordination needed.

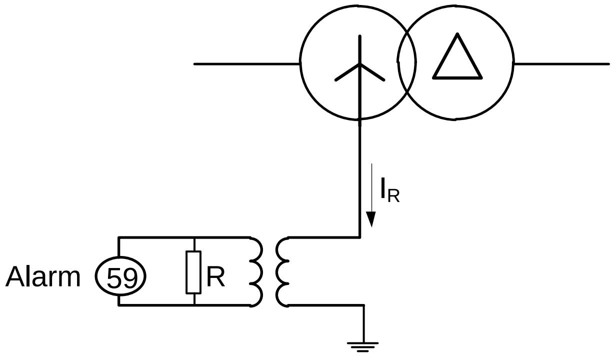

Figure 4-7: Schematic diagram showing the high-resistance detection method

4.5.3.2 Low-resistance grounded system

A low-resistance grounded system is mainly used in medium voltage systems of 11 kV and below. In a low-resistance grounded system, the objective is to limit the single-phase-to-ground fault currents to a range of 100 A to 1000 A, with 360 A being typical [34]. The value of the neutral resistor, *R,* shown in Figure 4-8 (a) is calculated using the system phase-to-neutral voltage and the desired single-phase-to-ground fault current. In the calculation below, the system source impedance and charging current are not taken into account, since they will have an insignificant impact [34]. Therefore,

$$R = \frac{V_{pn}}{I_g} \tag{4-6}$$

where,

R neutral resistor

V_{pn} system phase-to-neutral voltage

I_g desired single-phase-to-ground fault current

The advantage of low-resistance grounding system is the ability to detect both immediate and selective single-phase-to-ground faults. The most commonly used method to detect single-phase-to-ground faults is shown in Figure 4-8. A CT connected in series with the neutral resistor and the secondary windings of the CT are connected to the overcurrent relay, 51G [34].

During a single-phase-to-ground fault, the neutral potential will rise to the line-to-neutral voltage causing the fault current to flow through the neutral resistor. The fault current should be high enough to actuate the overcurrent relay to isolate the fault. Typical clearing fault time is between 10 seconds and 30 seconds, depending on the degree of security and application [34].

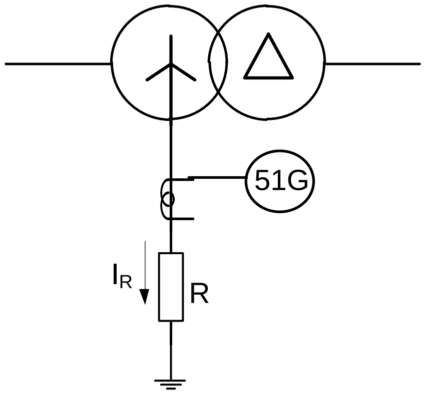

Figure 4-8: Schematic diagram showing the low-resistance detection method

4.5.3.3 Reactance grounded system

The reactance grounding method was employed by Eskom in the past on the delta connected MV networks feeding industrial, mining and rural areas at 33 kV and below. In the reactance grounding method the following criteria should be met [34],[35]:

$$\frac{X_0}{X_1} \leq 10 \tag{4.7}$$

In reactance grounded systems, the single-phase-to-ground fault currents are desired to be in the range of 25% ($X_0 = 10X_1$) and 60% ($X_0 = 3X_1$) of the three-phase fault current magnitudes. However, due to the higher magnitude of the zero-sequence reactance compared to the zero-sequence reactance in the resistively grounded system, the application of the reactance grounding characteristic is not an alternative to the resistive grounded characteristics. The equivalent zero sequence reactance in the reactance grounded system includes the zero-sequence grounding reactance ($3X_n$) and the zero-sequence reactance of the source X_0 [34].

The reactance grounded characteristic is used in less expensive applications and where there is a desire for single-phase-to-ground faults to be in the range of 1000 A or more [34]. In this method, the use of an NEC is not recommended as it can result in resonant and overvoltages, which could damage the healthy phases. The next section investigates the impact of the selection of the interface transformer on protection. Different vector groups and their benefits and drawbacks are discussed.

4.6 Implications of the DG interface transformer connection

The selection of the interconnection transformer has a major impact on how DG and the power system behave during abnormal conditions. There is no ideal connection, but care should be taken when selecting the interface transformer vector groups. This is to ensure that during a single-phase-to-ground fault there will be no zero-sequence current contribution from the DG interface transformer [34].

In South Africa, it is common practice to ground the neutral of the transformers solidly in order to limit the magnitude of the phase-to-neutral voltages to predictable limits during single-phase-to-ground faults. The other reason of implementing a solid grounded system in the HV and EHV network is to save on the cost of insulation due to transient overvoltages [35]. In Europe, the MV grid is grounded through the connections of the substation transformer or grounding transformer. The neutral point of the windings of the distribution system transformer can be solidly grounded or connected to ground through a current limiting device such as a resistor or reactor [67]. In the US, it is common practice to either connect the neutral conductor of the MV grid to earth several times (multi-grounded) or connect to earth at the source (unigrounded). The MV grid of the US is a four-wire system, which is typically an LV network in South Africa and Europe [68].

In the MV network, the emphasis is placed on reducing the magnitude of the single-phase-to-ground faults largely in order to ensure the safety of personnel and the plant rather than to ensure savings on the cost of insulation. This is achieved by using a neutral earthing resistor (NER) on the star connected transformer or using a combination of a neutral earthing compensator with a resistor (NEC/R) on the delta connection of the transformer [35].

Table 4-1 provides different transformer connections with their phase displacements. From table 4-1 the most commonly used transformer vector groups in the distribution network are group 3 and group 4. The groups are divided based on the phase shift between the primary and the secondary windings of the transformer.

Table 4-1: Transformer vector groups and phase shifts

Group	Phase shift	Transformer connections
1	Zero	Yny0, Dz0, Dd0
2	180˚	Yny6, Dz6, Dd6
3	30˚ lead	Ynd11, Dyn11, Yz11
4	30˚ lag	Ynd1, Dyn1, Yz1

where,

Y Transformer star connection

n Transformer neutral connection

D Transformer delta connection

z Transformer zigzag connection

In the next section the four different types of transformer connection, their benefits and drawbacks are discussed.

4.6.1 DG connected in the HV network

When the distributed generation is connected and operating in parallel in the distribution network, the grounding method on both sides should be matched. Otherwise the operation of the network is perturbed. Figure 4-9 below shows the DG connected on the HV side of the distribution network with the star point low resistance grounded and connected to the grid side.

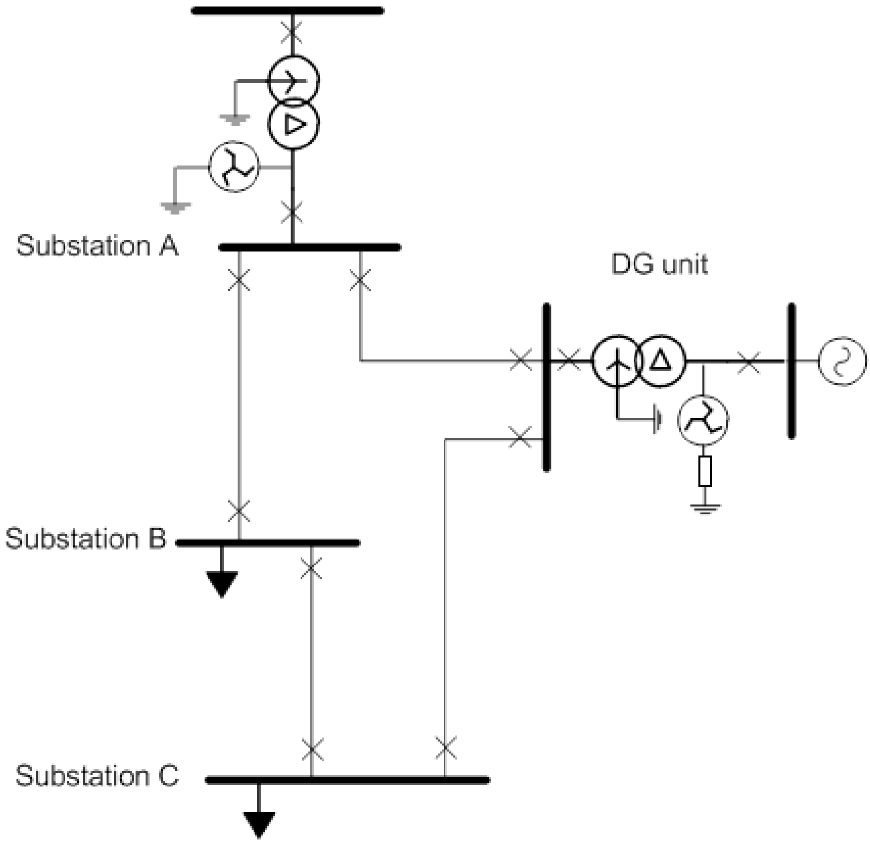

Figure 4-9: DG unit connected in the HV network

There are four types of interconnection transformer, which can be selected when connecting the DG in the distribution network. Different types of interconnection transformers are discussed in detail below.

4.6.1.1 Grounded Star (grid)/ Delta (DG) interconnection transformer

This section investigates the earth-fault protection on the feeder protection system for faults on either the DG or the feeder side. The first type of interconnection transformer considered is the star/delta connection, which is connected to the HV network of the distribution system as shown in Figure 4-9 above. The grounded star/delta interconnection transformer provides a zero-sequence path for a single-phase-to-ground fault in the interconnected network. There is a zero-sequence current contribution to the distribution system for faults on both the distribution system and DG side [37].

For a single-phase-to-ground fault on the distribution feeder from the network shown in Figure 4-9, the zero-sequence fault current is only flowing through the interface transformer high voltage side (i.e. utility side) and is not transformed into the low voltage side (i.e. the DG unit side). When a single-phase-to-ground fault occurs in the adjacent feeder, the interconnection transformer contributes a zero-sequence current, which may cause the protection on the other feeder to operate for fault in the adjacent feeder.

Table 4-2 below gives a summary of advantages and disadvantages of a star/delta interconnection transformer.

Table 4-2: Advantages and disadvantages of a star/delta transformer [36],[38]

Advantages	Disadvantages
For a fault at the DG side the zero-sequence current only flows through the generator and will not back-feed into the distribution system. Thus, an earth fault protection relay at the distribution substation will not detect a fault on the generator (DG) side.	Faults on the grid side are detected by the DG protection system because the transformer contributes to both the single-phase-to-ground and three-phase faults in the distribution network.
The tripled harmonics produced by the generator are blocked by the delta winding and therefore, cannot flow into the distribution system.	If proper coordination is not well applied, the possibility of one feeder operating for a fault on an adjacent feeder is high due to the contribution from the interconnection transformer.
During single-phase-to-ground faults on the distribution feeder, transient overvoltage on the unfaulted phases will not occur. Therefore, there is minimal damage to the insulation.	Tripled harmonics already in the system will tend to flow into the interconnection transformer, which will contribute to overheating of the transformer.

The sequence network diagram for the star/delta interconnection system is given in Figure 4-10 below.

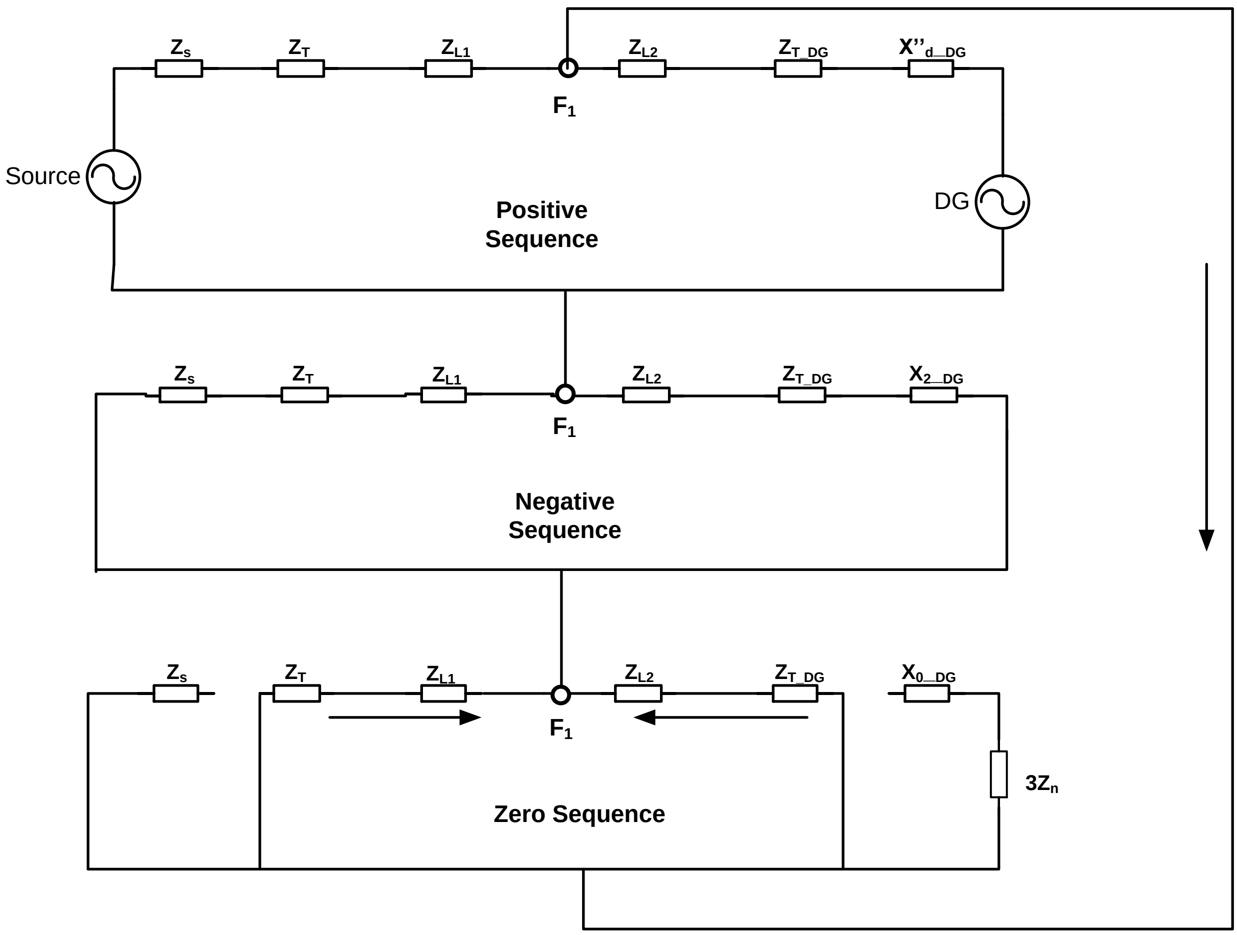

Figure 4-10: A star/delta interconnection transformer sequence network diagram

In the diagram Z_{T_DG} represents the impedance of the interconnection transformer, Z_T represents the impedance of the utility transformer, and Z_L represents the feeder impedance to the fault. The source impedance Z_s represents the equivalent source impedance of the network. The reactance of the generator of the distributed generation is represented by $X_d^{''}$ for positive sequence network, and X_{2_DG} and X_{0_DG} X_{0_DG} for negative and zero sequence networks, respectively.

4.6.1.2 Grounded Star (grid)/Star (DG) interconnection transformer

The second connection is a star/star interconnection transformer. This connection is most common in North America for three-phase loads. This connection is favoured because of its reduced susceptibility to ferro-resonance on the cable networks. Generally, it is well behaved in the application of DGs [36],[38].

In this case, the distribution system provides the zero-sequence fault current path during a single-phase fault. For a single-phase-to-ground fault on the DG side the fault is distributed. Most of the current flows in the least resistive path while less currents flow into the high resistive path.

For a single-phase-to-ground fault on the distribution feeder (i.e. utility side) the zero-sequence current is detected by the distribution feeder protection system. Thus, the feeder E/F protection is affected and problems with coordination can arise [37]. The relay at the substation (CB1) has to be well coordinated in order to avoid an undesired operation.

When the star/star connection is grounded on both sides, the zero-sequence current will be transformed by the interface transformer for a single-phase-to-ground fault either on the DG side or the utility side. However, for a star/star with only one side earthed, the single-phase fault current on the DG side is not detected by the feeder E/F protection in the utility side. Similarly, for a single-phase-to-ground fault on either feeder 1 or feeder 2 (i.e. utility side) the protection on the DG side will not detect the single-phase-to-ground fault.

The following Table 4-3 below gives a summary of the advantages and disadvantages of a star/star interconnection transformer.

Table 4-3: Advantages and disadvantages of a star/star transformer [36],[38]

Advantages	Disadvantages
Less concern for ferro-resonance.	Zero sequence harmonic currents are transformed (*i.e. 3rd harmonic currents*).
There is no phase-shift in system voltages. Can detect the faults on the primary side with low-voltage relays.	Faults on the utility side are detected by the DG protection unit. The DG system will contribute to the fault on the distribution system.
Provides an effective grounding system.	Triple voltage may be high in shell types units.
	This connection does not provide an effectively grounded source when islanded.

The sequence network diagrams are given in Figure 4-11. The Z_{T_DG} represents the impedance of the interface transformer, Z_T represents the impedance of the utility transformer, Z_L represents the feeder impedance to the fault. The source impedance Z_s represents the equivalent source impedance of the network. The reactance of the generator of the distributed generation is represented by $X_d^{''}$ for positive sequence network, and X_{2_DG} and X_{0_DG} for negative and zero sequence networks. The neutral earthing impedance of the generator is shown by the Z_n in the diagram.

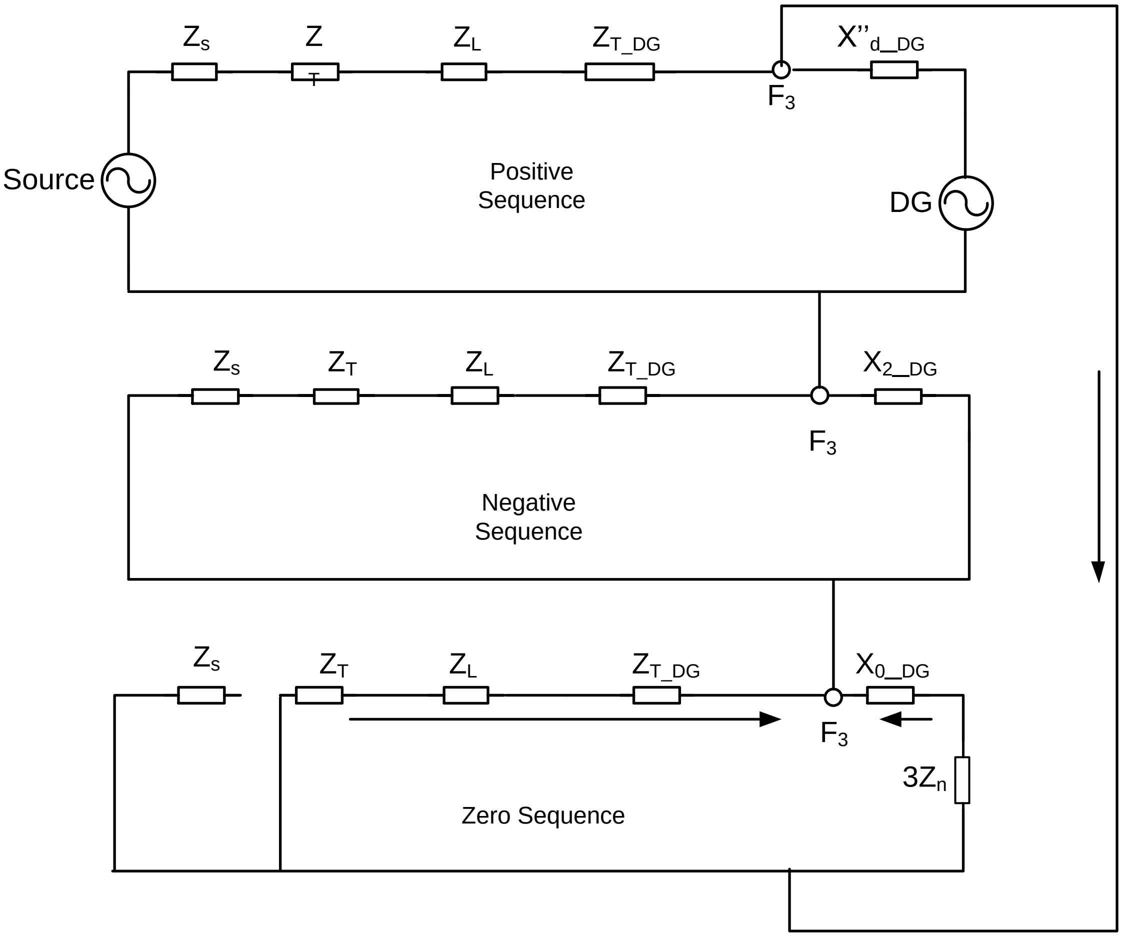

Figure 4-11: Star/Star interconnection transformer sequence network diagram

4.6.2 DG connected in the MV network

The distribution network is generally connected to ground through the connections of the distribution substation transformer. This is common practice in South Africa and Europe. The neutral of the transformer on the HV side is left ungrounded since the source transformers are solidly grounded. Therefore, the neutral earthing compensator is used with a resistor to provide a path for the zero sequence currents. When the DG is connected to the MV network it is a requirement that the grounding on both sides be matched. Thus, the interconnection transformer used in this interconnection system is the delta/star transformer [35].

In this section the two possible interconnection transformers, i.e. delta/star and delta/delta are investigated. The network in Figure 4-12 shows the distribution network with interconnected DG on the MV side. The DG is connected directly to the MV feeder via a delta (grid) /star transformer.

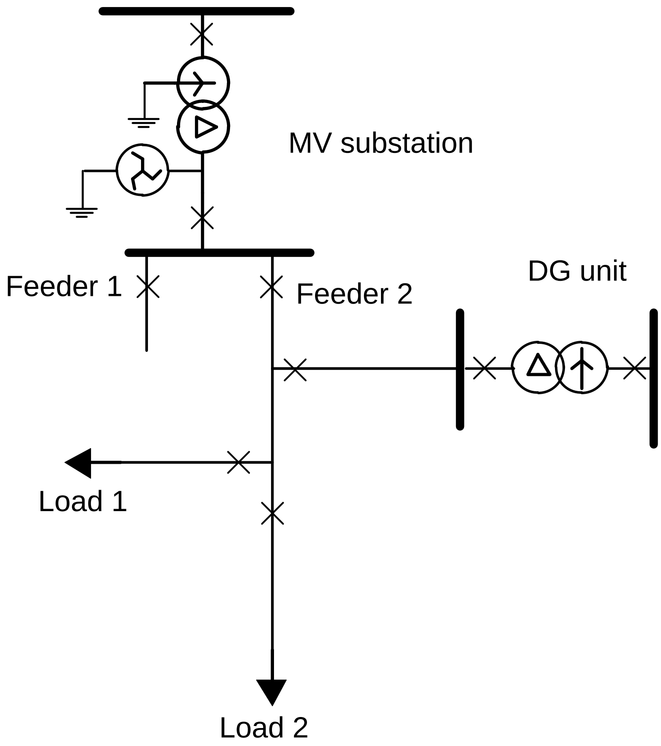

Figure 4-12: DG unit connected in the MV network

4.6.2.1 Delta (grid) / Delta (DG) interconnection transformer connection

In this case a delta/delta transformer winding connection is investigated. Consider a single-phase-to-ground fault on the distribution feeder 1. With this type of connection, the only source of zero sequence current is the distribution substation transformer. There is no path for the zero-sequence current. Therefore, there will be circulating current in the delta winding.

The advantage of this connection is that for a fault on the feeder, the zero-sequence current is flowing through the NEC/R and the feeder. There is no zero-sequence current transformed by the interface transformer [37]. Therefore, the DG will not detect this fault current.

For a single-phase-to-ground fault on the generator side (DG), zero sequence fault current will be flowing back to the DG generator’s neutral and the transformer. No current will be transformed into the high voltage side of the DG (i.e. utility side). Thus, the feeder earth-fault protection will not detect and operate for faults on the DG side.

The disadvantages of the selected winding connection are that for a three-phase fault there will be two sources of fault current and coordination problems may arise. For a single-phase-to-ground fault the voltages on the other two phases can rise beyond predictable limits.

The following Table 4-4 below gives a summary of the advantages and disadvantages of the delta/delta interconnection transformer.

Table 4-4: Advantages and disadvantages of a delta/delta transformer [36],[38]

Advantages	Disadvantages
Third harmonic currents are isolated.	There is no neutral point, therefore the phase-to-neutral voltages may rise beyond to line-to-line voltage.
Does not feed directly to the grid during single-phase-to-ground faults on the DG side.	Susceptible to ferro-resonance in a MV cable network. The effect is more pronounced during an open conductor fault.
Provides some isolation between the DG and utility systems from voltage sags during single-phase-to-ground faults. Therefore, the DG is allowed to ride through voltage sags.	Depending on the neutral grounding of the generator, the excessive third harmonic in the DG may cause damage to the generator neutral.
	During islanded operation, this connection does not provide an effectively grounded system. Therefore, overvoltages may result on the unfaulted phases.

4.6.2.2 Delta (grid) / grounded star (DG) interconnection transformer

This type of transformer is similar to the delta/delta connection transformer discussed above. It is not common practice to use a delta/star (ungrounded) transformer as there will be circulating current in the transformer due to the absence of a path for zero sequence currents.

4.7 Summary of impact of distributed generation on protection

The addition of DGs to the distribution network increases the risks of protection failures in the network. Listed below are a summary of potential failures due to DGs given in no order of priority:

a) The fault current contribution of the DG in the distribution network increases the power system current, which results in high fault currents. These high fault currents can exceed the rating of some equipment in the power system. Different generators will contribute to the fault differently. The synchronous generator increases both *make-current* and *break-current* respectively. An induction generator only increases the *break-current.* Generators with a power electronics interface have no contribution to either make-current or break-current due to their fast control systems [47].

b) In some cases, the fault current measured at the local substation can be reduced especially during a fault downstream. This situation occurs even under normal conditions, where for long lines, fault currents tend to decrease drastically. This results in relays not being able to detect the fault and failing to operate for such a fault, because it is below the relay current threshold setting. When there are no DGs connected, the fault can remain in the network for longer period [30].

c) When the DG is connected at the adjacent feeder and the fault occurs in the feeder where DG is not connected, the possibility of the overcurrent protection on the adjacent feeder to operate for faults on the other feeder due to the contribution of the DG is high. When DG is connected through a delta/star transformer with the neutral grounded, this creates a low impedance path for zero sequence current during a single-phase-to-ground fault. The probability of losing selectivity increases and may cause the feeder breaker to operate incorrectly [30].

d) Ferro-resonance is the phenomenon which may be experienced when DG is connected in the power system. This is likely to occur in the case where the feeder in which the DG is connected has been isolated from the power system. The occurrence of ferro-resonance in the network results in extreme overvoltages [37]. Single-phase reclosing can also result in ferro-resonance conditions with DG. It is therefore important to avoid using single-pole tripping when DG is connected [30].

4.8 Concluding remarks

This chapter has discussed impacts of DGs on network protection. In the first and second sections of this chapter the effects of excessive and reduced fault current from DGs are discussed and how each affects the utility network protection. The impact of excessive fault current from DGs is more pronounced when a DG is connected to a radial MV feeder of the distribution system. This is because in the MV network, non-directional relays are used as opposed to the sub-transmission network of the distribution system.

Different interface transformer vector groups were discussed together with each configuration’s advantages as well as disadvantages. It was shown that any vector group with a delta connection is better, since the zero sequence currents will not be transferred to the utility side for a fault on the DG side and vice versa.

5 Introduction and application of optimization algorithms

This chapter gives an introduction to optimization and classification of optimization problems. The second part of the chapter provides an overview of artificial intelligence optimization algorithms, makes a comparison between particle swarm optimization and genetic algorithms.

5.1 Introduction to optimization

An optimization problem is defined by various sets of equations, which are themselves defined by the design vector, design constraints, the objective function and the objective function surface. The general constraint optimization problems are formulated as follows [15],[48]:

Find

$$\bar{x} = [x_1, x_2, \dots x_n]^T \tag{5.1}$$

which minimizes the function $f(\bar{x})$

subject to

$$g_i(\bar{x}) \geq 0 \qquad i = 1, 2, \dots, m \tag{5.2}$$

$$h_j(\bar{x}) = 0 \qquad j = 1, 2, \dots, p \tag{5.3}$$

where,

$\bar{x}$ - design vector

$g_i(\bar{x})$ - inequality design constraint

$h_j(\bar{x})$ - equality design constraint

$f(\bar{x})$ - objective function to be minimized

The directional overcurrent relay coordination problem is a highly constrained optimization problem because of the many relay constraints considered [48]. The unconstrained optimization problem differs with constrained optimization in that the variables used in the design vector are not subjected to any constraints. Their values can be selected arbitrarily.

5.2 Optimization problem classification

The relationship which exists between the objective function and the design constraints determines the type of optimization problem, the level of difficulty encountered in solving it and the method to be used to solve the problem. It is important to check and verify the following key issues as a guideline to identifying the correct optimization method.

a) Is the optimization problem convex or non-convex?
b) Is the optimization problem continuous or discrete?
c) Is the optimization problem constrained or unconstrained?
d) Does the optimization problem have single or multiple objective functions?

There are various methods used to solve the directional overcurrent relay coordination problem. However, identifying the correct method requires knowledge of the nature of the design constraints, type of the function and the relationship between the objective function and the design variables. A brief discussion on the types of optimization problems follows.

5.2.1 Convex optimization problems

A function is said to be convex if the line segment joining the two points lies above or on the graph of $f(\bar{x})$ [48],[49]. With convex optimization problems, it becomes easier to determine if there is a feasible solution for the problem, determine the global optimal solution, and solve the problem up to a larger size. In general, all linear optimization problems are convex and some nonlinear optimization problems are convex [15].

The directional overcurrent relay coordination problem is a non-linear, mixed integer and non-convex problem, which is highly constrained [15]. Below is a proof which shows whether the directional overcurrent relay coordination problem is convex or non-convex.

A convex optimization problem is formulated as follows [49]:

$$\text{Minimize } f_0(\bar{x})$$

$$\text{subjected to} \qquad f_i(\bar{x}) \leq b_i \qquad i = 1,2, \ldots m \tag{5.4}$$

where functions $f_0, \ldots, f_m : R^n \rightarrow R$ are convex and should satisfy the following conditions:

$$f_i(\alpha x_1 + \beta x_2) \leq \alpha f_i(x_1) + \beta f_i(x_2) \tag{5.5}$$

where

$$\alpha + \beta = 1 \qquad \alpha \geq 0, \beta \geq 0 \tag{5.6}$$

The following graph shows a convex function. The line segment joining the two points x_1 and x_2 lie above the graph [48].

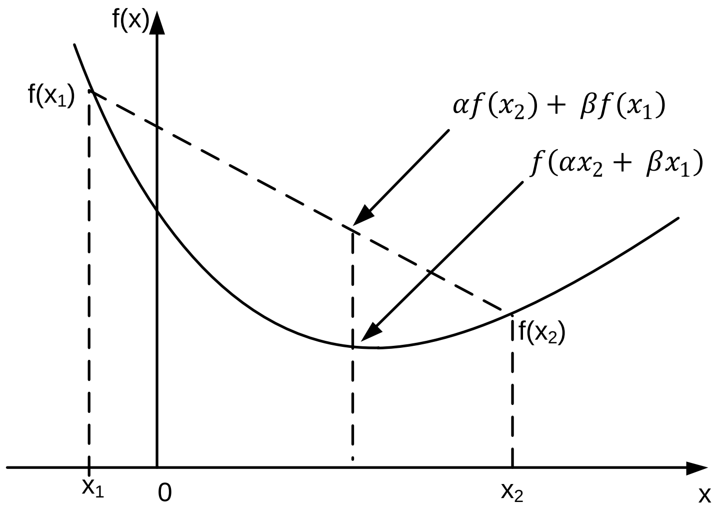

Figure 5-1: A convex function [1]

The time-current curve is plotted and tested for convexity. For all the points joining a line segment on the graph shown below (Figure 5-2) the condition in equation (5-5) is satisfied. However, there are three additional requirements, which need to be satisfied before making final decisions.

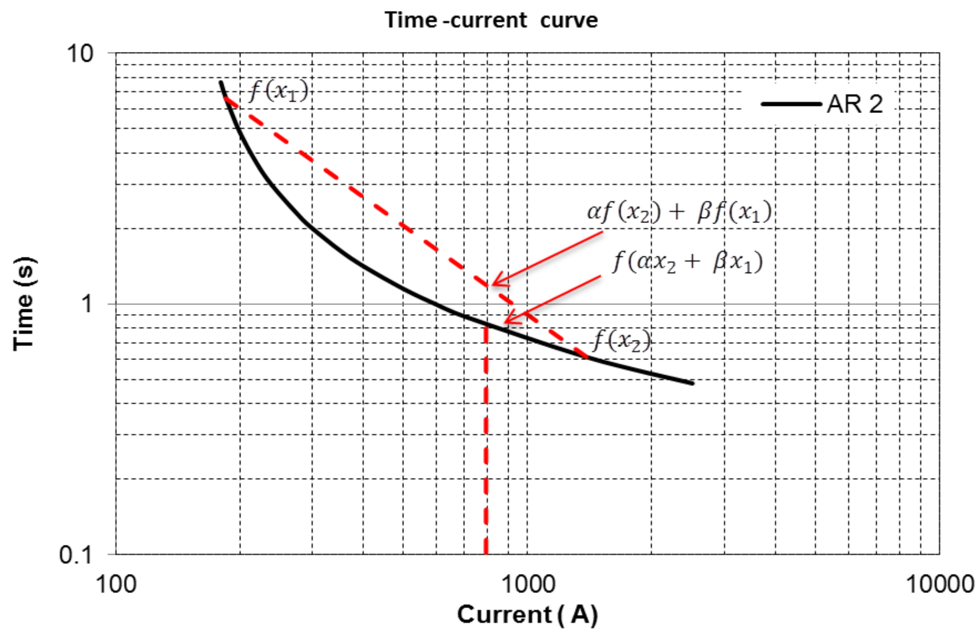

Figure 5-2: A time-current curve

Convex optimization problems should meet the following three additional requirements [49]:

a) The objective function of the optimization problem must be convex.

b) The inequality constraint functions must be convex.
c) The equality constraint function must also be convex.

5.2.2 Continuous vs. discrete

Models with continuous variables can take on any real value, whereas discrete variables take on values from a discrete set. Directional overcurrent relays allow for a continuous time multiplier and discrete pick-up currents. However, discrete pick-up currents during the simulations can be converted to be continuous, and final solutions are rounded off to the nearest discrete values. The original PSO was originally developed for continuous valued spaces [50].

5.2.3 Constrained vs. unconstrained

Unconstrained variables are optimization problems where variables are not bound in the search space. Most practical problems are constrained and design variables are bound by simple equations or sets of equalities and inequalities that model the relationship between the objective function.

5.2.4 Single vs. multi-objective functions

Multi-objective function optimization problems are used to determine a solution, which has more than one objective function. The following notation formulates a multiple objective optimization problem [50]:

Minimize

$$f(\bar{x}), \quad x = (x_1, x_2, \cdots, x_n) \tag{5.7}$$

subject to

$$g_i\,(\bar{x}) \le 0, \qquad i = 1, 2{,}3 \;\cdots n_g \tag{5.8}$$

$$h_i(\bar{x}) = 0, \qquad i = \; n_g + 1, \qquad \cdots, n_g + n_h \tag{5.9}$$

The distinction between the single and multiple objective functions is clarified in equation (5.9). The second equality constraint (eq. 5.9) has a different set of numbers compared to the constraint in equation (5.2).

For the directional overcurrent relay optimization problem, the proposed PSO algorithm can be used since PSO is suitable for both linear and non-linear functions, and for non-differentiable and convex and non-convex problems. The next section presents the theoretical background on the PSO algorithm.

5.3 Artificial intelligence optimization

Soft computing methods are advanced optimization methods used to determine the best solutions to various practical and theoretical problems. Figure 5-3 shows different categories of soft computing methods. The focus of this research is on the two stochastic methods, namely: particle swarm optimization (PSO) and evolutionary computing algorithms (e.g. GA). These methods differ from each other and apply to different types of problems.

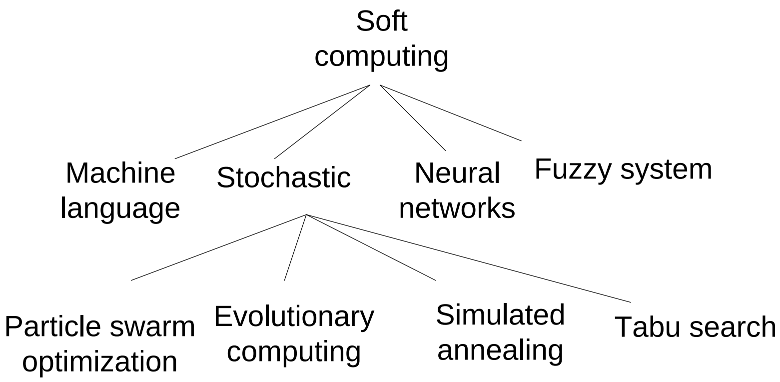

Figure 5-3: Soft computing methods

For the purposes of this research both PSO and GA (binary) algorithms are studied. The following section provides the background on PSO and its application.

5.3.1 Particle swarm optimization

The PSO technique is a biologically inspired metaheuristic search technique and optimization method developed by Eberhart and Kennedy in 1995. The algorithm emulates the behaviour of colonies of living things such as a swarm of insects, flock of birds or a school of fish. In this method individuals share information on their previous experiences. A particle represents a potential solution in the population. If an individual discovers a shorter path to the food source all other particles follow irrespective of how far they are from the newly found food source or better path to the food source [48],[51].

Every particle is represented by two quantities: position (x, y) and velocity (v_x, v_y) in the design space. Modification of the particle is based on the information on the current *position* and the *velocity* of the particle. This method is based on the experience of the individual particle and the experience of other particles [15],[48].

Figure 5-4 shows the search points of a single particle in the search space. Before a particle modifies its position (S^{k}) it uses the information of its current position $\left(\mathrm{S}^{\mathrm{k}}\right)$ and velocity (V^{k}). It compares the distance between its current position (S^k) and its best position (pbest). Lastly, it compares the distance between its current position (S^k) and the best position of another particle (gbest) in the population.

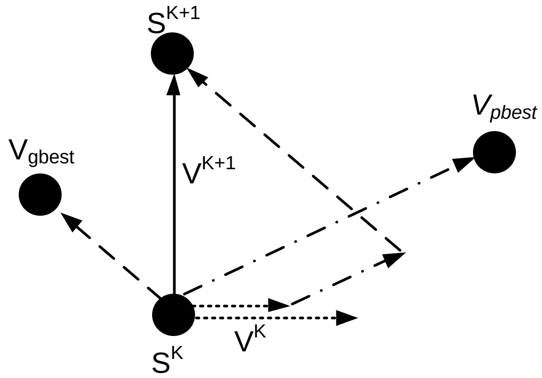

Figure 5-4: Searching points of PSO

Mathematically, the particle modifies its position using the velocity equation (5.10) below. This equation is known as the gbest model [7],[15].

$$v_i^{k+1} = wv_i^k + c_1 rand_1 \times \left(pbest_i - s_i^k\right) + c_2 rand_2 \times (gbest_i - s_i^k) \tag{5.10}$$

where

w	- weighting factor
v_i^k	- particle velocity i at iteration k
c_1	- weighting coefficient
c_2	- weighting coefficient
$rand$	- random numbers between 0 and 1
s_i^k	- particle's position i at iteration k

In equation (5.10) above the weighting coefficients c_1 and c_2 provide a balance between *exploration* and *exploitation*. The word exploration refers to the particle's ability to hunt for an optimal solution in the search space. Exploitation refers to the particle's ability to concentrate the search space around a promising area in order to refine the particle solution [7].

The particle updates its position using the current position (s_i^k) and the modified velocity (v_i^{k+1}) as calculated in equation (5.10). From the results, the $pbest$ position is updated after the k^{th} interval.

$$s_i^{k+1} = s_i + v_i^{k+1} \tag{5.11}$$

The PSO algorithm is not a continuous iterative algorithm. Before proceeding to the next step $(k+1)$ the best position is updated. Thus, the fitness function is evaluated at the new position and compared with the previous best solution.

$$pbest = \begin{cases} pbest^k, & if\ f(s^{k+1}) \geq f(pbest) \\ s^{k+1}, & if\ f(s^{k+1}) < f(pbest) \end{cases} \tag{5.12}$$

The basic algorithm of the particle swarm optimization technique is shown in Figure 5-5 below. The algorithm is based on random initialization of the particles. The details of the calculations inside the main loop are discussed below.

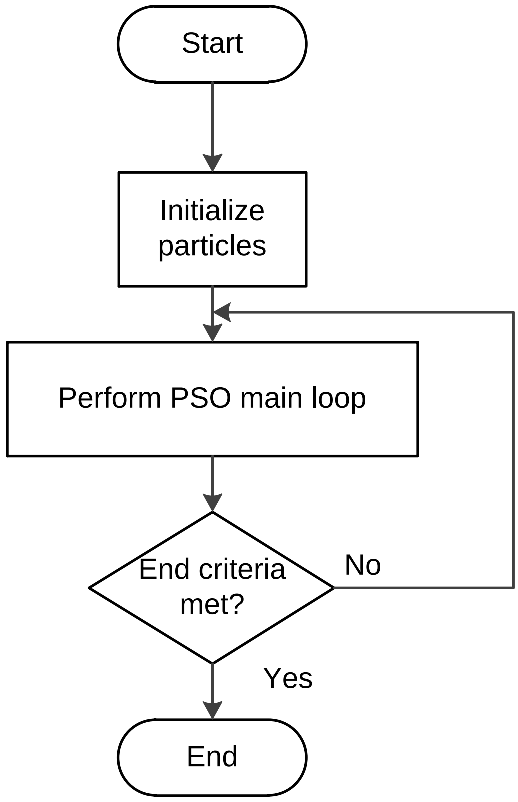

Figure 5-5: Basic PSO flowchart

The PSO technique can be used to solve scientific and engineering problems. The advantages of using the particle swarm optimization technique are summarized below [50]:

a) it optimizes both continuous and discrete problems,
b) it does not require derivative information,
c) it accepts real number codes,
d) it does not have the overlapping and mutation calculations as are required by genetic algorithms,
e) the speed of the search of the PSO algorithm is faster the genetic algorithms and
f) the number of the dimensions of the PSO algorithm equals the number of possible solutions.

Basic PSO has four variants, which are used to enhance the performance of the algorithm. The drawback of the PSO technique is that the method easily suffers from partial optimism, which reduces the accuracy and speed of finding the velocity and position vectors [50].

5.3.2 The variants of basic PSO

The shortcomings of the PSO algorithm have been modified by implementation of the variants, which improves the speed of convergence and the quality of the solution. The basic PSO technique consists of the following variants:

a) Velocity clamping
b) Inertia weight
c) Constriction weight
d) Synchronous and asynchronous updates

The PSO algorithm can be modified in three ways [50]:

a) expansion of the search space,
b) adjustments of parameters,
c) hybrid with another technique.

Figure 5-6 shows the difference between the basic PSO and modified PSO algorithms. The modified particle swarm has more variants than the basic PSO and this is to ensure that the results are optimal and of good quality [50].

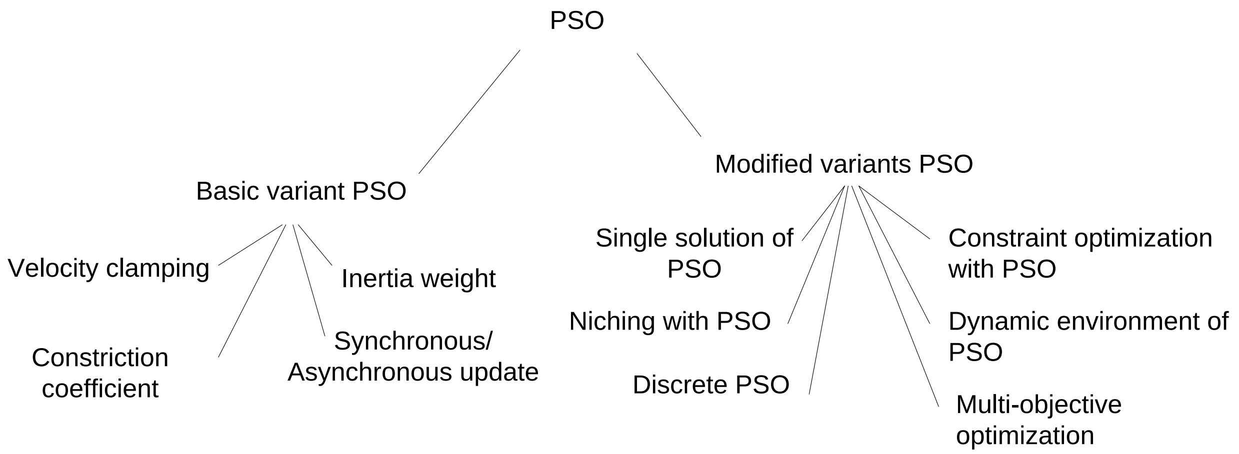

Figure 5-6: Variants of particle swarm optimization technique

The impact of variants of the basic PSO on the particle's velocity, solution and the convergence of the algorithm is discussed in the subsequent paragraphs.

a) Velocity clamping

The velocity of a particle is limited to a certain minimum and maximum value (i.e. pre-defined range). The reason for limiting the velocity is to reduce the possibility of the particle flying out of the search space [50],[51]. The speed (velocity) of a particle is adjusted using the following equation:

$$v_{ij}^{k+1} = \begin{cases} v_{ij}^{k+1}, & v_{ij}^{k+1} < v_{max,j} \\ v_{max,j}, & Otherwise \end{cases} \tag{5.13}$$

where

v_{ij}^{k+1} - the velocity of a particle

$v_{max,j}$ - is the maximum velocity of a particle.

The maximum and minimum velocity values are calculated using the equations below, where the constant δ is typically set to either 0 or 1.

$$v_{max} = \delta(x_{max} - x_{min}) \tag{5.14}$$

$$v_{min} = \delta(x_{min} - x_{max}) \tag{5.15}$$

where

x_{max} - maximum position of the particle

b) Inertia weight

From the velocity equation (5.10), the inertia weight is the coefficient of the velocity obtained from the previous iteration. As seen in equation (5.10), the inertia weight controls the exploitation and exploration of the swarm. A higher coefficient of the velocity accelerates the particle velocity to the maximum. This implies that the particle will explore the search space widely. While a small coefficient encourages the particle to exploit other particles [50]. The value of the inertial weight of the basic PSO variant is calculated as:

$$w = w_{max} - \frac{w_{max} - w_{min}}{k_{max}} \times k \tag{5.16}$$

where

k - iteration number

w_{min} - final weight

w_{max} - initial weight

The values for the initial and the final weight are typically set to 0.9 and 0.4 respectively. These settings are used to ensure that during the initial stages, there is enough space for particles to explore and with time the search space narrows. Secondly, this decreases the oscillations around the global position ($gbest$) [7].

c) Constriction coefficient

The constriction weight ensures that the PSO technique converges to a stable point without the need to constrict the velocity [50]. In the case where the constriction weight is used, the velocity equation in (5.10) is changed to the following equation:

$$v_i^{k+1} = x\left[v_i^k + \emptyset_1\left(pbest_i - s_i^k\right) + \emptyset_2(gbest_i - s_i^k)\right] \quad (5.17)$$

where

$$x = \frac{2k}{\left|2 - \emptyset - \sqrt{\emptyset(\emptyset - 4)}\right|} \quad (5.18)$$

and,

$$\emptyset = \emptyset_1 + \emptyset_2 \quad (5.19)$$

$$\emptyset_1 = r_1 c_1 \quad (5.20)$$

$$\emptyset_2 = r_2 c_2 \quad (5.21)$$

where $\emptyset \geq 4$ and $k \in [0\ 1]$

d) Synchronous vs. Asynchronous update

The synchronous update approach updates the results iteratively and separately from the particle position and global position update. This method is slower and provides feedback update at the end of iteration. This approach is extensively used to determine the global best position. The asynchronous update approach is better for pbest, calculates new best position after each particle position update, and gives immediate feedback about a region of the search space [50].

Table 5-1 below summarizes the functions of all four variants and gives their advantages and disadvantages.

Table 5-1: Advantages and disadvantages of the basic PSO variants [50]

Basic variant	**Function**	**Advantages**	**Disadvantages**
Velocity clamping	Controls the global exploration and exploitation of the particle in the search space.	Reduces the size of the step velocity in order to control the particle's movement.	As the particle's velocity reaches maximum velocity, the particle will remain in the upper limit and not converge to the local area.
Inertia weight	Controls the momentum of the particle.	Fosters the convergence ability.	The particle velocity is strongly influenced.
Constriction coefficient	Ensures a stable convergence of the algorithm.	Foster the convergence rate.	Unnecessary fluctuations of the particles when the algorithm converges.
Synchronous vs. Asynchronous update	Parallel processing of the optimization.	Improves the convergence rate.	More complex finite element formations.

5.4 Evolutionary computing optimization

Evolutionary algorithm is based on the theory of natural evolution and the principle of survival of the fittest. Natural evolution is a hypothetical population-based optimization process [15],[48]. As depicted in Figure 5-7, there are four stochastic optimization techniques, which belong to evolutionary optimization techniques, namely:

a) Genetic algorithms (GA)
b) Genetic programming (GP)
c) Evolutionary strategy (ES)
d) Evolutionary programming (EP)

All these methods are guided and randomized stochastic optimization techniques. The evolutionary programming technique is similar to an evolutionary strategy in that both place emphasis on the relationship between parents and their offspring, rather than seeking to emulate specific genetic operators as observed in nature. Both techniques are well suited for combinatorial optimization problems [15]. The main focus from Figure 5-7 is on the genetic algorithm optimization technique. A general background on the technique is presented and compared with the PSO technique at the end of the chapter.

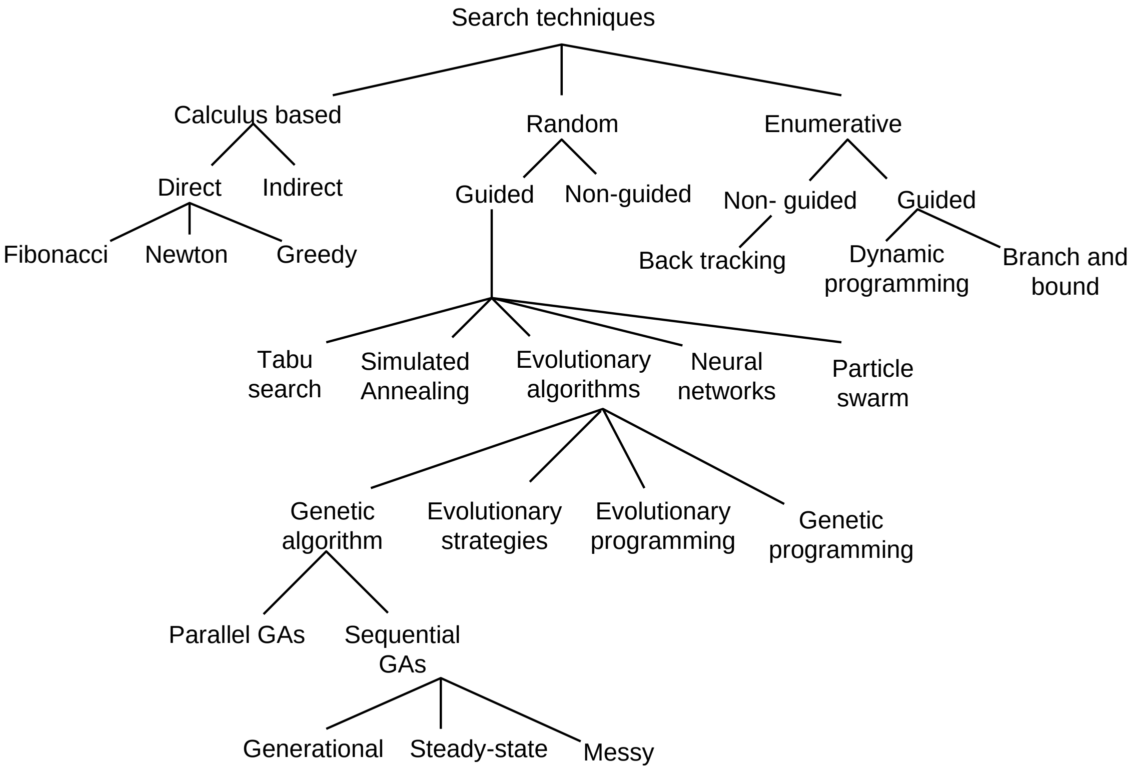

Figure 5-7: Search techniques taxonomy

5.4.1 Genetic algorithm

The basic elements of natural genetics are reproduction, crossover and mutation [15]. GA operates on a population of individual basis. Each individual is a potential solution in the population. In binary GA, the actual chromosomes are represented by a string of fixed-length binary, which encodes each individual in the population. The first generation is created randomly by a generated initial population, which has to go through the three different stages of GA in a sequential and iterative way.

The execution of a genetic algorithm is a two-stage process. In the first stage, a random generation is created. Then reproduction takes place where an intermediate population is created. In the second stage, crossover and mutation take place where the newly created intermediate population is used to create the next generation of potential solutions [15],[48]. The basic algorithm is shown with the flowchart in Figure 5-8 below. The operators of the genetic algorithm technique are discussed in detail in the subsequent section.

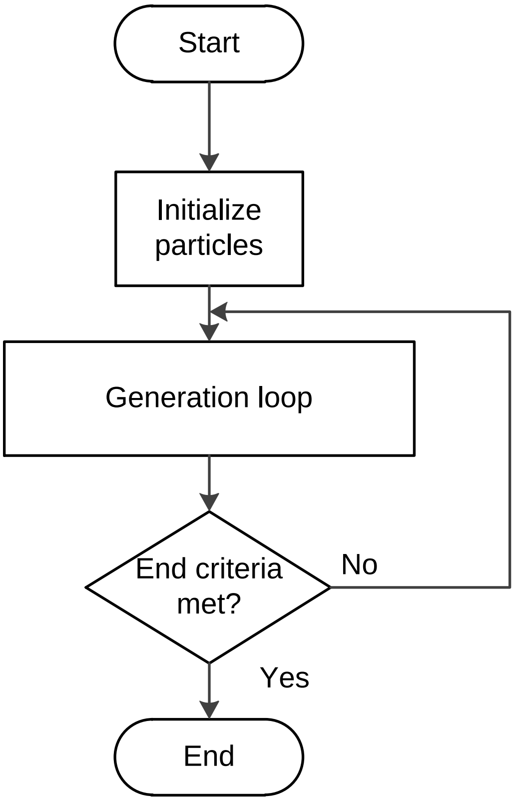

Figure 5-8: Basic algorithm of the genetic algorithm technique

5.4.2 Genetic algorithm operators

The genetic algorithm uses more operators compared to other algorithms such as the PSO algorithm. These operators are discussed in this section to provide detail of how each functions. In the binary genetic algorithm the design vectors are represented by binary numbers i.e. a 0 or 1. Each design variable $\bar{x} = [x_1, x_2, \ldots, x_n]$ is coded in a string of length (q), which is represented by a string of total length (nq) [15],[48].

a) Encoding and decoding

Since most problems are not defined using binary numbers, a conversion from real to binary numbers is done in order to transform the problem to binary. Quantization samples the range of continuous values and sorts them into a non-overlapping sub range. In the range, variables are assigned to either high or low range [52].

Mathematical formulations for binary encoding and decoding are given below [52]:

For encoding:

$$P_{norm} = \frac{P_n - P_{lo}}{P_{hi} - P_{lo}} \tag{5.22}$$

$$gene = round\left\{P_{norm} - 2^{-m} - \sum_{p=1}^{m-1} gene[P]2^{-p}\right\} \tag{5.23}$$

For decoding:

$$P_{quant} = \sum_{m=1}^{N_{gene}} gene[m]2^{-m} + 2^{-(m+1)} \tag{5.24}$$

$$q_n = P_{quant}(P_{hi} - P_{lo}) + P_{lo} \tag{5.25}$$

In each case,

P_{norm} - normalized variable, $0 \leq P_{norm} \leq 1$

P_{lo} - smallest variable value

P_{hi} - highest variable value

P_{quant} - quantized variable of P_n

$gene[m]$ - binary version of P_n

q_n - quantized version of P_n

P_n - the number of variables (n^{th})

b) Selection operator

At this stage, the survival of the fittest principle is applied. Individuals with higher fitness functions are selected so that they may increase the chances of reproducing new individuals in the new generation [15],[52]. The selection operator is implemented by the mathematical equation given below.

$$N_{keep} = X_{rate} - N_{pop} \tag{5.26}$$

where,

N_{keep} – number of chromosomes in the mating pool

N_{pop} – number of chromosomes in the population from generation to generation

X_{rate} - crossover rate

The population cost is arranged in ascending order (i.e. from lowest to highest). The chromosomes with highest cost are excluded from the generation to provide space for the new offspring [52].

c) Crossover operator

Crossover and mutation are used to explore the search space. The crossover represents the reproduction of new individuals. During the process of reproducing new offspring, the strings of the mating individuals exchange [15].

d) Mutation operator

The mutation operator ensures that there are more different individuals in the new population. The second function of this operator is to ensure that premature convergence does not occur [15]. Mathematically, the mutation operator is formulated using the notation below.

$$M = \mu(N_{pop} - 1)\times N_{bits} \tag{5.27}$$

and,

$$N_{bits} = N_{gene}\times N_{par} \tag{5.28}$$

where,

M - mutation operator

μ – mutation rate

N_{bits} – number of bits in the chromosomes

N_{gene} – number of bits in the gene

N_{par} – number of parameter variables

e) Fitness function

In genetic algorithms, there are two important functions, namely: fitness function and objective function $f(\bar{x})$. Due to the fact that GA is based on the principle of survival of the fittest, the optimization problem is maximized instead of being minimized. This implies that the function $F(x)$ should be maximized. Therefore, for unconstrained maximization problems GA becomes a more suitable optimization algorithm to use. When using this algorithm to minimize the optimization problem, it is vital to first transform the problem to a maximization problem by using the transformation equation below [15],[48]:

$$F(x) = \frac{1}{1 + f(X)} \tag{5.29}$$

Where a general constraint optimization problem is stated as:

Minimize $f(\bar{x})$

subject to:

$$g_i(\bar{x}) \leq 0 \qquad i = 1, 2,3 , \dots m \tag{5.30}$$

$$h_j(\bar{x}) = 0 \qquad j = 1,2, 3 \ \dots \ p \tag{5.31}$$

The genetic algorithm has been implemented on various problems and has proven to be one of the best optimization algorithms to solve minimization problems. The advantages of using a genetic algorithm are summarized below, in no order of priority [52]:

a) has the ability to solve both continuous and discrete variables,
b) does not require derivative information,
c) deals with a large number of variables,
d) provides a list of optimum variables instead of a single variable, and
e) it is suited for parallel computation of the solution.

On the other hand, for simple and non-complex problems other optimization algorithms perform faster than the genetic algorithm due to the fact that the genetic algorithm deals with a large population [52].

5.5 Concluding remarks

This chapter presented the two most popular stochastic optimization methods, which are used globally to solve scientific and engineering problems. A summary of the two methods is provided in Table 5.2 below.

From the table below, the following conclusions are made: PSO algorithm is less complex than GA. PSO presents more benefits than GA. The PSO algorithm searches faster than GA in the search space, uses two variables for the particle in the search space while GA only uses one (i.e. position). The number of solutions equal the number of the problem dimension. Lastly, the population diversity is mainly around the local region. Based on these benefits, PSO is chosen to improve on the calculated overcurrent settings calculated by the conventional method.

Table 5-2: Comparing GA and PSO algorithms [51],[52]

Parameter / Function	**GA**	**PSO**
General feature	Population, guided and random search	Population, guided and random search
Memory	Yes	Yes
Individual operator	Mutation	Individual's best position (pbest) history, velocity inertia
Social operator	Selection and crossover	Global best position gbest) history
Particle's variables	Position	Position and velocity
Population diversity	Variable $\frac{P_c}{P_m}$ Ratio and Selection schema	Mainly via local region
Design search space	Discrete (but can solve continuous value problems)	Continuous (can solve discrete value problems)
Global/local search balance	Can be tuned $\frac{P_c}{P_m}$ Ratio and Selection schema	Can be tuned Inertia weight (w) Higher (w) – global search Lower (w) – local search
Number of solutions	Provides a list of optimum variables	Provides optimum variables equals the number of problem dimension
Speed of search	Slower *(large population)*	Faster

6 Mathematical modelling of the directional overcurrent relay

This chapter presents mathematical modelling of the directional overcurrent relay coordination problem. The first section models the problem for the conventional coordination method. The second part of this chapter models the problem as a linear and constrained optimization problem for particle swarm optimization algorithm. Lastly, the induction generator is modelled mathematically and steady-state fault current is calculated.

6.1 Introduction

The distribution system is not designed to have multiple sources connected in various positions. When distributed generation is connected to the distribution network the direction of the fault current changes and increases in magnitude. The overcurrent relay depends explicitly on the fault current, pick-up current, time-current curve and time multiplier settings respectively. Therefore, the operating time of the overcurrent relay is influenced by the change in the magnitude of the fault current in the distribution network. The consequence of the increasing fault current is miscoordination of relays in the distribution network.

Directional overcurrent relays are mainly used in the sub-transmission system in the distribution network, which is mainly interconnected. The main challenge encountered when coordinating directional overcurrent relays, especially in an interconnected network, is setting the last relays in the loop. The reason is that often in an interconnected network a relay is paired with more than one relay. Therefore, manual computation of overcurrent relay settings becomes a serious challenge, cumbersome and time consuming [8].

The directional overcurrent relay coordination problem is formulated and is used to compute the relay's settings using both the conventional and PSO algorithm. The IEEE 8-bus case is modelled in PowerFactory to obtain three-phase fault currents measured by the main and backup relays. The relays are paired and coordinated accordingly. The second case study is a test case consisting of a DG source.

The following section formulates the coordination problem mathematically taking into account the information discussed in the previous two chapters. The first approach is to formulate the problem using mathematical equations, identifying factors which describe the important aspects of the coordination problem, and translating them into a mathematical set of equations.

6.2 Problem formulation for conventional method

The directional overcurrent relay modelled in this section is a generic model of the overcurrent relay family. Emphasis is placed on the time equation, which plays a major role in coordination. The standard equation to calculate the operating time of an overcurrent relay is given in equation (6.1) below. From the equation, the operating time (t) is a function of the pick-up current (I_r), fault current (I) and time multiplier setting (*TMS*). The assumption is that a normal inverse characteristic is used.

Overcurrent relay characteristics were discussed in detail in chapter 2, therefore the values of α and β are 0.02 and 0.14 respectively taken from table 2-2.

$$t = \frac{\beta}{\left(\frac{I}{Ir}\right)^{\alpha} - 1} \times TMS \qquad (6.1)$$

The operating time of the relay is a positive quantity. Therefore, the calculated operating times of the protective relays should be positive numbers. The inequality constraints given below in equations (6.2) and (6.3) govern the operating time of the coordinated relays, ensuring that in the calculation the operating times of both main and backup relays will not be a negative number.

$$t_{ii} \geq 0 \qquad \forall\, i = 1, 2 \dots n \qquad (6.2)$$

$$t_{min} \leq t_{ii} \leq t_{max} \qquad \forall\, i = 1, 2 \dots n \qquad (6.3)$$

The minimum and maximum operating times of the relays are at least 0.2 seconds for close in faults and 1.8 seconds for a far bus fault, respectively. The time value 1.8 seconds is selected such that it does not exceed the short time rating of the system equipment (*e.g. circuit breakers, transformers and conductors*). Most of the system equipment has a short time rating of at least 2 seconds in order to minimise damage to equipment.

The overcurrent relay has three settings which are important in determining the operating time of the relay namely; the pick-up (I_r), time multiplier (TMS) settings, which have predefined ranges, and the time-current curve. The range for the pick-up and TMS depends on the model of the relay simulated or used. For the selected relay, the minimum and maximum range of the time multiplier and pick-up current are assumed to be as:

Time multiplier setting (TMS):

$$TMS_{min} \leq TMS_i \leq TMS_{max} \qquad \forall\, i = 1,2 \dots n \qquad (6.4)$$

$$0.05 \leq TMS_i \leq 1.0 \qquad \forall\, i = 1,2 \dots n \qquad (6.5)$$

Pick-up currents (PU):

$$PU_{min} \leq PU_i \leq PU_{max} \forall\ i = 1,2 \dots n \qquad (6.6)$$

The pick-up setting depends on the thermal rating of the conductor carrying the current or maximum load current, and the minimum and maximum fault current in the network.

$$PU_{min} = 1.05 \times I_{load} \qquad (6.7)$$

$$PU_{max} = 1.20 \times I_{fault} \qquad (6.8)$$

where

TMS_{min} – minimum time multiplier setting of the relay

TMS_{max} – maximum time multiplier setting of the relay

PU_{min} – minimum pick-up current of the relay (A)

PU_{max} – maximum pick-up current of the relay (A)

The relay operating time equation is a linear function of the time multiplier setting and a non-linear function to the ratio of the fault current and pick-up current. Keeping the pick-up current fixed throughout the calculations, equation (6.1) becomes a linear coordination problem. Thus, equation (6.1) is reduced to equation (6.9) below.

$$t_{ii} = \alpha_i \times TMS_i \qquad \forall\ i = 1, 2 \dots n \qquad (6.9)$$

where α_i is a known constant and represented below by equation (4.10):

$$\alpha_i = \frac{\beta}{\left(\frac{I}{I_r}\right)^{\alpha} - 1} \qquad \forall\ i = 1, 2 \dots n \qquad (6.10)$$

Once the equation for the relay operating time is set, then coordination between the main and backup relays is considered.

The coordination criterion refers to the coordination measure between the main relay and the back-up relay. The coordination time interval (CTI) depends on the type of the relays used: either a digital or electromechanical relay. For this research, only digital relays are assumed. Therefore, the CTI ranges between 0.25 seconds to 0.3 seconds.

The operating time of the back-up relay should be greater than the operating time of the primary relay plus the coordination time interval of a fixed value of 0.3 seconds.

$$t_{ji} \geq CTI + t_{ii} \tag{6.11}$$

where

t_{ii} - primary relay operating time at location i for the fault current at i (s)

t_{ji} - back-up relay operating time at location j for a fault at location i (s)

In order to compute the settings of the directional overcurrent relays in Matlab®, the following data is required: three-phase fault currents at all relay locations, coordination margins (CTI), relay constraints and settings of relays to be coordinated and those close to the loads and at boundaries of other networks.

The overall procedure is summarized in the following steps:

a) identify the relay pairs to be set, determining the primary and back-up relay pairs,
b) simulate three-phase faults at 5% of the protected line and measure the current measured by both the primary and back-up relay,
c) verify that the calculated relay settings that they meet the requirements stated in chapter 2, (i.e. coordination constraints and settings constraints discussed in sections 2.3.1 and 2.3.2).

The program calculates the time multipliers and operating times of the identified primary relays. The back-up relays' operating time is also calculated and coordination between primary and back-up relays is checked.

A Matlab® program is compiled to calculate the overcurrent relay settings in order to minimize the time for calculating the relay settings. A simple radial feeder shown in Figure 6-1 is used to illustrate the procedure followed in Matlab® to calculate the relay settings for relays in the IEEE 8 bus case. A flowchart in Figure 6-2 summarizes the conventional coordination steps as discussed in chapter 2 for a radial system.

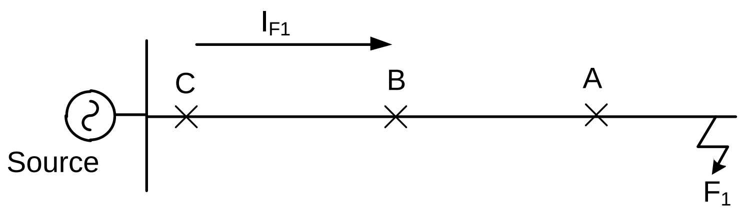

Figure 6-1: A simple radial feeder with a fault at F_1

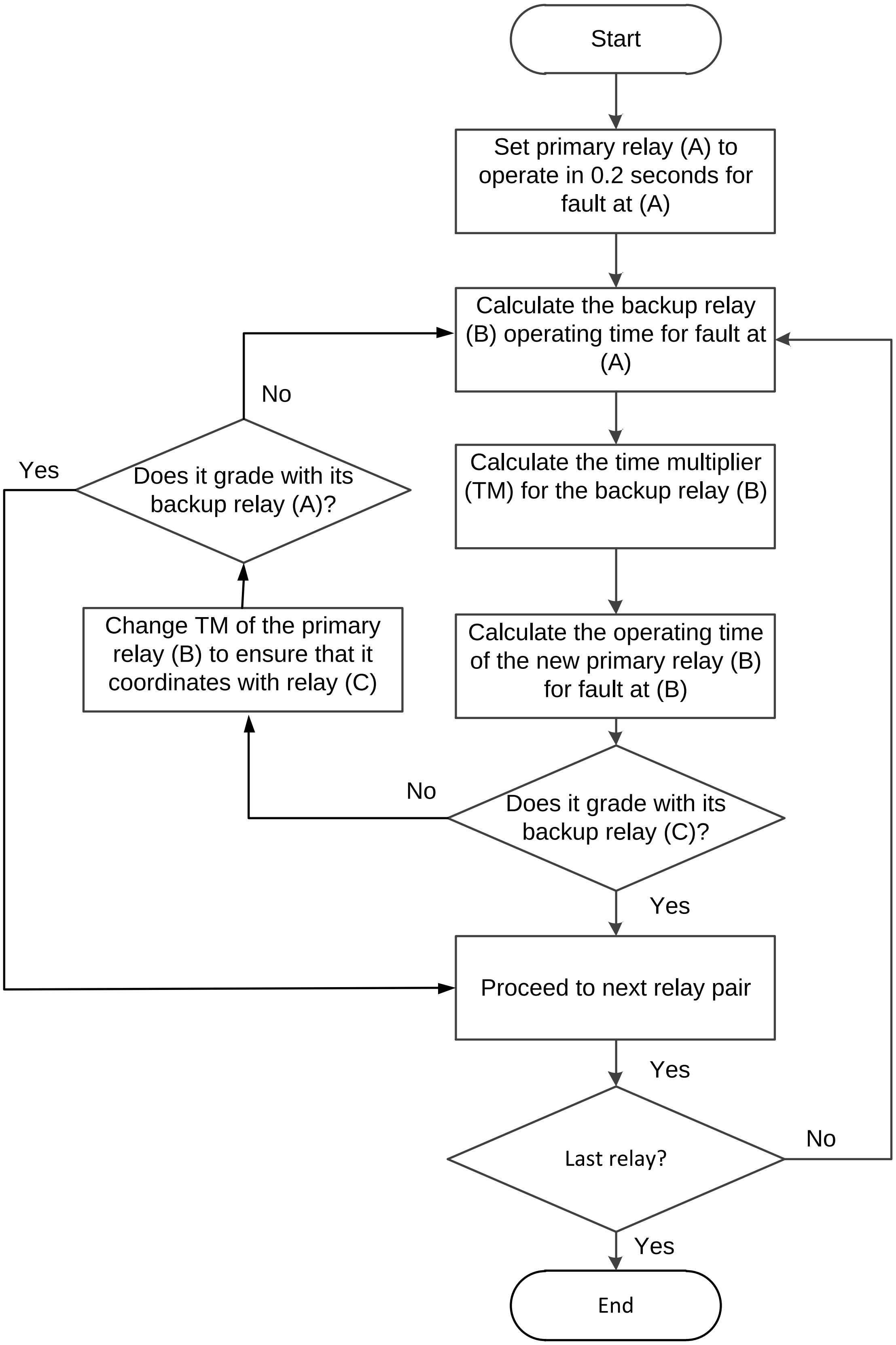

Figure 6-2: Conventional method flow chart

6.3 Problem formulation for PSO algorithm

The objective of this research is to compute optimum settings of the directional overcurrent relays in the distribution network with DGs using the PSO algorithm. The proposed algorithm should meet the following minimum requirements:

a) Minimize the operating times of the primary relays for close-in three-phase faults in a distribution network with distributed generation.
b) Maintain a coordination time interval of 0.3 seconds between the primary and back-up relays in a distribution network with distributed generation.

The objective is to find $\bar{x} = [x_1, x_2, \cdots x_n]$, which minimizes the function $f(\bar{x})$, the function $f(\bar{x})$ is the sum of the primary relays' operating times for close-in three-phase faults.

$$f(\bar{x}) = \alpha_i \sum_{i=1}^{n} t_{ii} \qquad \forall\, i = 1, 2 \dots n \tag{6.12}$$

subject to the following constraints,

$$x_i^{lb} \le x_i \le x_i^{ub} \qquad \forall\, i = 1, 2 \dots n \tag{6.13}$$

$$t_{ji} - t_{ii} \ge CTI \qquad \forall\, i = 1, 2 \dots n \tag{6.14}$$

The design vector $\bar{x}$ represents a set of time multipliers. The design vector constraints are: x_i^{lb}, which is the time multiplier lower bound and is equal to 0.05 and x_i^{ub} is the time multiplier upper bound, which is equal to 1.0. The coordination time interval (CTI) is the coordination time difference between the main and backup relays. The difference between the backup (t_{ji}) and primary relay (t_{ii}) for a close-in fault at location i should be at least 0.3 seconds.

The basic PSO is generally used for unconstrained optimization problems in Matlab®, therefore using a basic PSO results in miscoordination between the operating times of the main and the backup relays. Secondly, when boundaries are not set, particles search all over the design space, which returns an optimal solution that is out of relay setting bounds. To ensure that these challenges do not occur, a constrained optimization problem is implemented in Matlab® by introducing penalty functions to the objective function $f(\bar{x})$. Details on how the penalty function is used in the objective function are discussed in the following section.

6.3.1 Constrained objective function

Penalty functions are the methods used to transform the unconstrained optimization problem into a constrained optimization problem.

The constraint functions G_i and L_i is either added to- or subtracted from the original objective function $f(\bar{x})$ based on violation present in the solution [55].

There are two types of the penalty functions, namely: the *exterior* and the *interior* penalty function. The most commonly used are the exterior penalty functions because they are easily implemented. The exterior method does not require any feasible region starting point. The particles are allowed to search for a solution in the infeasible region, then move to the feasible region. The interior method requires a feasible region starting point. In this method, particles are allowed to search first in the feasible region and then move to the constraints barriers. The drawback with the interior penalty method is its initial requirement (*feasible region starting point*) [55].

The general formula of the penalty function is defined below as:

$$f(\tilde{x}) = f(x) \pm \left[\beta_1 \sum_{i=1}^{n} G_i \ + \ \beta_2 \sum_{i=1}^{n} L_i\right] \tag{6.15}$$

$$G_i \ = max[0, g_i]^{\gamma} \tag{6.16}$$

$$L_i = \left[h_j(x)\right]^{\tau} \tag{6.17}$$

Where, β_1 and β_2 are the penalty factors, $f(\bar{x})$ is the expanded objective function to be optimized and G_i and L_i are the constraint functions. The positive constant γ and τ normally range between 1 and 2 [2].

The objective function implemented in Matlab® is formulated in equation (6.8) below. The coordination criteria constraint eq. (6.3) is easily violated. Thus, the penalty factor β_1 is set to a higher positive number. The penalty rule states that the penalty should be as low as possible. This is due to the fact that the penalty is either too high or too low. For a higher penalty factor the optimum solution lies on the boundary of the feasible solution [55].

$$f(\bar{x}) = \ \alpha_i \sum_{i=1}^{n} f(x_i) \ + \ \left[\beta_1 \sum_{i=1}^{n} \Delta t_{mb} \ + \ \beta_2 \sum_{i=1}^{n} g_i\right] \tag{6.18}$$

The following flowcharts summarize the formulation and the process of the PSO algorithm simulated in Matlab. The first one shown below in Figure 6-3 details the formulation of the constrained objective implemented in Matlab.

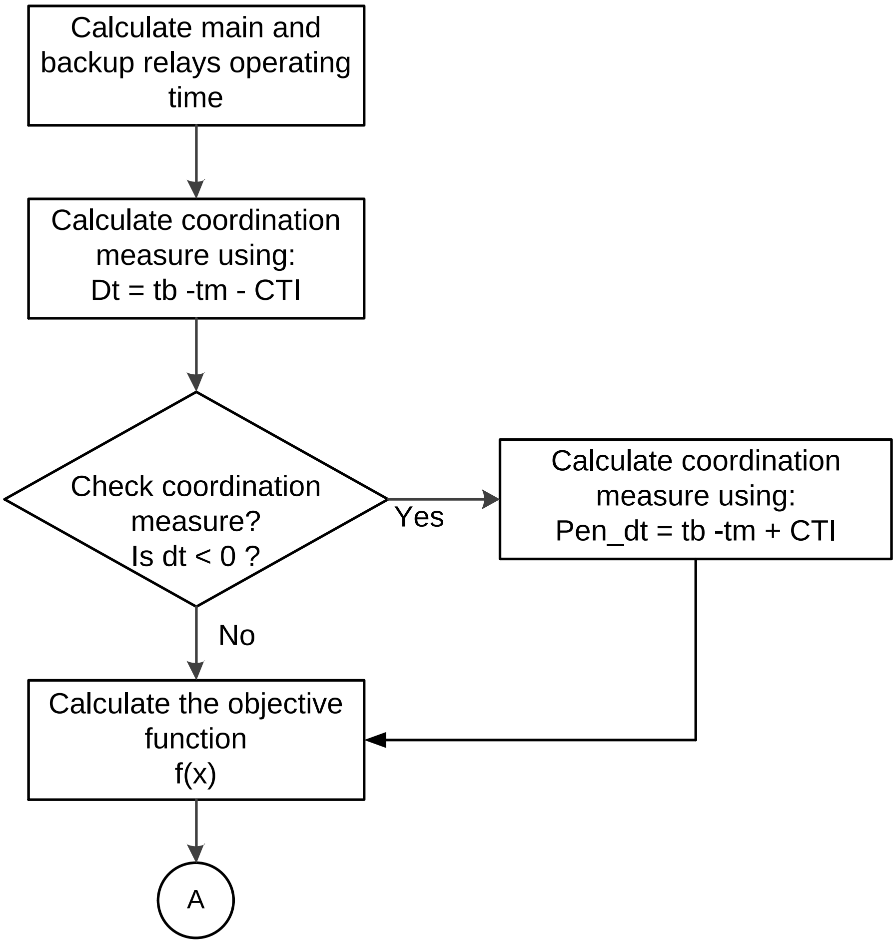

Figure 6-3: Objective function calculation

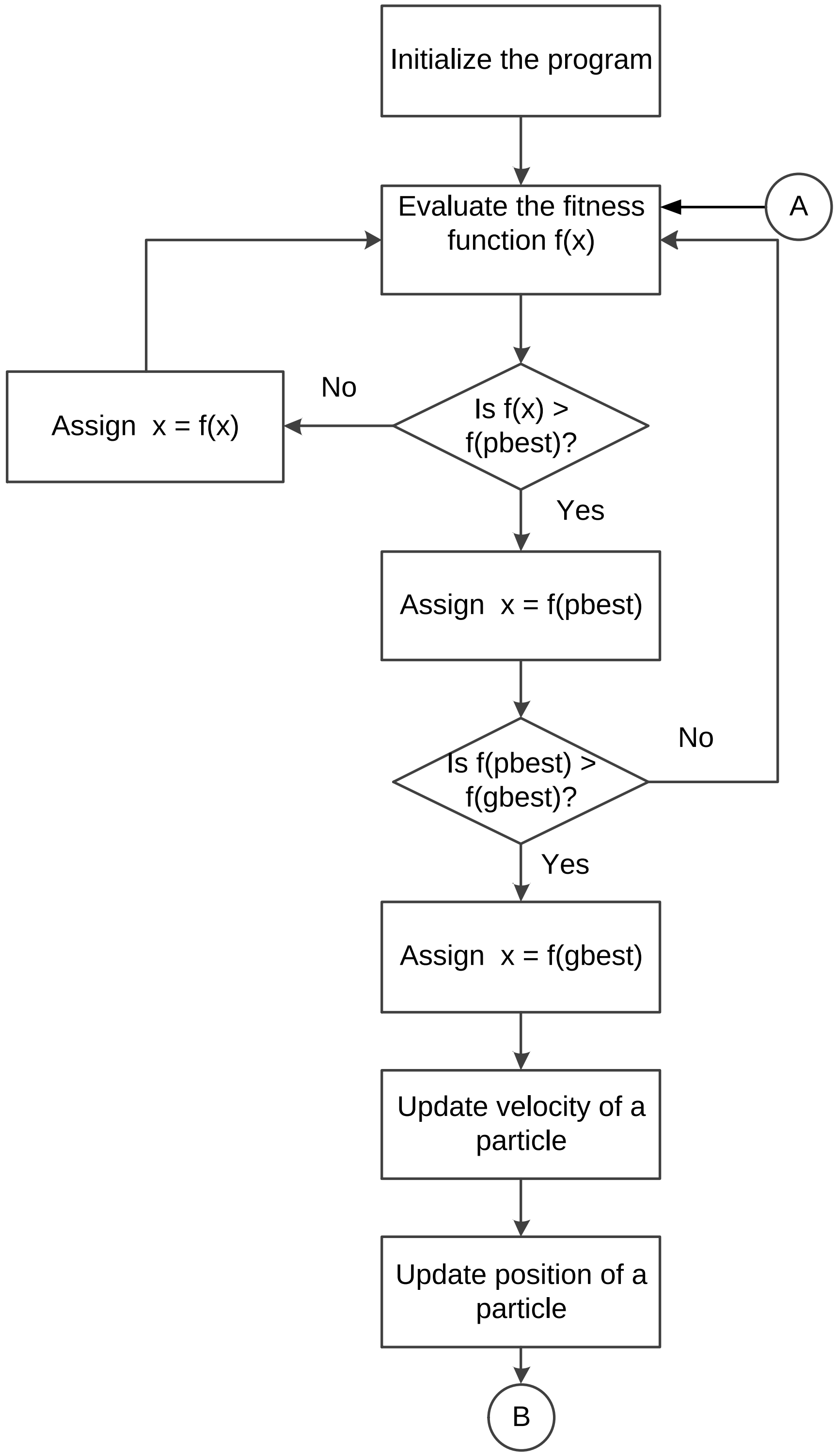

Figure 6-4: Application of PSO technique on coordination problem

The final step is to calculate the best times using the global best positions. The global best position is the best *time multiplier setting*. These new time multipliers are used to calculate optimized operating times of the primary and backup relays.

The two constraint violations checked are:

a) coordination criteria and

b) the range of the time multiplier setting

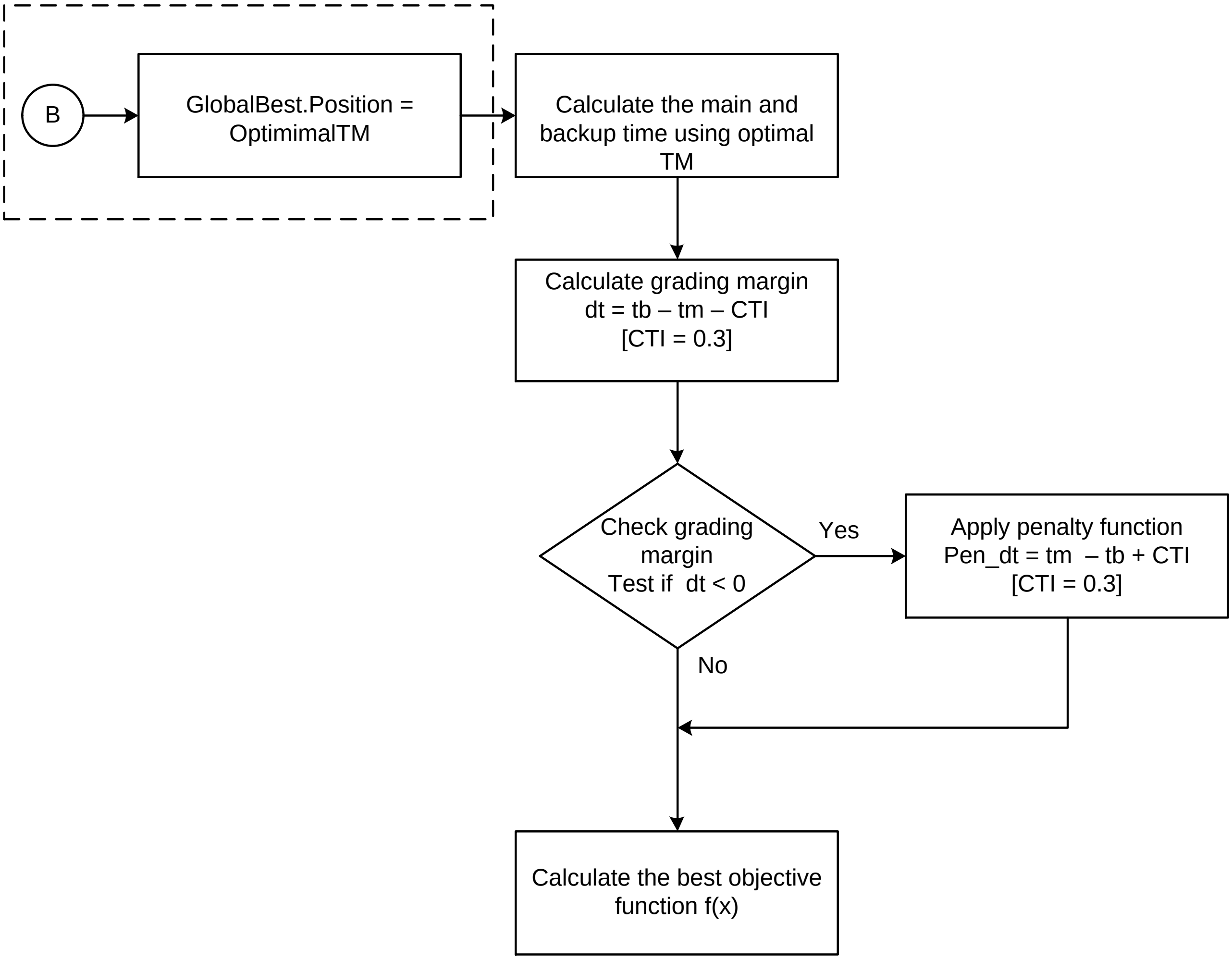

Figure 6-5: Optimized overcurrent coordination results

The next section details the mathematical modelling of the wind turbine and the induction machine. The generic models are used, since obtaining manufacturers data for these models is not easily accessible.

6.4 Modelling of the distributed generation sources

6.4.1 Modelling the wind turbine

A generic dynamic model for all four generators has been used to perform EMT study analysis in order to get a clear idea of how each type responds to fault conditions. For a SCIG, the generic model consists of four blocks of the generic model of the turbine. The four blocks represent the pitch angle controller, turbine, drive train shaft using a two-mass model and the generator. The internal details of the turbine model (e.g. equations, assumptions and approximations) are not accessible and therefore the models are used as standard models existing in DIgSILENT PowerFactory [42].

6.4.2 Modelling the induction generator

According to IEEE / ANSI method, the induction generator in the short circuit analysis is modelled as a 1 pu voltage source with a direct axis sub-transient inductance ($X_d^{''}$) as shown below in Figure 6-6. Both positive and negative sequence impedances for induction generators are equal to $X_d^{''}$.

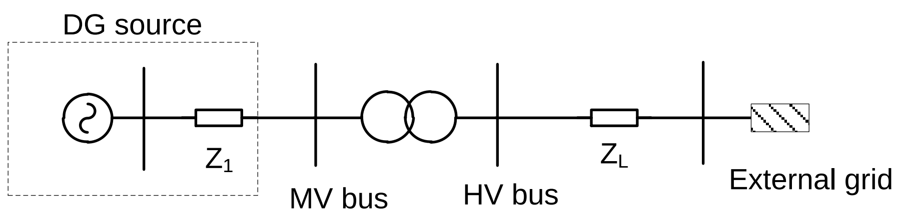

Figure 6-6: Equivalent model of an induction generator for short circuit analysis

The parameters of the DG sources modelled in Chapter 3 and base quantity values are given below and in Appendix A.

Table 6-1: Induction generator's data

Parameter Name	SCIG
Power rating (Srated)	2.2 MVA
Voltage (Vrated)	0.69 kV
Number of pole pairs (N)	2
Magnetizing reactance (X_m)	3.5 pu
Stator leakage reactance (X_s)	0.1 pu
Rotor leakage reactance (X_r)	0.1 pu
Stator resistance (R_s)	0.01 pu
Rotor resistance (R_r)	0.01 pu
Inertia (J)	75 kg m^2

If the locked rotor current is known, thus the value of the sub-transient inductance can be calculated as:

$$X_d''(pu) = \frac{1}{I_{locked\ rotor}(pu)} \tag{6.19}$$

From the above equation (6.19) a three-phase-to-ground fault at the turbine terminals can be approximated to be close the magnitude of the locked rotor current ($I_{locked\ rotor}$) during the first cycle [42].

The circuit shown in Figure 6-7 shows IEEE recommended equivalent circuit of the induction machine with the rotor referred to the stator circuit. The induction machine's parameter shown in the circuit in Figure 6-7 are given in Table 6-1 and are used in the steady state short circuit calculations.

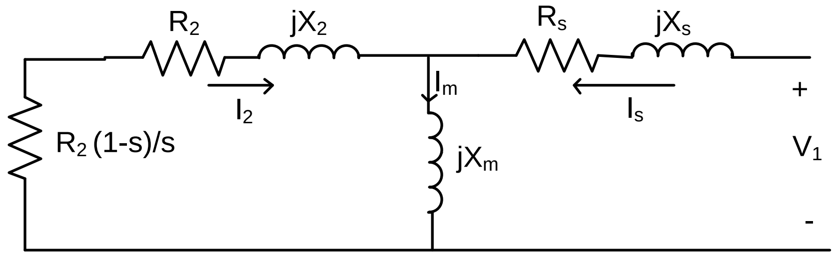

Figure 6-7: Steady-state equivalent circuit of an induction machine

For three-phase short circuit on the LV bus as shown in Figure 6-6, the network remains symmetrical, since there is no negative and zero sequence current flowing. Therefore, the network can be represented by a positive sequence network as shown below in Figure 6-8.

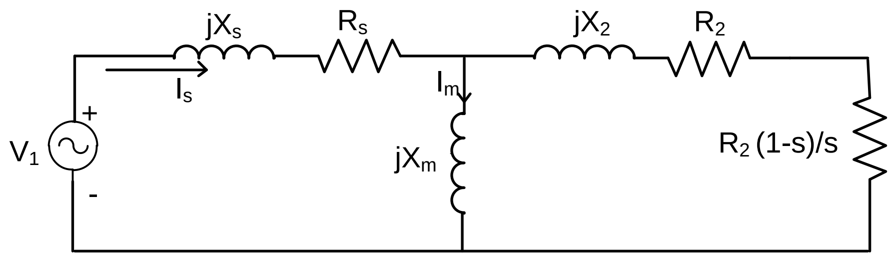

Figure 6-8: Equivalent circuit of the DG unit

The above circuit is used to calculate the steady state short circuit contribution of the induction machine. Since the network remains symmetric for three-phase faults, the initial short circuit current contribution is calculated using the following equations derived from Figure 6-8. The effective impedance of the induction generator is calculated as:

$$Z_m = R_s + jX_s + \frac{jX_m(R_2/_s + jX_2)}{R_2/_s + j(X_m + X_2)} \tag{6.20}$$

$$\therefore Z_m = 0.198\ \angle 84.36°\ pu$$

When a DG source is connected through a cable or an overhead conductor as shown in Figure 6-6, the parameters of the conductor are calculated using the following equation (6.22) [42].

$$Z_L = R_L + jX_L \tag{6.21}$$

Since the bus voltage is known, therefore V_s is converted to a per unit value for calculations. The base quantities are provided in Table A-1 in Appendix A.

$$V_{s,pu} = \frac{V_{nom}}{V_{base}} \tag{6.22}$$

$$V_{s,pu} = 1 \angle 0° \, pu$$

Thus, from the equivalent circuit the steady state short circuit current (I_s) can be calculated, since all parameters are known. DG source is not connected via an overhead conductor. Therefore,

$$I_s = \frac{V_s}{Z_m + Z_L} \tag{6.23}$$

$$\therefore I_{s,pu} = 5.051 \angle -84.37° \, pu$$

where,

I_s	Steady state current (A)
V_s	Voltage (V)
Z_m	Effective impedance of the induction machine (pu)
R_2	Rotor resistance (pu)
X_2	Rotor reactance (pu)
R_s	Stator resistance (pu)
X_s	Stator reactance (pu)

To convert the steady state current to the actual value (i.e. in Amps), the base current calculated in Appendix A is used to convert the pu current to actual currents in Amps.

$$I_{s,actual} = (5.051 \angle -84.37°) \times I_B \tag{6.24}$$

$$I_{s,actual} = 9297 \angle -84.37° \, kA$$

For a three-phase fault on the LV bus, the network remains symmetrical. Therefore, the current's magnitude is equal and displaced $120°$ apart. Using the matrix below, the phase currents and their angles are calculated. The negative and zero sequence components are equated to zero, since they are not present during balanced faults.

$$\begin{bmatrix} I_a \\ I_b \\ I_c \end{bmatrix} = \begin{bmatrix} 1 & 1 & 1 \\ 1 & a^2 & a \\ 1 & a & a^2 \end{bmatrix} \begin{bmatrix} I_1 \\ I_2 \\ I_0 \end{bmatrix} \tag{6.25}$$

$$\begin{bmatrix} I_a \\ I_b \\ I_c \end{bmatrix} = \begin{bmatrix} 1 & 1 & 1 \\ 1 & a^2 & a \\ 1 & a & a^2 \end{bmatrix} \begin{bmatrix} I_1 \\ 0 \\ 0 \end{bmatrix}$$

$$\begin{bmatrix} I_a \\ I_b \\ I_c \end{bmatrix} = \begin{bmatrix} 9297 \angle -84.37° \\ 9297 \angle +35.63° \\ 9297 \angle -204.37° \end{bmatrix}$$

where,

I_a, I_b, I_c	Phase current quantities
I_1, I_2, I_0	Sequence component quantities
a	The “*a*” operator, where a = 1∠120º and a^2 = 1∠240º

The calculated short circuit results in equation (6.25) are used in the following chapter to verify the simulation results for the induction machine used in the second case study.

6.5 Concluding remarks

The directional overcurrent relay coordination problem has been modelled in this chapter by a set of equations for both conventional method and particle swarm optimization (PSO) algorithm. These equations are set up in Matlab® for coordination calculations. The flowcharts given in the chapter outline the procedure on how the calculations are executed.

The second part of this chapter modelled the Type I induction generator and the generic turbine model is assumed, since obtaining data for DG sources is a challenge. The induction generator is modelled in PowerFactory for simulations. The results are compared in the next chapter for model verification in order to perform fault studies for coordination and compare the two methods.

7 Results analysis and verification

This chapter provides the fault responses of the DG sources as well as coordination results obtained from both coordination methods. The first part of the chapter details how the test and calculation models are set up in PowerFactory simulation tool. Secondly, the verification process and the performance comparison of both methods are discussed. The last section validates the PSO algorithm by comparing the applied overcurrent settings with the new settings obtained when calculating the settings using the PSO algorithm. One of the problematic HV ring network (Makalu 88 kV) in the border of Free-State and Gauteng is selected for validation process.

7.1 Test model setup

7.1.1 Case study 1 model setup

The 8-bus test case is modelled in PowerFactory with data provided in Tables 7-1 to 7-4 respectively [7] [9]. There are fourteen (14) primary overcurrent relays and twenty (20) relay pairs in total to be coordinated.

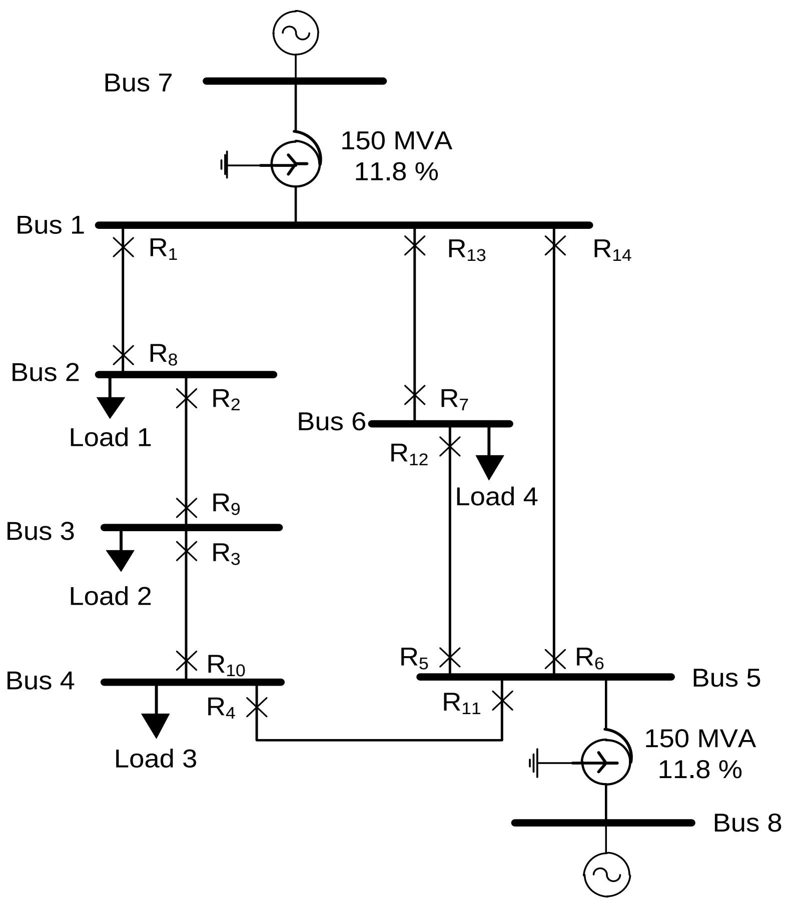

Figure 7-1: IEEE 8 bus test case

The information of the line parameters is provided in Table 7-1 below. The lines are modelled as line type elements where only positive sequence parameters are provided.

Table 7-1: Feeder positive sequence parameters

Name	Terminal i	Terminal j	Length (km)	R (Ω)	X (Ω)
Line 1	Bus 1	Bus 2	70	0.0057	0.00714
Line 2	Bus 2	Bus 3	80	0.005	0.0563
Line 3	Bus 3	Bus 4	100	0.005	0.045
Line 4	Bus 4	Bus 5	110	0.0045	0.0409
Line 5	Bus 6	Bus 5	90	0.0044	0.05
Line 6	Bus 1	Bus 6	100	0.005	0.05
Line 7	Bus 1	Bus 5	100	0.04	0.05

Table 7-2 below provides the details of the transformers used in the test case. The other researchers used an impedance of 4% for both transformers T1 and T2. However, the rating of the transformers and their selected impedance are not a true reflection of standard impedance for a 150 MVA transformer. Thus, a positive impedance of 11.8% is selected based on the information provided in Appendix B, which shows all the impedances of different ratings for transformers.

Table 7-2: Transformer data

Name	Terminal i	Terminal j	$S_n\ (MVA)$	$V_P\ (kV)$	$V_S\ (kV)$	$X_T(\%)$
Transformer 1	5	8	150	10	150	11.8
Transformer 2	1	7	150	10	150	11.8

Below in Table 7-3 and Table 7-4 respectively is the data for generators (G1) and (G2) as well as loads connected to different buses in the 8-bus test case.

Table 7-3: Generator data

Name	Terminal i	$S_n\ (MVA)$	$V_P\ (kV)$	$X_G(\%)$
Generator 1	8	150	10	15
Generator 2	7	150	10	15

Load flow study results are provided in Appendix C. As the test case is modified, it is expected that the results differ due to transformer impedances.

Table 7-4: Load data

Name	$P(MW)$	$Q(MVAr)$
Load 1	40	20
Load 2	60	40
Load 3	70	40
Load 4	70	50

Table 7-5 provides the values of the full-load currents, the pick-up currents, secondary currents and the CT ratio. The secondary current is the measured current in the secondary side of the CT. The secondary currents are calculated to ensure that the pick-up current do not exceed the continuous rated current of the relay. Lastly, a three-phase fault current is simulated at 5% of the protected feeder and measured at the relay location. All relays used in the modelled network are directional.

Table 7-5: Values of the full-load, pick-up, maximum fault currents and CT ratios

Relay ID	Load currents (A)	Pick-up currents (A) $(1.2 \times I_{FL})$	CTR	Secondary Currents (A) $\left[I_{sec} = \frac{I_{pu}}{CTR}\right]$	Maximum Fault Currents (A)
R_1	456	547	600/1	0.912	3858
R_2	102	122	200/1	0.612	2551
R_3	297	356	400/1	0.891	1734
R_4	715	858	1000/1	0.858	1034
R_5	365	438	600/1	0.73	3030
R_6	304	365	400/1	0.912	3556
R_7	93	112	200/1	0.558	2003
R_8	456	547	600/1	0.912	1107
R_9	102	122	200/1	0.612	1812
R_{10}	297	356	400/1	0.891	2655
R_{11}	715	858	1000/1	0.858	2655
R_{12}	304	365	400/1	0.912	1859
R_{13}	93	112	200/1	0.558	3564
R_{14}	365	438	600/1	0.73	3030

The second case study is modified to accommodate a connection of a DG source. The DG data used is obtained is provided in Table A-2 in Appendix A. Details on how the case study is modelled are given in the next section.

7.1.2 Case study 2 model setup

The steady-state parameters shown in the equivalent circuit in Figure 6-8 (in Chapter 6) are given in Table A-2 in Appendix A. The circuit shows a generic model of the induction generator used in this research for short circuit calculation analysis. The information used to model the three different types of WTGs used in chapter 3 and also in the calculations of new fault level studies is given in Appendix A. Due to difficulties obtaining DG sources information from the manufacturers, the machine data is taken from the models used in the South African electricity utility distribution network for short circuit contribution analysis.

The modified IEEE 8 bus test case is given below in Figure 7-2. The new DG is connected via a step-up delta/star transformer. Detailed model of the DG plant is shown in Figure 7-3.

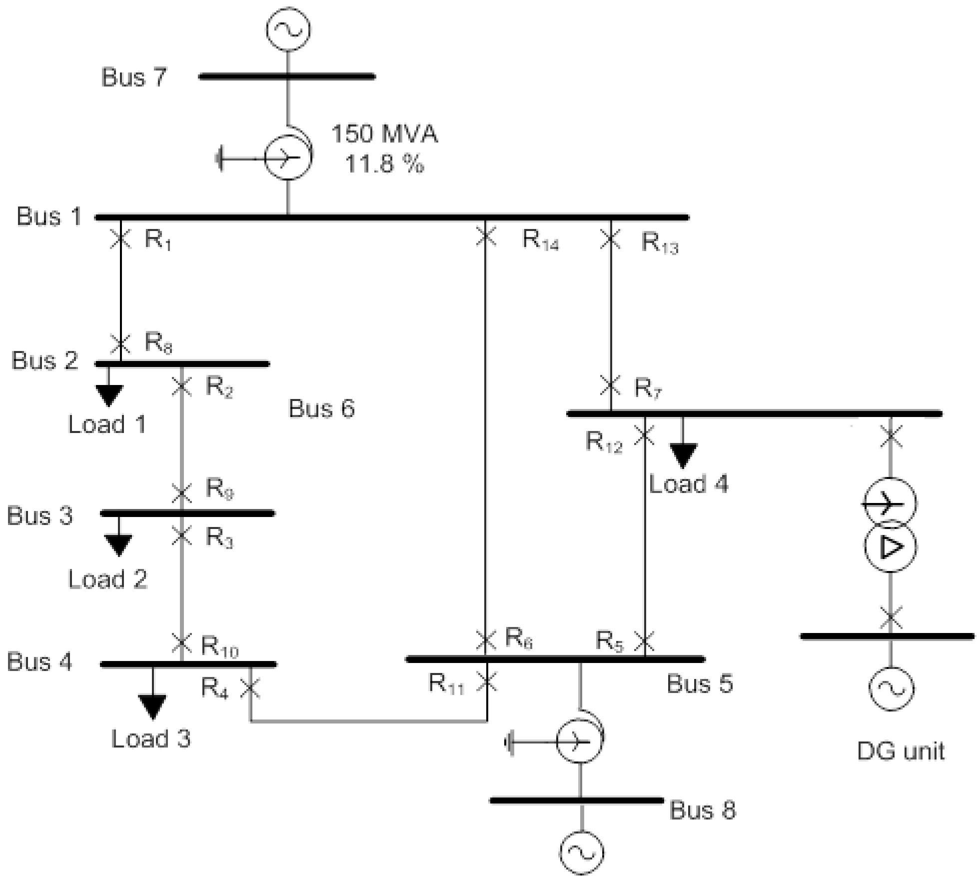

Figure 7-2: Modified 8 bus test case with a DG source

The delta connection is used to ensure that the zero sequence currents on the DG side are not transformed to the utility side. The wind power plant is made up of ten units of wind turbine generators each rated 2.2 MVA (i.e. 22 MVA in total). The shunt capacitor at the LV bus is used for compensation since the type I and type II are known to consume the reactive power.

In the second case study, a DG source is connected to bus 4. The DG source used is type I and type II since it was shown from Chapter 3 that the DFIG and fully-rated converter (FRC) induction generator will have no contribution to the system faults. The maximum fault current that can be contributed from the DFIG is the full-load current. Therefore, the first two types are investigated in this research, since their contribution is different from the other two types (i.e. DFIG and FRCIG).

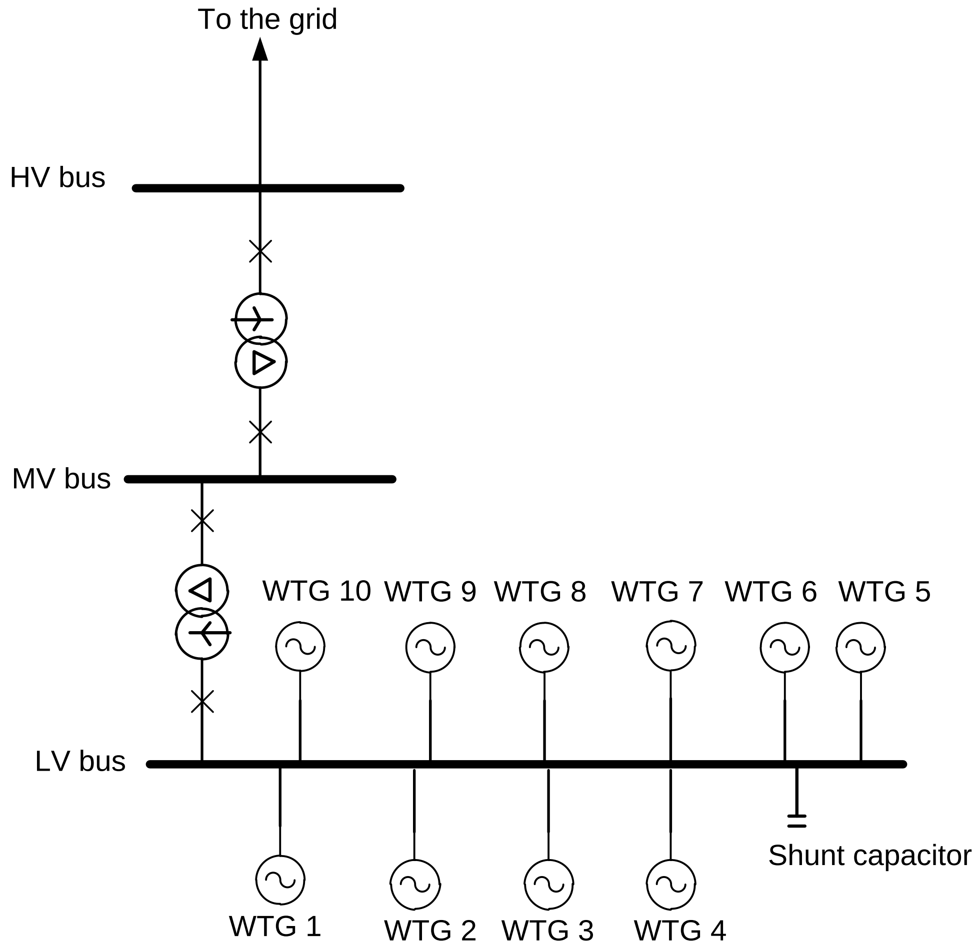

Figure 7-3: The detail plant model of the DG unit

The following section verifies the correctness of the models used. The results obtained after modelling the IEEE 8-bus test case are provided in Table 7-6. The induction generator hand calculations and simulation results for verification of the generator models are also provided in Table 7-7.

7.2 Case study test model verification

The IEEE 8-bus test system is used predominately by many researchers in the directional overcurrent relay coordination research studies [7],[9],[65]. The results obtained in this research using PowerFactory are provided in Table 7-6 and compared with results obtained by Ezzeddine *et al.* [65].

The fault studies in the second column are the results obtained in this research using PowerFactory simulation tool. The fault currents in the third column represent the currents, which are compared with [65]. The last column calculates the percentage error between the two results. Since, the transformer impedances were revised, the following significant error margin is expected, because the impedance is changed almost 3 times the impedance used by most researchers who used the same test case for their overcurrent relay coordination studies.

By increasing the impedance of the transformers from 4% to 11.8%, it is expected that the fault currents in the interconnected network decrease according to Ohm's law. Secondly, the current is not expected to drop by a factor of 3 since the impedance is increased by almost a factor of 3, because the network is interconnected.

Table 7-6: Verification of simulated three-phase fault results

Relay ID	**Maximum fault currents** (I_{f1})	**Maximum fault currents [65]** (I_{f2})	**% Error** $\left(\frac{I_{f1}}{I_{f2}}\right)\times 100\%$
R_1	3858	5390	71.58
R_2	2551	3347	76.22
R_3	1034	2243	46.10
R_4	1034	1361	75.97
R_5	3030	4267	71.01
R_6	3556	4995	71.19
R_7	2003	2703	74.10
R_8	1107	1353	81.82
R_9	1812	2345	77.27
R_{10}	2655	3495	75.97
R_{11}	2655	5391	49.25
R_{12}	1859	2507	74.15
R_{13}	3564	4995	71.35
R_{14}	3030	4267	71.01

The results shown below in Figure 7-4 are the three-phase fault currents simulated in this research and compared with the results obtained in [7],[65].

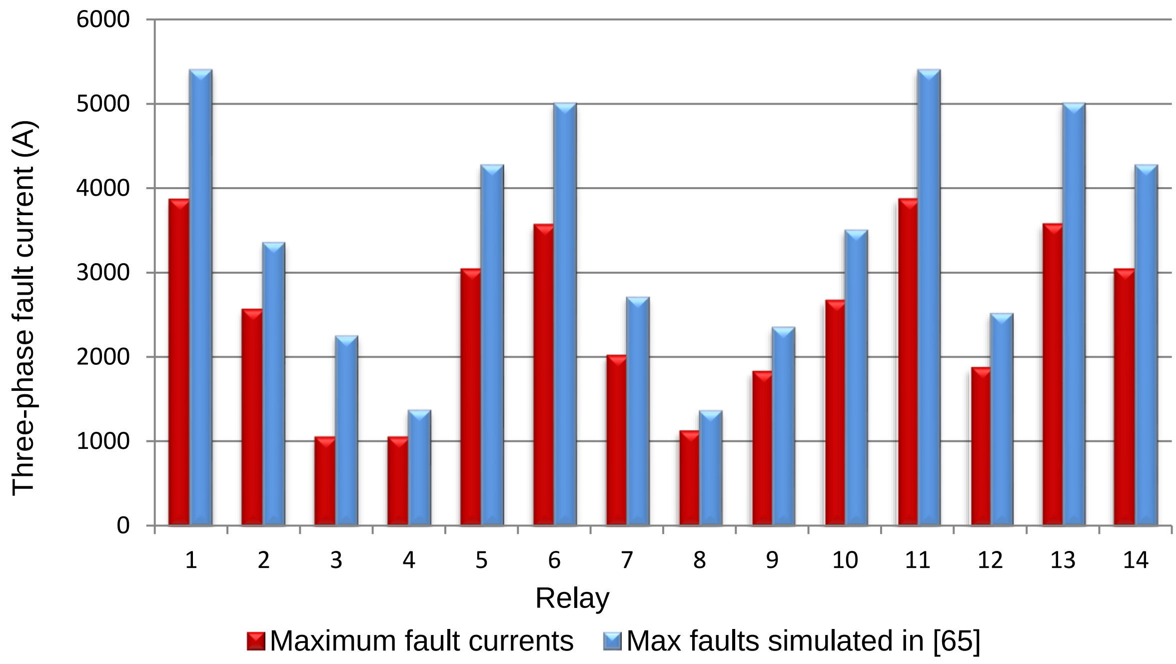

Figure 7-4: verification of three-phase fault current simulation results

The following Table 7-7 compares the results to verify that the DG source is modelled correctly before analysing the results. The simulated results obtained in PowerFactory are compared with the results calculated in the previous chapter (section 6.4.2).

Table 7-7: Comparison of the induction machine simulation results

	Calculated results		Simulated results	
	Magnitude	**Angle**	**Magnitude**	**Angle**
I_a	9297	-84.36	9235	99.27
I_b	9297	35.64	9235	-20.73
I_c	9297	154.36	9235	219.27

The above results are calculated using equations (6.20) to (6.25) for three-phase fault currents at the generator terminal. The magnitude error between the calculated and simulated results is less than 1% and the phase angle error is completely different. The reason for different angles could be different reference angles used in hand calculations and PowerFactory. However, this will not have a negative impact on the calculations since only magnitudes of fault currents are used in the calculations.

7.3 Case study 1 results and analysis

The following sections provide the results for case study 1. These are the primary and back-up relay's three-fault currents simulated at 5% of the protected line length. The primary and back-up fault currents are measured at the relay location. Relays are arranged in an ascending order and each pair is shown in column 1 (primary relay) and column 2 (back-up relay).

The usual procedure for grading relays in the ring network is to open the ring at the supply end and grade relays in a clockwise direction first and then anti-clockwise. Considering the network shown in Figure 7-1, relays looking in a clockwise direction are arranged to operate in the following tripping sequence R_7-R_6-R_5-R_4-R_3-R_2-R_1 and relays looking in the anti-clockwise are arranged in the same tripping sequence R_8-R_9-R_{10}-R_{11}-R_{12}-R_{13}-R_{14} respectively [26].

Table 7-8: Primary and back-up relay's fault currents

Primary relay	Back-up relay	Primary relay's Fault current (A)	Back-up relay's Fault current (A)
R_1	R_5 R_7	3858	1119 590
R_2	R_1	2551	2551
R_3	R_2	1734	1734
R_4	R_3	1034	1034
R_5	R_4 R_{12}	3030	298 582
R_6	R_4 R_{14}	3556	301 1115
R_7	R_5	2003	2003
R_8	R_9	1107	1107
R_9	R_{10}	1812	1812
R_{10}	R_{11}	2655	2655
R_{11}	R_{12} R_{14}	3859	590 1120
R_{12}	R_{13}	1859	1859
R_{13}	R_5 R_8	3564	1113 301
R_{14}	R_7 R_8	3030	582 298

The operating times of the primary and back-up relays for close-in[4] faults are recorded in Table 7-9 below. The primary relay is expected to clear the fault as fast as possible and only when the primary relay fails, the back-up relay can clear the fault. Analysing the results in Table 7-9, the primary relay's operating times should be faster than the back-up relay's. A coordination time interval (CTI) $\geq$ 0.3 seconds between the primary and back-up relay should be maintained.

Table 7-9: The comparison of the primary and back-up relays' operating times

Relay pairs		**Conventional**		**PSO**	
Primary relay	**Back-up relay**	**Primary relay's operating time (s)**	**Back-up relay's Operating time (s)**	**Primary relay's operating time (s)**	**Back-up relay's Operating time (s)**
R_1	R_5 R_7	0.703	1.003 1.003	0.698	1.003 1.003
R_2	R_1	0.543	0.843	0.590	0.890
R_3	R_2	0.653	0.953	0.367	0.676
R_4	R_3	0.412	0.719	0.242	0.548
R_5	R_4 R_{12}	0.533	0.833 0.833	0.485	1.011 1.011
R_6	R_4 R_{14}	0.751	1.051 1.051	0.659	0.986 0.986
R_7	R_5	0.679	0.979	0.586	0.886
R_8	R_9	0.402	0.702	0.224	0.536
R_9	R_{10}	0.631	0.931	0.436	0.783
R_{10}	R_{11}	0.854	1.154	0.632	0.936
R_{11}	R_{12} R_{14}	0.917	1.217 1.217	0.701	1.022 1.022
R_{12}	R_{13}	0.614	0.914	0.504	0.804
R_{13}	R_5 R_8	0.782	1.082 1.082	0.649	0.950 0.950
R_{14}	R_7 R_8	0.739	1.039 1.039	0.577	0.974 0.974

[4] Close-in fault is a bolted fault in front of the relay i.e. the fault is at the primary relay location.

The graph below plots the operating times of the primary relays calculated using both the conventional method and PSO algorithm. From the graph below, it is shown how the primary relay's operating times have been minimized by the PSO algorithm as compared to the conventional method. From Table 7-9 and Figure 7-5 the operating time of R_2 is not minimized. The time increases from 0.543 seconds to 0.590 seconds instead. However, this is the only relay and compared to other relays in the network, the operating time has been minimized drastically.

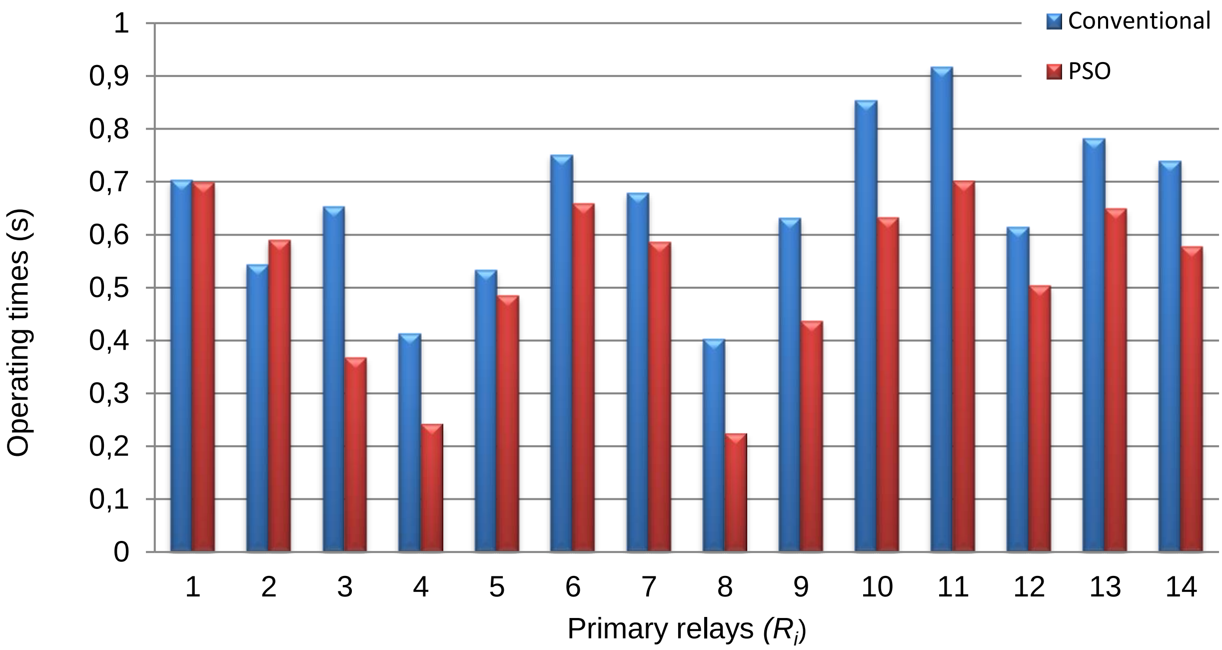

Figure 7-5: Comaprison of the primary relay's operating times

As discussed in Chapter 2, regarding five requirements of a protection system, speed is one of the critical protection design requirements, which cannot be compromised. The objective of this study is to ensure that the primary relays operate faster for close-in three-phase faults.

The results provided in Table 7-10 below shows the sum of the primary and back-up relay's operating times obtained from both the conventional and PSO algorithm. The sum of the primary relay's operating time is the defined objective function. This is the function being minimized. Thus, comparing the two values calculated using the conventional method and PSO algorithm, it is evident that the objective function ($f(x)$) is minimized from 9.22 seconds to 7.35 seconds.

Comparing the back-up operating times, the sum of the relay's operating times has reduced from 19.65 seconds to 17.95 seconds. This implies that the relays in the network are operating faster for close-in and far-bus faults. Therefore, minimum damage to system equipment, protection for the public and personnel is improved since the fault is cleared faster.

Table 7-10 : Primary and back-up relays' summed operating times

	Conventional	PSO
Primary relay's operating time ($\sum_{i=1}^{n} t_{ii}$)	9.220	7.350
Back-up relay's operating time ($\sum_{i=1}^{n} t_{ji}$)	19.645	17.953

In order to minimize the objective function, the best global positions (TMS) are calculated using both conventional method and PSO algorithm. Throughout the calculations, the pick-up currents are kept constant. In both conventional method and PSO algorithm, time multipliers are calculated using pick-up currents (in Table 7-5), fault levels calculated in Table 7-8 and the IDMT NI[5] curve is assumed for all calculations.

Table 7-11: Overcurrent relay calculated parameters

Calculated (TM_i)	Conventional	PSO
TM_1	0.20	0.20
TM_2	0.40	0.25
TM_3	0.15	0.10
TM_4	0.10	0.05
TM_5	0.15	0.10
TM_6	0.25	0.20
TM_7	0.30	0.25
TM_8	0.10	0.05
TM_9	0.25	0.15
TM_{10}	0.25	0.20
TM_{11}	0.20	0.15
TM_{12}	0.20	0.15
TM_{13}	0.40	0.30
TM_{14}	0.25	0.20

The results obtained by the conventional method are the same irrespective of how many times the program is executed (trials). However, the conventional coordination results obtained depend mainly

[5] NI refers to the normal inverse overcurrent relay characteristic

on the initial guess of the initial relay's settings. It is indicated in Chapter 6 that the initial operating times for all primary relays is set to operate in 0.2 seconds. Thus, if the time could be changed from 0.2 seconds to 0.3 seconds, longer operating times are expected.

In contrast to the conventional method, PSO algorithm is a stochastic search algorithm and calculates the time multipliers randomly. This implies that, different results can be obtained depending on how many times the algorithm is executed (trials). The results given in Table 7-11 are obtained after the fifth trial. The reason for executing the algorithm more than once is that PSO searches randomly through the search space and the results are different for each execution. Therefore, it is critical to execute the algorithm more than once and compare the results obtained per execution (or trial). The minimum cost function (objective function) is taken.

The inverse-time curves for the primary relays in the clockwise and anti-clockwise loops are drawn and shown in Figure 7-6 (a) to (h) below. The dotted lines in the time-current graph shows the maximum fault levels at the primary relay's (R_i) fault location.

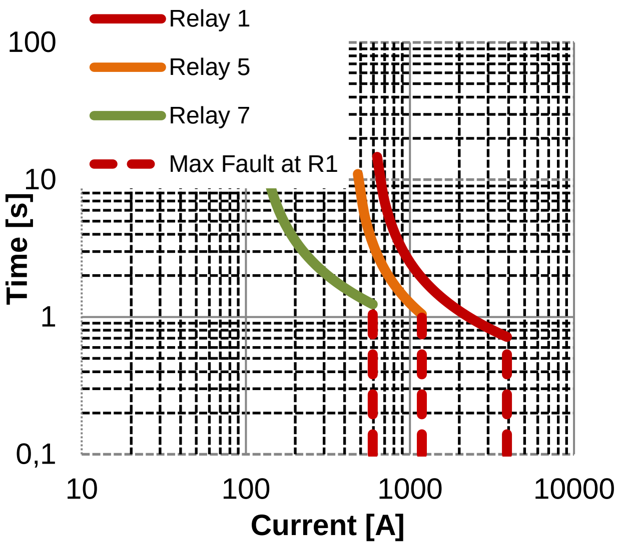

(a)

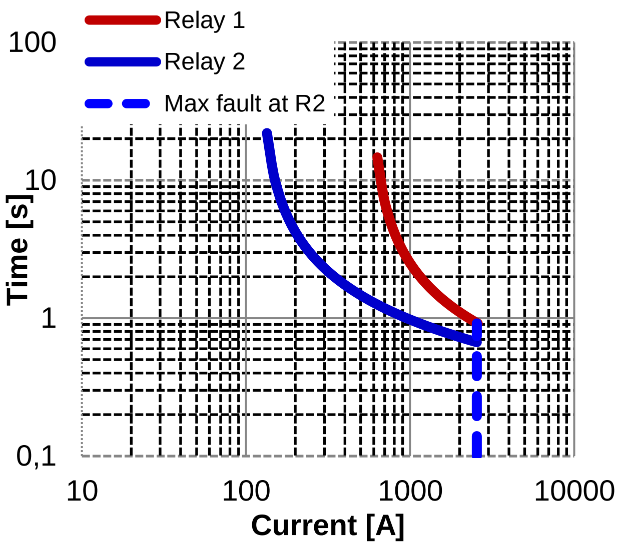

(b)

Using the graph provided in Figure 7-6(a) above to calculate coordination time interval for conventional method results, the first pair is used. Since, the primary relay R_1 measures a fault current of 3.858 kA, the back-up relay R_5 measures 1.119 kA for the same fault. Thus, the primary relay's time from the graph is 0.73 seconds and the back-up relay's time is 1.088 seconds. CTI = 1.088 – 0.73 = 0.358 seconds. The reason why this CTI is not the same as the calculated CTI is that the approximated fault levels are used when plotting the graphs in Microsoft Excel®.

The IDMT O/C curves plotted in (c), (d) and (f) shows the coordination between the relay pairs where both the primary and back-up relays detect the same magnitude of fault current. In (c), the pick-up current of the back-up relay (R_2) is set to be sensitive than the primary relay (R_3) due to the small magnitude of the load current. The drawback with the selected setting is that for faults below 700 A, the back-up relay will operate faster than the primary relay. However, setting relay R_2 to be less sensitive than relay R_3 will make relay R_2 not to pick-up for faults it is supposed to operate for.

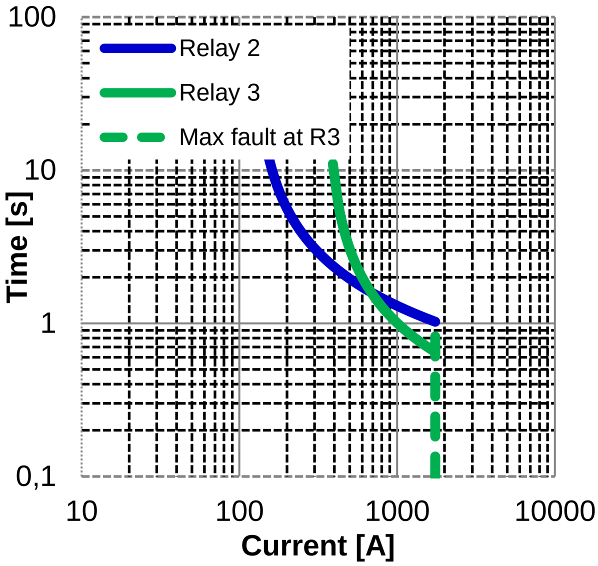

(c)

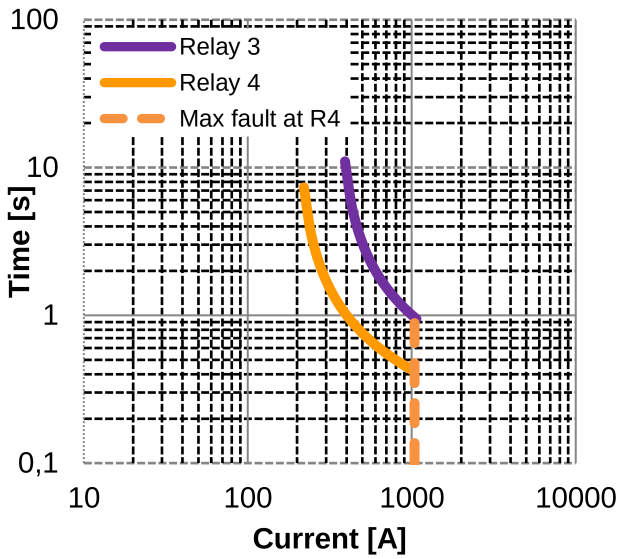

(d)

The graph in (e) below, shows a pair consisting of three relays, that is, one primary and two back-up relays respectively. The back-up relays do not measure the same magnitude of fault current, because they are connected to different circuits in the IEEE 8-bus test case. The quickest back-up relay operating time is coordinated with the primary relay (R_5).

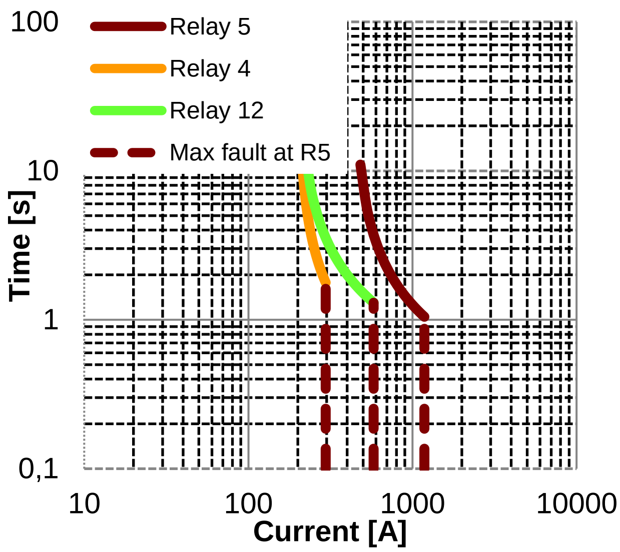

(e)

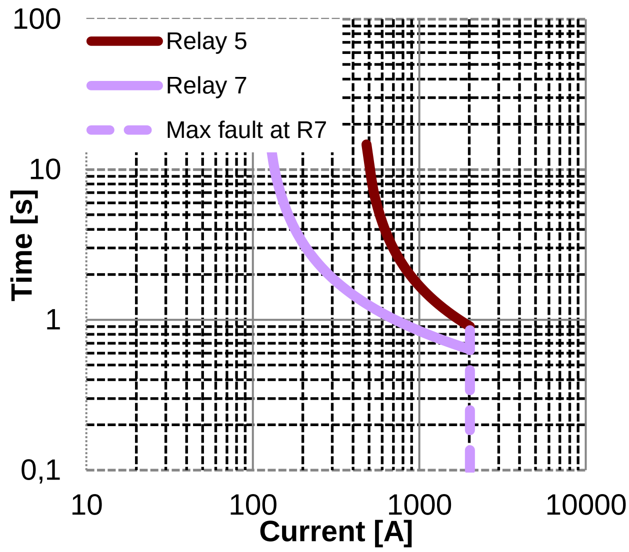

(f)

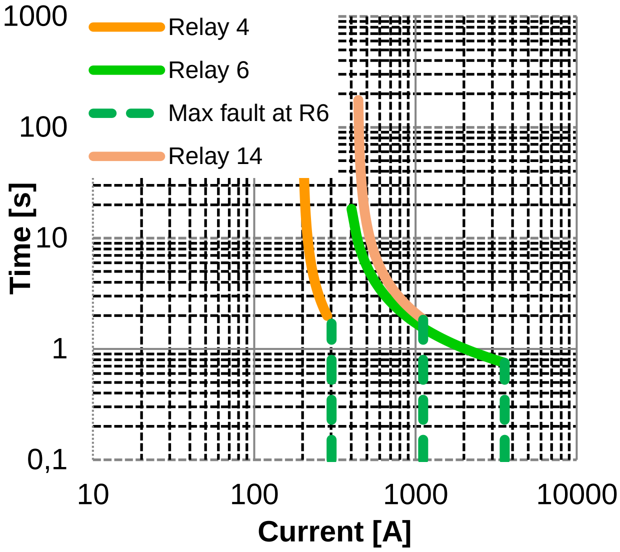

(h)

Figure 7-6: The IDMT O/C curves for relay pairs in the clockwise loop

The time-current graph plotted below in Figure 7-7(a) to (h) are the relay pairs in the anti-clockwise loop. The first and second pair are shown in (a) and (b) below. In (a) and (b) both the primary and back-up relays detect the same magnitude of fault current of 1.1 kA and 1.8 kA respectively. The primary relay (R_8) operates in 0.50 seconds and the back-up relay (R_9) operates in 0.85 seconds as shown in the graph. Thus, the grading margin of 0.85 – 0.50 = 0.35 seconds is obtained. In the second pair, the obtained grading margin is 1.05 – 0.70 = 0.35 seconds.

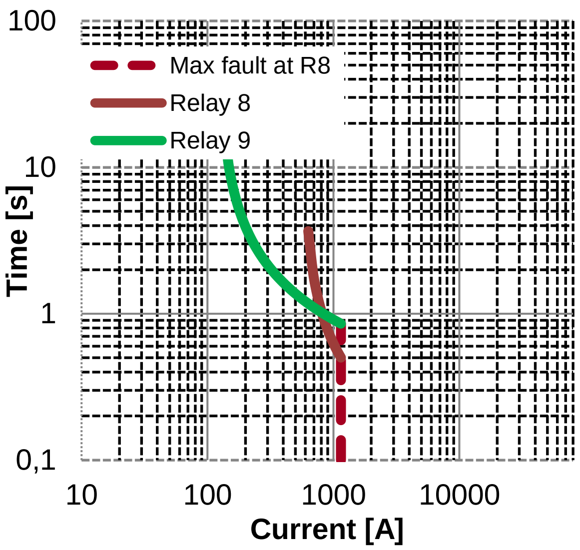

(a)

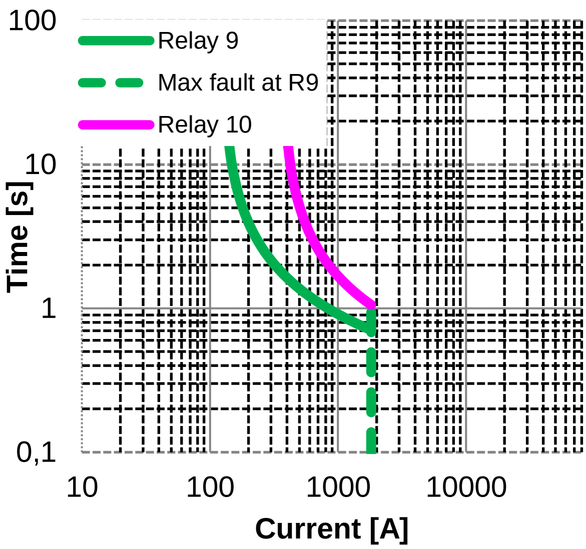

(b)

Considering the relay pair in Figure 7-7(d), the primary relay is R_{11}, which measures a current of 3.8 kA with R_{12} and R_{14} are back-up relays measuring 590 A and 1.1 kA respectively. Considering the conventional method results, the primary relay clears the fault in 0.91 seconds and the minimum time between the back-up relays is selected, which is 1.22 seconds, thus CTI = 0.31 seconds. Because of an interconnected network, the back-up relays do not often measure the same current as the primary relay.

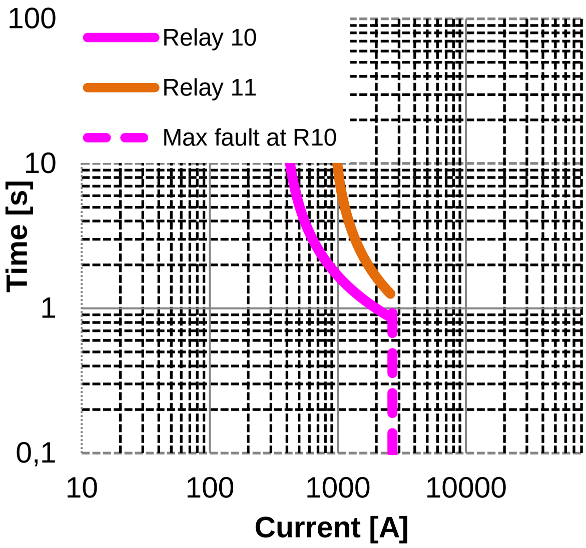

(c)

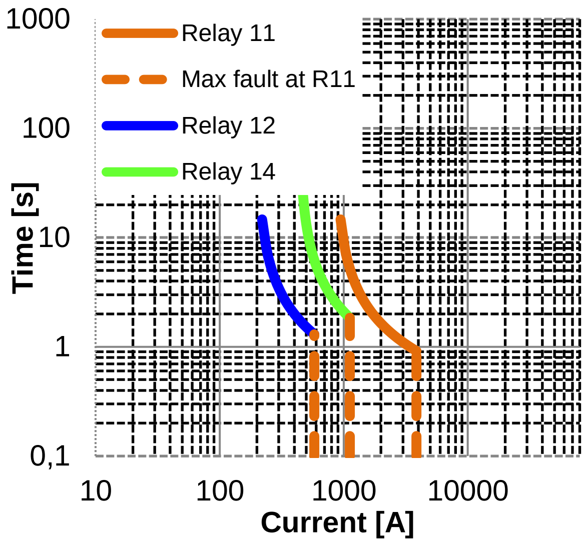

(d)

In Figure 7-7(f), the primary relay R_{13} is paired with two relays R_5 and R_8 respectively. Due to an interconnected network, back-up relays detect different magnitude of currents and operates at different times. The quickest relay between the two (i.e. R_5 and R_8) is coordinated with the primary relay. In the graph, R8 is not plotted, because it measures a current of 300 A, which operates longer than the other back-up relay.

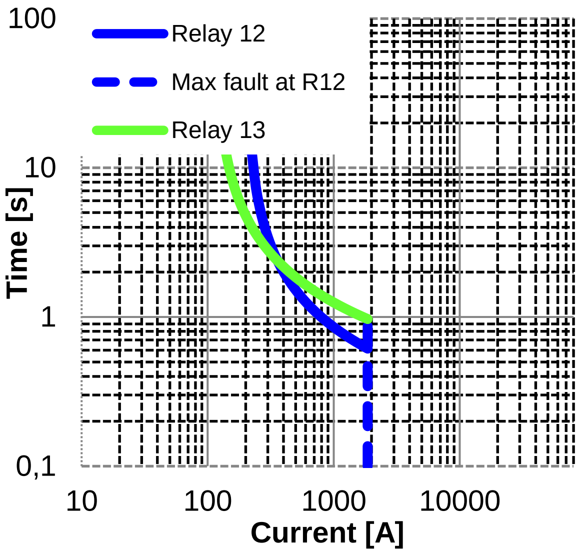

(e)

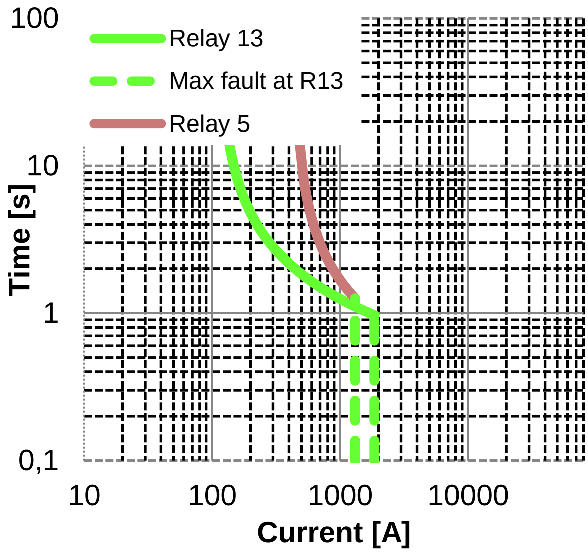

(f)

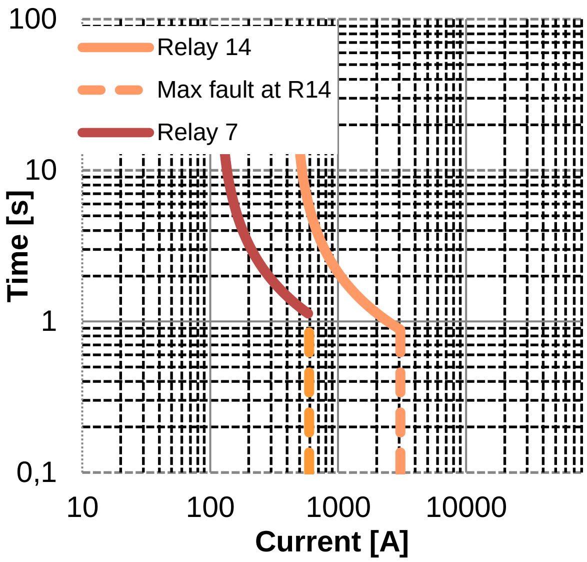

(h)

Figure 7-7: The IDMT O/C curves for relay pairs in the anti-clockwise loop

Observing the results given in Table 7-9 to 7-11 including the time-current graphs in Figures 7-6 and 7-7, the following conclusions are made in case study 1:

a) the operating times for both primary and back-up relays is faster,
b) the time multiplier settings (TMS) are minimized and
c) the sum of the primary relay's operating time $f(x)$, has been minimized from 9.22 seconds to 7.35 seconds.

The next section modifies the network to accommodate a wind power plant by adding a non-inverter coupled wind power plant to the 8-bus test case. The non-inverter coupled DG source is used to assume the worst-case scenario, since it was shown in Chapter 3 how each machine respond to system faults.

Adding either type III and type IV in the 8-bus test case will not have any significant impact, since the maximum fault current the two DG sources can contribute to the grid is maximum load current. Depending also on the power electronics control systems used, the current contribution can be very small. The same applies to the PV plant, they are connected to the grid through inverters and tend to disconnect faster during fault conditions. As shown in Chapter 3, the contribution from a PV plant is zero for the duration of the fault and after the fault is cleared, it will reconnect to the grid depending on the control system's settings.

It is therefore necessary to consider the cases where the contribution of the WTG is unpredictable and unknown and has a significant impact to the grid protection.

7.4 Case study 2 results and analysis

When a DG source is connected to the existing distribution network, it is expected to increase the fault currents in the network, since the selected WTG is can contribute a significant magnitude of fault current. Secondly, the direction of both the power flow and fault current is expected to change as indicated in Chapter 1. Load-flow studies are provided in Appendix C and fault current results are given in the next page.

Table 7-12 below provides the new simulated fault currents in the modified 8-bus tests case for both primary relays in the first column and back-up relays in the second column.

Table 7-12: Primary and back-up relay's fault currents

Primary relay	Back-up relay	Primary relay's Fault current (A)	Back-up relay's Fault current (A)
R_1	R_5 R_7	3549	743 390
R_2	R_1	2368	2370
R_3	R_2	1610	1611
R_4	R_3	1034	959
R_5	R_4	1058	366
R_6	R_4 R_{14}	2997	378 1277
R_7	R_5 R_6	1597	387 1598
R_8	R_9	901	901
R_9	R_{10}	1553	1554
R_{10}	R_{11}	2333	2259
R_{11}	R_{12} R_{14}	3309	681 1299
R_{12}	R_{13}	1781	1782
R_{13}	R_5 R_8	3345	719 202
R_{14}	R_7 R_8	2993	355 191

The fault currents given in Table 7-12 when compared to fault current in Table 7-8 instead of increasing, they have decreased. Some currents have decreased significantly and others marginally.

Each machine contributes approximately 2.91 kA and the total fault current at the LV bus is the sum of the entire machine's contribution. A step-up transformer (0.69/10 kV) is used. Therefore, the fault current on the MV bus is transformed by the ratio of $k = 0.069$, which will decrease the current significantly. The DG source is connected to the network through a transformer, which is rated 150/10 kV, again the current is transformed to the HV side, which is 133 A on the 150 kV network.

With a peculiar behaviour of the network when the DG source is connected, therefore the following results in Table 7-13 are the newly calculated operating times.

Table 7-13: Primary and back-up relay's operating times

Relay pairs		**Conventional**		**PSO**	
Primary relay	**Back-up relay**	**Primary relay's operating time (s)**	**Back-up relay's Operating time (s)**	**Primary relay's operating time (s)**	**Back-up relay's Operating time (s)**
R_1	R_5 R_7	0.735	1.035 1.035	0.968	1.268 1.268
R_2	R_1	0.445	0.475	0.939	1.239
R_3	R_2	0.685	0.985	0.779	1.079
R_4	R_3	0.419	0.719	0.893	1.193
R_5	R_4	0.787	1.087	0.757	1.832
R_6	R_4 R_{14}	0.488	0.788 0.788	0.489	0.789 0.789
R_7	R_5 R_6	0.330	0.630 0.630	0.402	0.702 0.702
R_8	R_9	0.312	0.612	0.305	0.605
R_9	R_{10}	0.536	0.836	0.473	0.774
R_{10}	R_{11}	0.731	1.031	0.604	0.904
R_{11}	R_{12} R_{14}	0.767	1.067 1.067	0.646	0.946 0.946
R_{12}	R_{13}	0.313	0.613	0.525	0.825
R_{13}	R_5 R_8	0.498	0.798 0.798	0.668	0.968 0.968
R_{14}	R_7 R_8	0.743	1.043 1.043	0.598	1.052 1.052

The sum of the operating times of both the primary and back-up relays is presented in Table 7-14. In this case study, the conventional method seems to perform better than PSO. This is clearly shown in summary in Table 7-14. Instead of minimizing the operating times, the sum of the primary relay's operating time is higher than the results obtained from the conventional method. This is the case with the back-up relay's operating times too.

Table 7-14: The sum of the primary and back-up relays' operating times

	Conventional	PSO
Primary relay's operating time ($\sum_{i=1}^{n} t_{ii}$)	7.7898	9.045
Back-up relay's operating time ($\sum_{i=1}^{n} t_{ji}$)	17.808	21.031

The graph below plots the operating times of the primary relay's operating times when using both methods, which are compared in this research. The conclusion drawn from this case study is that the conventional method is still capable of optimizing the operating times of the primary relays. However, the only disadvantage with the conventional method is that it is deterministic. To get different results, either the pick-up current or CTI should be increased and then the results will be different. Otherwise with the same inputs, the results will always be the same.

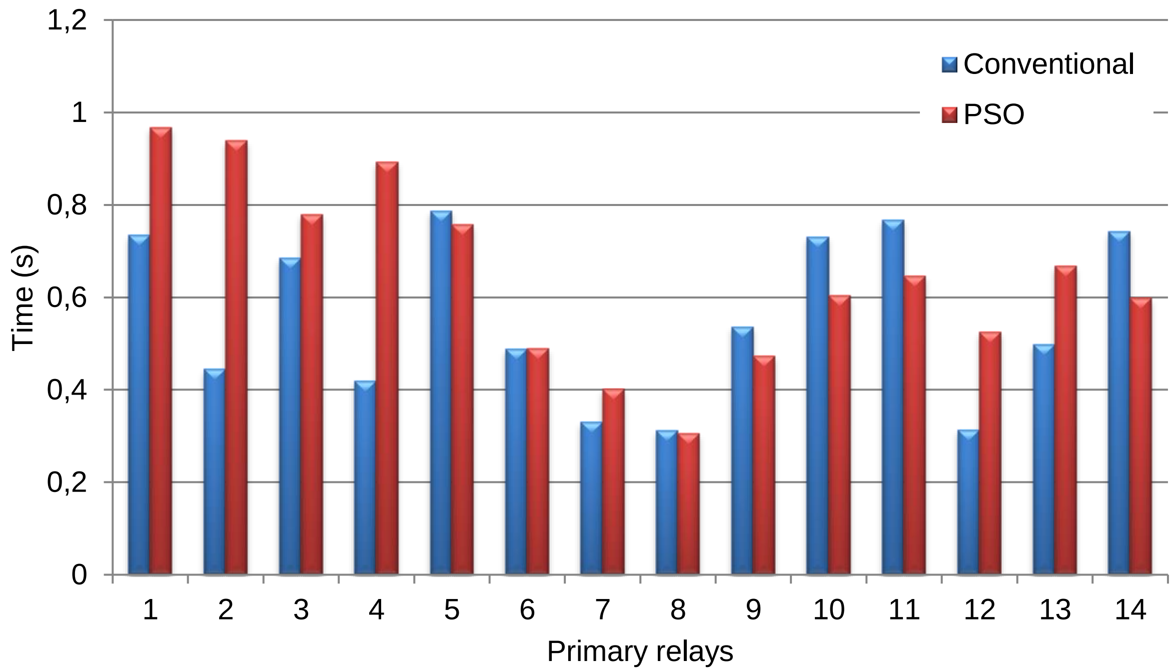

Figure 7-8: Comparison of the primary relay's operating times

Considering the TM settings obtained in this case study, it is expected that the TM settings obtained with the conventional method to be smaller than the results obtained with PSO based on the operating times.

Table 7-15: Best calculated TMs

Calculated $(\boldsymbol{TM_i})$	**Conventional**	**PSO**
TM_1	0.20	0.25
TM_2	0.40	0.40
TM_3	0.15	0.15
TM_4	0.10	0.20
TM_5	0.10	0.10
TM_6	0.15	0.15
TM_7	0.10	0.10
TM_8	0.10	0.10
TM_9	0.20	0.25
TM_{10}	0.20	0.15
TM_{11}	0.15	0.10
TM_{12}	0.10	0.15
TM_{13}	0.25	0.35
TM_{14}	0.25	0.20

Based on the results in Tables 7-13 and 7-14, the following conclusions are drawn from case study 2:

a) the operating times for both primary and back-up relays are slower compared to the calculated operating times by the conventional method,
b) the time multiplier settings (TMS) are not all minimized and
c) the sum of the primary relay's operating time $f(x)$ increased from 7.789 seconds to 9.045 seconds.

Therefore, PSO did not perform well in this case study as the conventional method has shown to perform better.

7.5 Performance of the PSO algorithm

This section analyses the performance of the PSO algorithm in both case studies. The capabilities of the PSO algorithm to maintain selectivity and produce the best results are analysed.

7.5.1 Case study 1 best fitness functions

The best fitness function of the results in Figure 7-11 is shown below. The simulation is executed 5 times and each simulation's best fitness is recorded, then the best amongst the pool is selected. In this case, the best fitness function is 7.3504.

Table 7-16: Best calculated fitness function per execution

Execution number	Best fitness
1	7.4607
2	7.4218
3	7.4592
4	7.3504
5	7.3810

The number of iterations selected is 500, since it is proved by many studies that PSO converges faster to the global minimum. The graph in Figure 7-9 shows the best fitness obtained during the fourth interval.

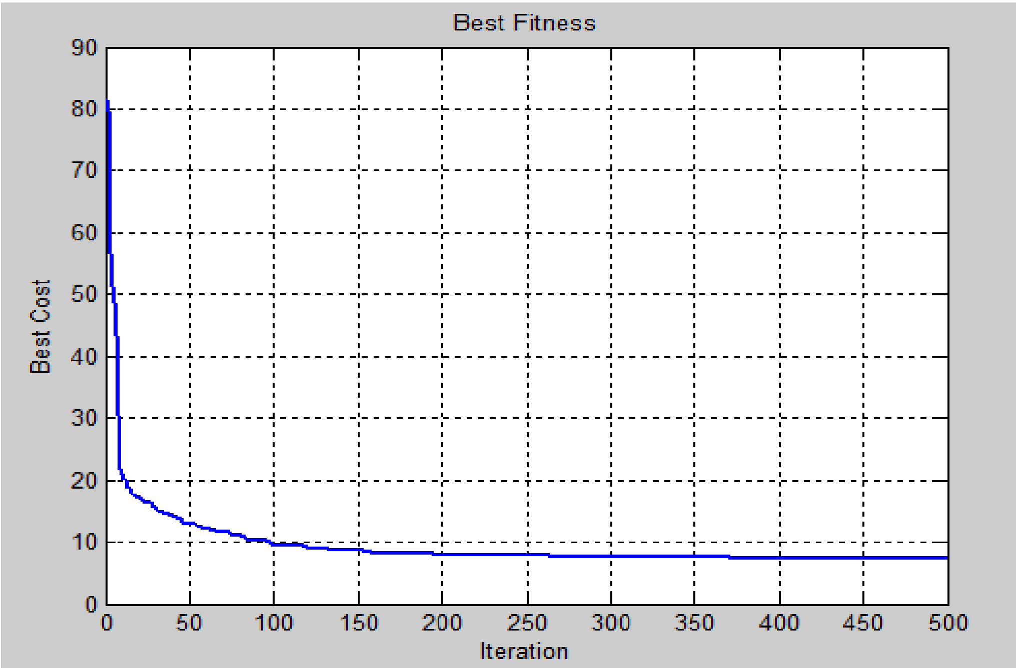

Figure 7-9: Best fitness function obtained in Matlab®

7.5.2 Case study 1 penalty functions

Penalty functions are methods used to transform the unconstrained optimization problem into a constrained optimization problem. The constraint functions G_i and L_i is either added to- or subtracted from the original objective function $f(\bar{x})$ based on violation present in the solution.

The objective function implemented in Matlab® is formulated in equation (7.1) below. The coordination criteria constraint can easily be violated. Thus, the penalty factor β_1 is set to a higher positive number. The penalty rule states that the penalty should be as low as possible. This is due to the fact that the penalty is either too high or too low. For a higher penalty factor the optimum solution lies on the boundary of the feasible solution [55].

$$f(\bar{x}) = \alpha_i \sum_{i=1}^{n} f(x_i) + \left[\beta_1 \sum_{i=1}^{n} \Delta t_{mb} + \beta_2 \sum_{i=1}^{n} g_i\right] \tag{7.1}$$

Where, the following values were used in the above equation to implement the penalties in the objective function. The value of β_1 is obtained through a trial and error process. The value of β_1 is selected in such a way that the coordination criteria and the boundaries of the TMs are not violated. From equation (7.1), the function (g_i) is used to sum all the operating times of the back-up relays. The value of (β_2), which is the penalty factor applied to the sum of all the back-up relays is set to zero, since it does not have a significant improvement on the final results.

Table 7-17 : Constants used in the objective fucntion

Constant	Value
α_i	1
β_1	17
β_2	0

In the following Table 7-18, the penalty function is calculated and coordination measure. The penalty is implemented only when there is no coordination between the primary and back-up relays. Where the penalty is a zero, therefore coordination measure between the primary and back-up relays is greater than 0.3 seconds. Otherwise the penalty will take effect and apply the following equation to ensure that coordination is met.

$$penalty = t_{primary} - t_{back-up} + 0.3 \tag{7.2}$$

Effectively, the coordination time interval of 0.3 seconds is added to the previous coordination time interval, which is less than 0.3 seconds. Coordination measure calculates the difference between the primary and back-up relay's operating time for a close-in three-phase fault.

Table 7-18: Coordination measure and penalty factors in case study 1

Primary relay	Back-up relay	Penalty factor	Coordination measure $[dt = t_{bu} - t_{pri} - CTI]$
R_1	R_5 R_7	0	0.31
R_2	R_1	0	0.30
R_3	R_2	0	0.31
R_4	R_3	0	0.31
R_5	R_4 R_{12}	0	0.53
R_6	R_4 R_{14}	0	0.33
R_7	R_5	0	0.30
R_8	R_9	0	0.31
R_9	R_{10}	0	0.35
R_{10}	R_{11}	0	0.30
R_{11}	R_{12} R_{14}	0	0.32
R_{12}	R_{13}	0	0.30
R_{13}	R_5 R_8	0	0.30
R_{14}	R_7 R_8	0	0.40

7.5.3 Case study 2 best fitness function

The best fitness function is calculated every time the position and velocity of the particle is updated. In Table 7-19 is the best objective function calculated every time the algorithm is executed. Out of the calculated best cost functions, the best function is the function with minimum values. The number of iterations selected is 1000. However, many studies indicate that PSO converges faster to the global minimum.

Table 7-19: Best calculated fitness function per execution

Execution number	Best fitness
1	11.7701
2	11.7634
3	11.7704
4	11.7761
5	11.7730

The graph in Figure 7-10 shows the best fitness obtained during the fourth interval.

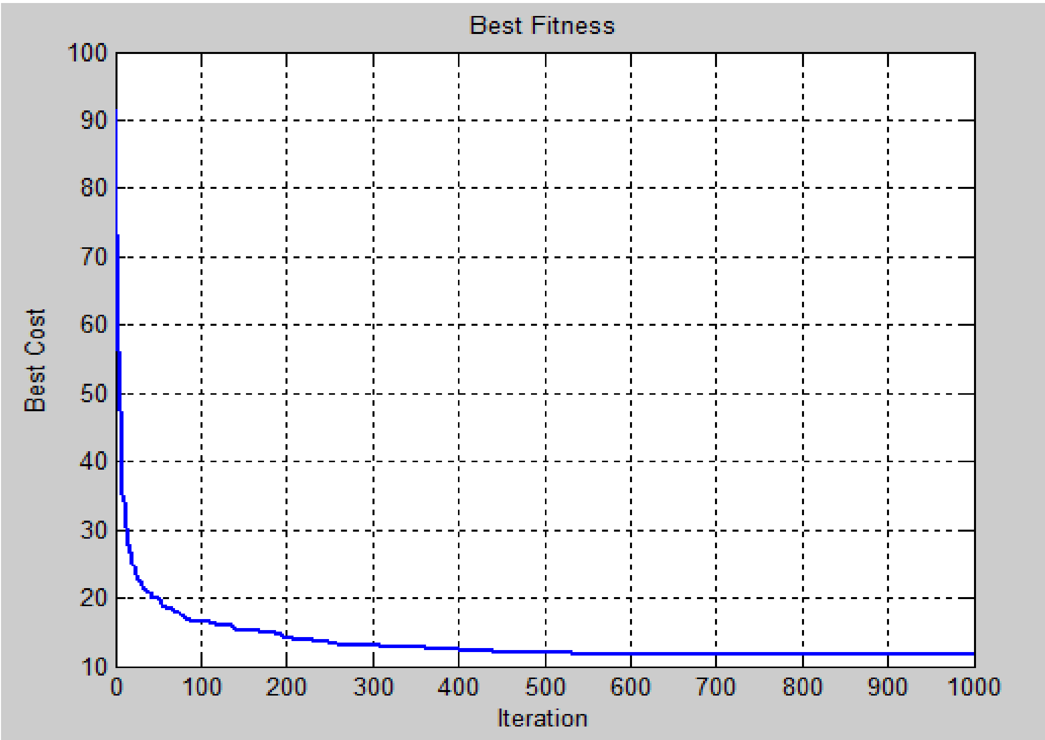

Figure 7-10: Best fitness function for IEEE network with DG source

The next section provides the performance of the PSO algorithm for case study 2. The same penalty functions and best fitness function plot is presented. Lastly, coordination measure is also presented, which calculates coordination between the primary and back-up relays.

7.5.4 Case study 2 penalty functions

Table 7-20: Coordination measure and penalty factors in case study 2

Primary relay	Back-up relay	Penalty factor	Coordination measure $[dt = t_{bu} - t_{pri} - CTI]$
R_1	R_5 R_7	0 0	0.30
R_2	R_1	0	0.30
R_3	R_2	0	0.30
R_4	R_3	0	0.30
R_5	R_4	0	1.075
R_6	R_4 R_{14}	0 0	0.30
R_7	R_5 R_6	0 0	0.30
R_8	R_9	0	0.30
R_9	R_{10}	0	0.30
R_{10}	R_{11}	0	0.30
R_{11}	R_{12} R_{14}	0 0	0.30
R_{12}	R_{13}	0	0.30
R_{13}	R_5 R_8	0 0	0.30
R_{14}	R_7 R_8	0	0.45

Based on the results provided in Tables 7-18 and 7-20, the following conclusions are drawn:

In both cases, coordination time interval of 0.3 seconds and above is maintained. When comparing with the conventional method, the conventional method maintains a coordination time interval of 0.30 seconds for all relay pairs. There are only a few pairs whose CTI is more than 0.3 seconds.

7.6 Validation of PSO algorithm

The objective of this research is to propose an optimization algorithm, which can be used to improve on the settings of the directional overcurrent relays in a distribution network with DG sources as calculated by the conventional method. To obtain optimal coordination results, the conventional and PSO methods are used and the analysis of their performance is done through comparison. The comparison between the conventional method and PSO algorithm is done in the previous sections using the IEEE 8-bus test case. In this section the proposed algorithm (PSO) is validated by selecting one of the HV network from the South African utility network. The Makalu 88 kV ring network which is in the border of the Free-State and Gauteng province is selected to validate the proposed optimization algorithm. The ring network is shown in Figure 7-11. The Makalu substation belongs to the transmission division. Therefore, the feeder settings at Makalu 88 kV busbar (R_1, R_7 and R_{11}) are calculated by the transmission settings department and the other relay's settings in the ring are calculated by the distribution settings department.

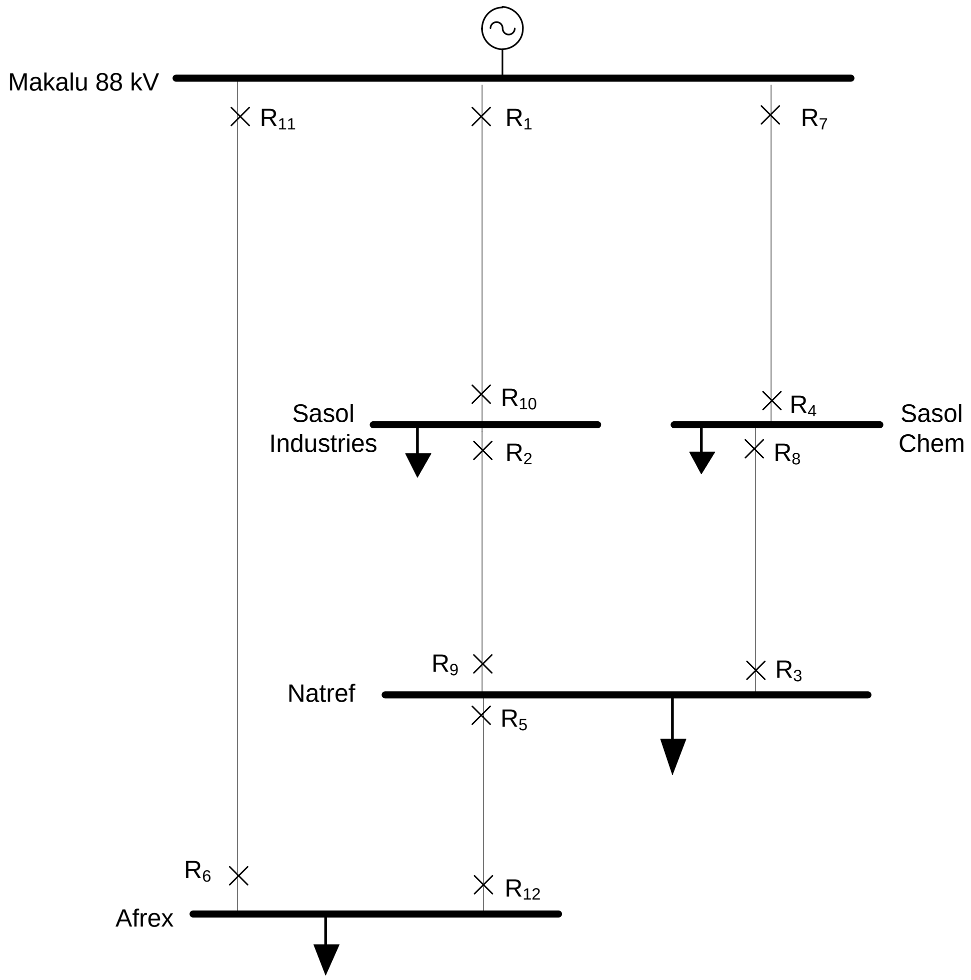

Figure 7-11 : The 88 kV Makalu ring network

In the selected network, there are 12 directional overcurrent relays and 18 relay pairs to be coordinated. The relays are numbered from R_1 to R_{12} as shown in the diagram. The overcurrent settings provided in Table 7-21 provides the applied settings of the overcurrent relays in the network. These settings are implemented and verified with the field technicians in the distribution network.

Table 7-21: The applied overcurrent settings in the Makalu ring

Substation	**Feeder**	**Relay number**	**CTR**	**Plug setting**	**TM**
Makalu	Sasol Industries	R_1	1200/1	75%	0.30
Sasol Industries	Natref	R_2	600/1	100%	0.35
Natref	Sasol Chem	R_3	600/1	100%	0.30
Sasol Chem	Makalu	R_4	600/1	100%	0.15
Natref	Afrex	R_5	600/1	100%	0.30
Afrex	Makalu	R_6	600/1	100%	0.15
Makalu	Sasol Chem	R_7	1200/1	75%	0.50
Sasol Chem	Natref	R_8	600/1	100%	0.40
Natref	Sasol Industries	R_9	600/1	100%	0.25
Sasol Industries	Makalu	R_{10}	600/1	100%	0.10
Makalu	Afrex	R_{11}	1200/1	75%	0.50
Afrex	Natref	R_{12}	600/1	100%	0.40

The maximum fault currents measured by the primary and back-up relays are simulated in PowerFactory and recorded in Table 7-22 below. These fault currents are used when calculating the new settings of the identified 12 primary relays in the ring. The applied settings are later compared with the new calculated settings using the proposed PSO algorithm and discussed at the end of the chapter.

Table 7-22 : Primary and back-up relays fault currents

Primary relay	Back-up relay	Primary relay's fault current (A)	Back-up relay's fault current (A)
R_1	R_4 R_6	30495	285 226
R_2	R_1	8171	8171
R_3	R_2 R_{12}	11548	5305 6245
R_4	R_3	10377	10377
R_5	R_2 R_8	12959	5207 7753
R_6	R_5	8077	8077
R_7	R_6 R_{10}	30391	336 286
R_8	R_7	8760	8760
R_9	R_8 R_{12}	13890	7761 6135
R_{10}	R_9	10377	10377
R_{11}	R_4 R_{10}	29901	419 281
R_{12}	R_{11}	9805	9805

7.6.1 Relay coordination results analysis

The operating times of the primary and back-up relays are calculated and tabulated in the following Table 7-23. The operating times in the third and fourth column are calculated using the applied settings obtained from the settings departments (i.e. Transmission and Distribution). The fifth and sixth columns present the results of the newly calculated settings using PSO algorithm.

The back-up operating times are not considered that much, since the probability of main protection and its back-up protection failing is minimal. However, it is also crucial to ensure that the back-up relays do not operate longer than 2 seconds or 3 seconds. In the first relay pair, the back-up operating time is 2.6 seconds. This is a very long operating time, but the reason why these relays (R4 and R6) are operating longer is the small magnitude of fault currents they measure when there is a fault near R1.

Table 7-23: Comparison of the applied setting with the PSO calculated results

Relay pairs		Applied settings		PSO	
Primary relay	**Back-up relay**	**Primary relay's operating time (s)**	**Back-up relay's Operating time (s)**	**Primary relay's operating time (s)**	**Back-up relay's Operating time (s)**
R_1	R_4 R_6	0.575	0.975 0.975	0.764	2.589 2.589
R_2	R_1	0.912	0.922	0.835	1.236
R_3	R_2 R_{12}	0.689	1.089 1.089	0.604	1.004 1.004
R_4	R_3	0.256	0.656	0.224	0.628
R_5	R_2 R_8	0.663	1.063 1.063	0.474	0.876 0.876
R_6	R_5	0.274	0.674	0.162	0.536
R_7	R_6 R_{10}	0.960	1.360 1.360	0.789	1.195 1.195
R_8	R_7	1.017	1.417	0.835	1.235
R_9	R_8 R_{12}	0.540	0.940 0.940	0.462	0.876 0.876
R_{10}	R_9	0.170	0.570	0.104	0.511
R_{11}	R_4 R_{10}	0.964	1.365 1.365	0.835	1.235 1.235
R_{12}	R_{11}	0.975	1.375	0.838	1.239

Table 7-24 presents the summation of the primary and back-up relays. Evidently, the conventional method maintains selectivity although slower when compared to PSO. However, PSO tends to be faster than the conventional method, especially when observing the primary relay's performance.

Table 7-24: Comparison of the sum of the primary and back-up times

	Applied	**PSO**
Primary relay's operating time ($\sum_{i=1}^{n} t_{ii}$)	7.605	6.926
Back-up relay's operating time ($\sum_{i=1}^{n} t_{ji}$)	19.198	20.935

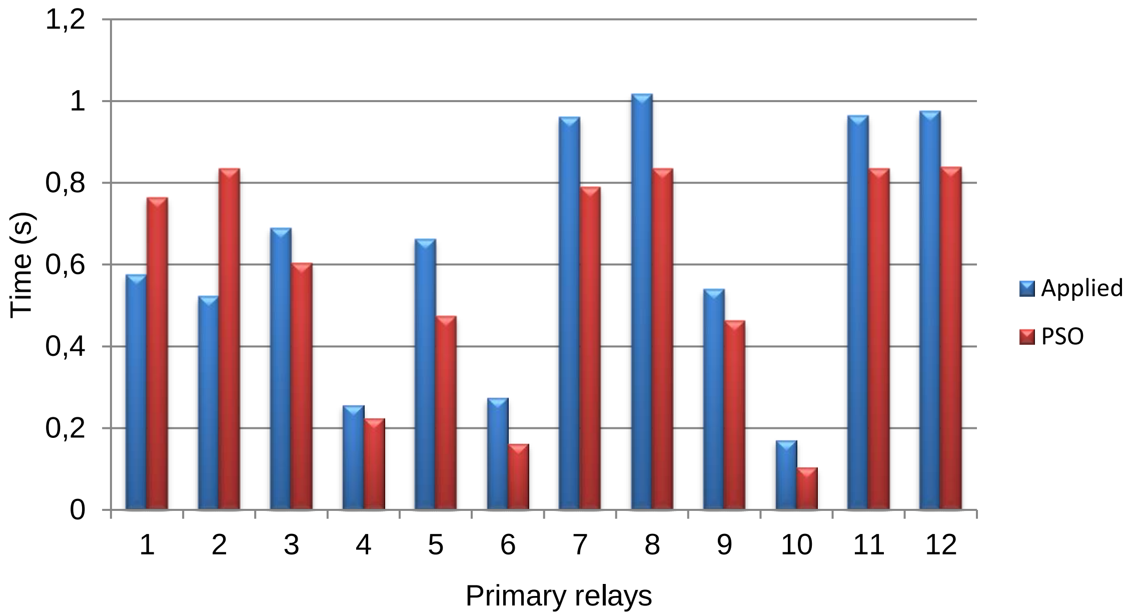

Figure 7-12: Comparison of the operating times of the primary relays in the Makalu ring

When comparing, the results obtained from the conventional method used primarily in the industry and PSO algorithm, it is evident from the graph in Figure 7-12 that the operating times of the primary relays are minimized (i.e. reduced operating times), therefore yields faster operating times compared to the old settings calculated by the conventional method. Figure 7-13 below shows a comparison of the TMs calculated by both the conventional method and PSO algorithm. There are only two relays whose results are not improved.

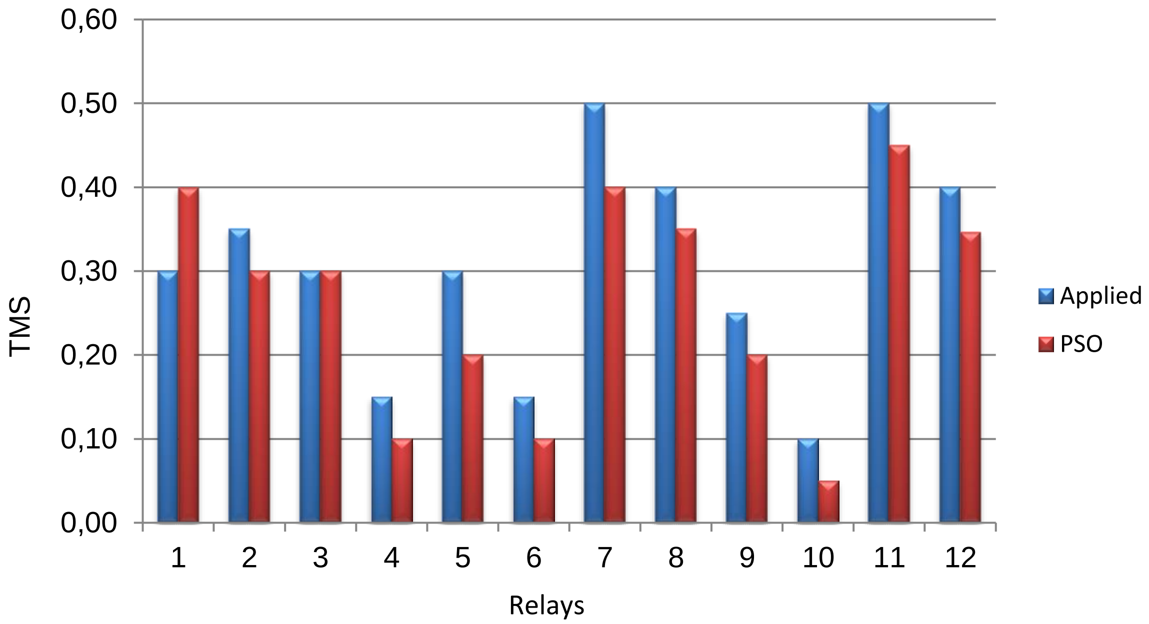

Figure 7-13: Comparison of the calculated TMS of the primary relays in the Makalu ring

7.6.2 Overcurrent relay's time-current graphs

The following IDMT O/C curves provided below in Figure 7-14 (a) to (n) show how the PSO algorithm has improved the operating times of the relays in the Makalu network. The IDMT O/C curves on the left-hand side show the results as calculated by the conventional method. While the IDMT O/C curves on the right-hand side show the results as calculated by the PSO algorithm.

In the first pair, it is evident that the two relays operate at approximately the same time for a fault at relay R_2 in Figure 7-14(a). However, by recalculating the same relay's settings using PSO algorithm the operating times of both relays are improved as shown in Figure 7-14(b).

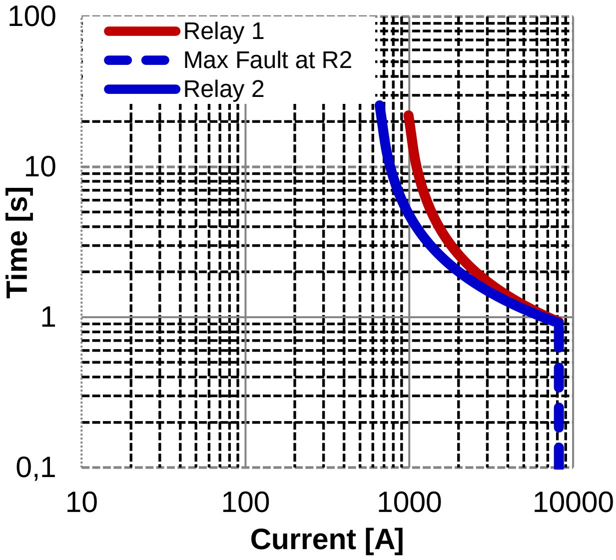

(a)

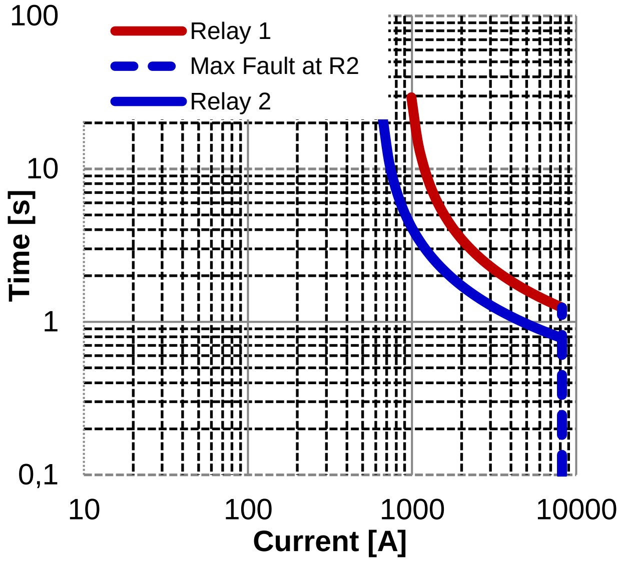

(b)

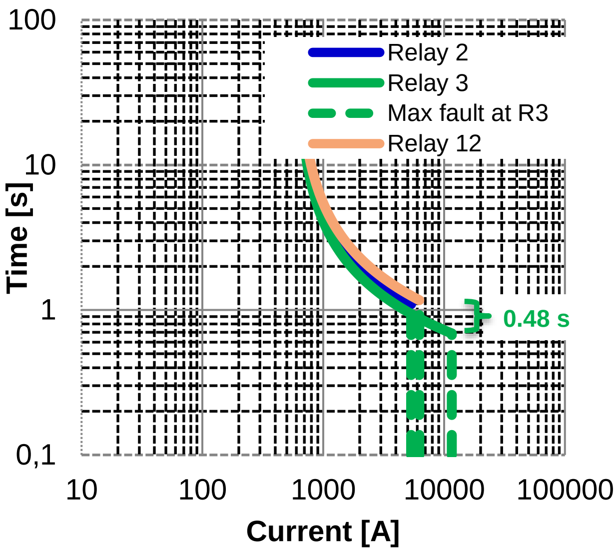

(d)

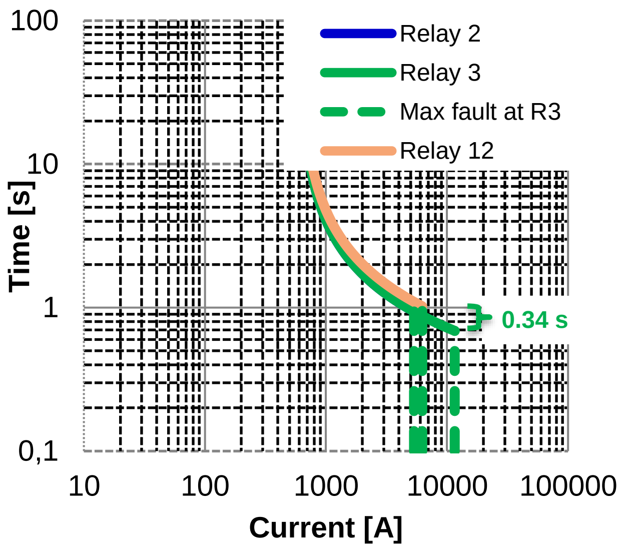

(c)

Analysing the results in Figure 7-14(c) and (d), the operating time of R_{12} (back-up relay) as calculated by the conventional method is 1.16 seconds and the new operating time as calculated by PSO is 1.02 seconds. In this case the primary relay settings remain the same and the settings, which are improved are the back-relay's R_{12}. Thus, the coordination time interval of 0.34 seconds is obtained as compared to a coordination time interval of 0.48 seconds.

The operating time of the primary relay R_4 (orange) has been improved from 0.37 seconds to 0.23 seconds as shown in Figure 7-14(f). The back-up relay R_3 settings remains the same and the grading margin in this relay pair is bigger than the grading margin as calculated by the conventional method. However, the fast-operating time of the primary relay for a close-in three-phase fault is better than a grading margin of 0.3 seconds as calculated before by the conventional method.

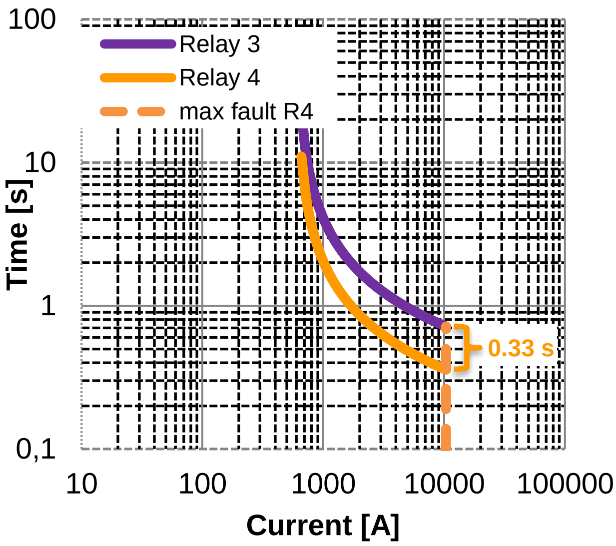

(e)

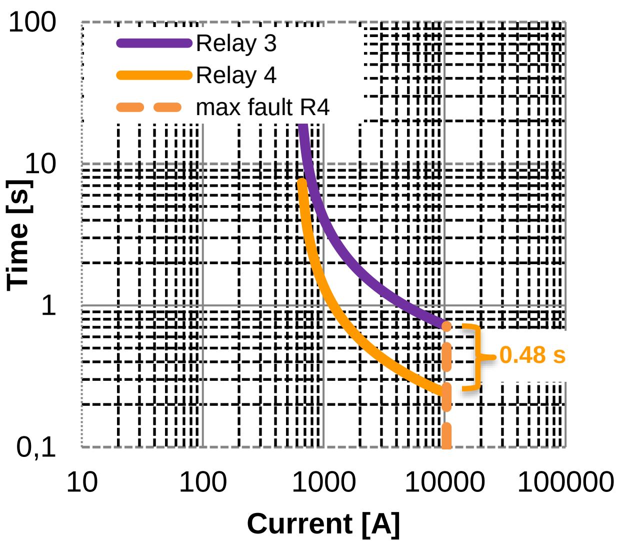

(f)

In Figure 7-14(h) and (g), both primary and back-up relay's operating times are minimized. The primary relay's operating time has been reduced from 0.67 seconds to 0.55 seconds and the back-up relay from 1.06 seconds to 0.93 seconds. These newly calculated operating times of both the primary and the back-up relays yield a coordination time interval of 0.39 – 0.38 = 0.01 seconds. In the next pair, the coordination time interval obtained by the PSO algorithm is 0.02 seconds. The operating times of both relays are minimized.

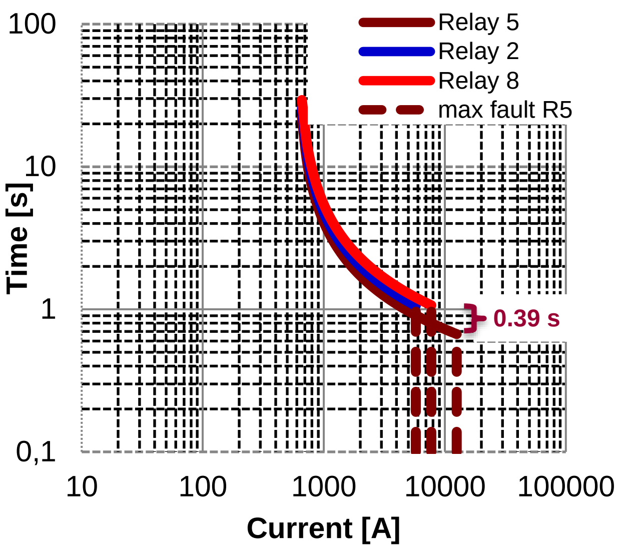

(g)

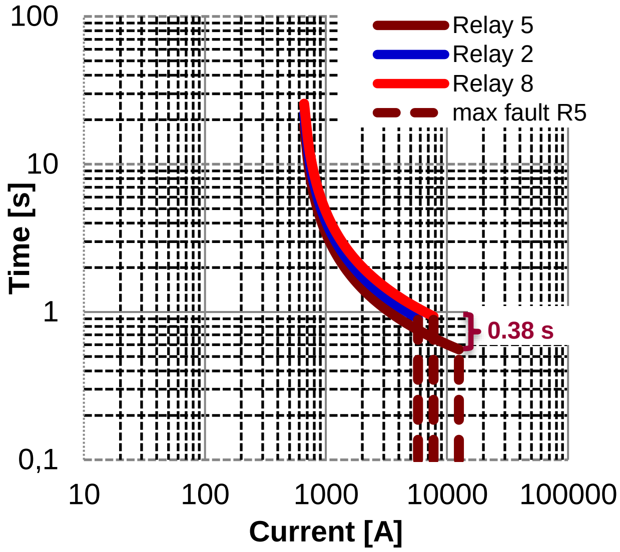

(h)

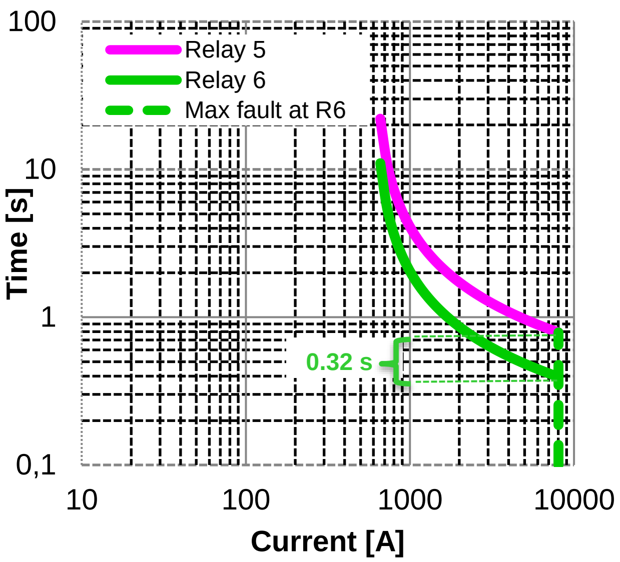

(i)

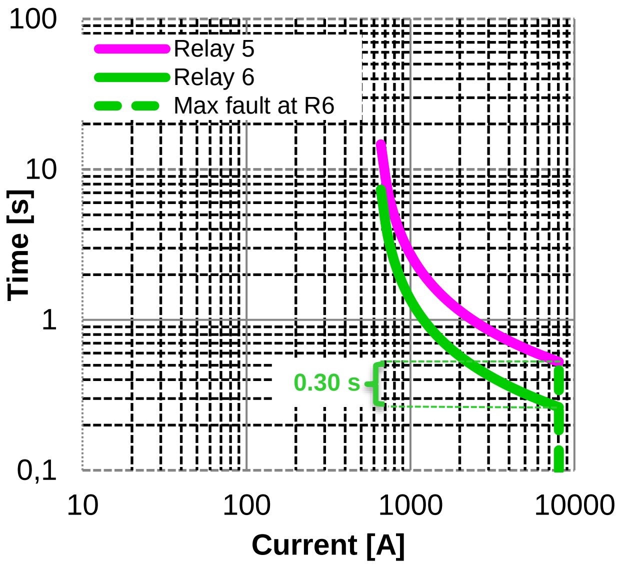

(j)

In the last two set of time-current curves, both times are minimized and improved. However, the coordination time interval increases from 0.32 seconds to 0.41 seconds and from 0.45 seconds to 0.48 seconds resepctively.

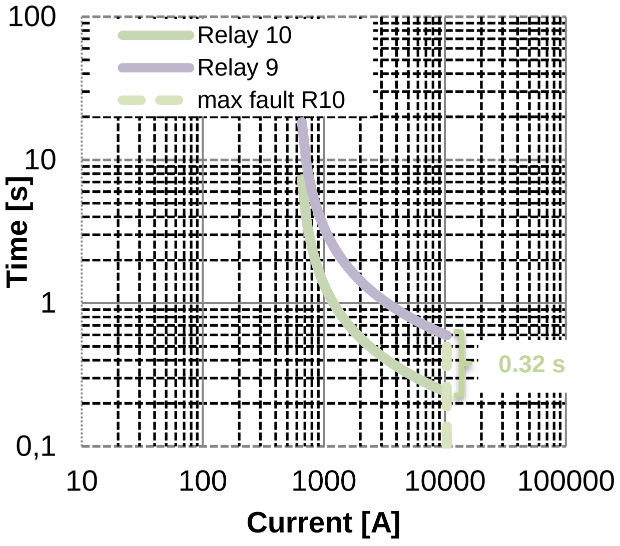

(k)

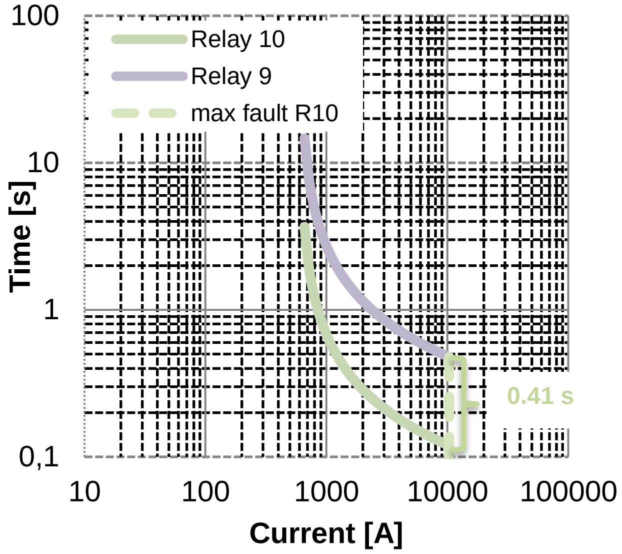

(l)

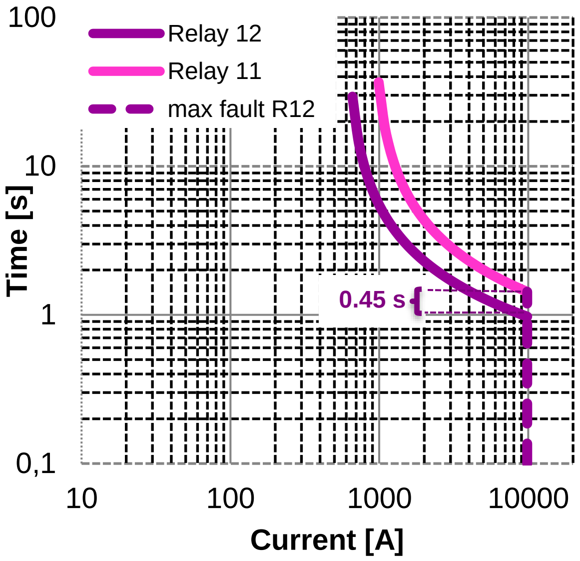

(m)

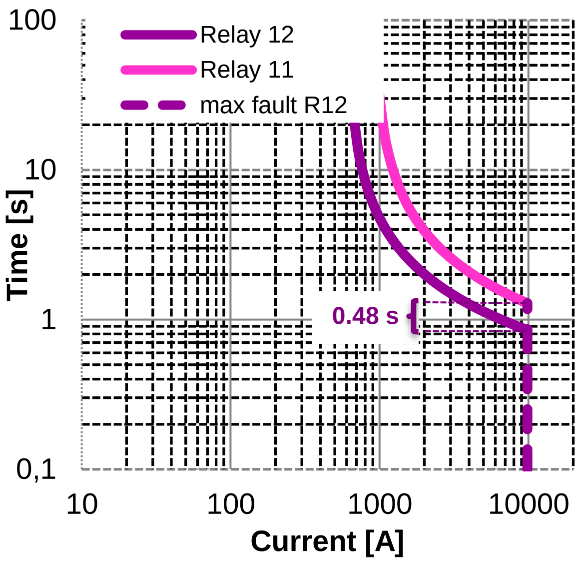

(n)

Figure 7-14: Relay pairs in the Makalu network

The time-current curves provided in the above Figure 7-14 show how the PSO algorithm has minimized the sum of the operating times for the primary relays in the Makalu network. Most of the relay pairs shown in Figure 7-14 from (a) to (n), there are only three cases where the coordination time interval exceeds 0.3 seconds. But, it is less than 0.5 seconds. The highest recorded is 0.48 seconds. The remaining pairs, improved both the operating times and the coordination time interval between the primary and back-up relays.

7.7 Concluding remarks

In Chapter 2, the basic design requirements of any protection scheme are discussed and a few are used to compare the two methods used in this research to calculate the directional overcurrent relay's settings. By optimizing the sum of the primary relay's operating times (i.e. speed of operation) and selectivity are inevitably one of the main factors.

The proposed PSO algorithm should meet the following objectives as stated in Chapter 1:

a) Minimize the operating times of the primary relays for close-in three-phase faults in the IEEE 8-bus test case in both study cases.
b) Maintain a coordination time interval of 0.3 seconds between the primary and backup relays in the IEEE 8-bus test case in both study cases.

From the coordination study conducted in the Makalu network, the primary relay's operating times have been minimized as calculated the PSO algorithm. Therefore, the operating times of the primary relays are improved. In all relay pairs in the Makalu ring, the coordination time interval of 0.3 seconds is not violated, but maintained throughout the calculation process.
The following table 7-25 summarizes the results of the PSO algorithm and the conventional method. The conclusions drawn from this study are based on all three case studies investigated in this chapter.

Table 7-25: Performance comparison between PSO and conventional method

	PSO algorithm	**Conventional method**
Speed ***(relay's operating times speed)***	Faster	Slower
Selectivity ***(coordination)***	Maintains selectivity	Maintains selectivity
Speed of search/ calculation	Faster *(Matlab® based)*	Slow *(mainly hand calculations)*
Population diversity	Mainly via local region	Based on initial guess of the initial relay's settings

8 Conclusion and recommendations

This chapter summarizes all the work discussed in this research. The second part of the chapter provides recommendations for future work on the particle swarm optimization technique and other findings.

8.1 Conclusion

The objective of this research is to calculate the optimal settings of the directional overcurrent relays in the distribution network with DGs. Two case studies are used to test the following hypothesis: *A particle swarm optimization algorithm can be used to improve on the protection settings for a distribution network with DGs as calculated by the conventional method.*

8.1.1 Performance of the proposed PSO algorithm

The PSO algorithm is proposed in this research to improve on the directional overcurrent relay's settings for a distribution network with DGs. The results compared to are calculated by the conventional method, which is mainly the method that is used in the industry. The Makalu HV ring network is used to validate the results of the PSO algorithm. The directional overcurrent settings were calculated by hand by the settings department.

From the results, the following conclusions are drawn:

- The PSO algorithm converges faster to the global minimum solution and does not require a large population. A population between 30 and 50 is sufficient to obtain the best solution.

- PSO has been tested on two case studies. The first case study is an IEEE 8-bus test case and the second is the modified IEEE 8-bus test case. PSO has shown the capability of maintaining selectivity and calculating faster operating times as compared to the conventional method although some cases coordination time interval is more than 0.3 seconds.

- In terms of speed of search, the PSO algorithm calculates settings faster since it takes less than a minute to execute 500 to 1000 iterations in Matlab®.

A summary of the calculated primary relay's operating times obtained in all three cases in presented in Table 8-1. From the table, it is clear how the PSO algorithm has minimized the operating times of the primary relays.

Therefore, the proposed PSO algorithm has more benefits than the conventional method, since it has shown to calculate fast operating times for primary relays, able to maintain selectivity in all the scenarios studied in chapter 6 and can perform the setting calculations faster than the conventional method.

Table 8-1: Summary of the calculated primary relay's operating times

	PSO algorithm	**Conventional method**
	Primary relay's operating time ($\sum_{i=1}^{n} t_{ii}$)	Primary relay's operating time ($\sum_{i=1}^{n} t_{ii}$)
Case study 1	7.35	9.22
Case study 2	9.04	7.79
Makalu ring	6.93	7.61

The conventional method, on the other hand has also shown to have the capability to maintain selectivity. The calculations can be calculated by hand or automated either in Matlab® or Excel. But, comparing the speed of calculations, PSO outperforms the conventional method.

Based on the results from Chapter 7, the following conclusions are drawn:

- The final results are based on the initial guess of the initial relay's settings. Hence, the primary relay operating times for close-in three-phase faults are longer when compared with the operating times calculated using the PSO algorithm. In both case studies, minimum operating time of 0.2 seconds was selected for relay's initial operating times.

- Analysing the results in Table 8-1, it is only in the second case study where the conventional method performed better than the PSO algorithm. This proves that the final results depend on the initial selection of the primary relay's settings and the number of trials allowed (i.e. 10, 20 or more).

The speed at which protection operates has major benefits to the power system. This includes power system faults being cleared in shorter periods and minimization of damage to the equipment.

8.1.2 Summary of impacts of DGs in the existing distribution network

The impacts of DGs in the existing distribution network are discussed in detail in Chapter 3 and Chapter 4. A summary is therefore given below in no order of priority:

- The magnitude of the fault current can flow in both forward and reverse directions as seen from the load studies. In long distribution feeders (MV) where the fault currents are inherently low, DGs are most likely to detect and operate for faults in the distribution feeders.

- During a transient fault in the power system, DGs continue operating while auto-reclosing devices attempt to clear the fault. The first reclosure cycle is at least 180 seconds and during this period, DG will continue operating thereby sustaining the power system voltage and contributing to the fault current. This prevents the arc of a transient fault from being extinguished and the device clearing the fault will have an unsuccessful auto-reclose operation. Therefore, a transient fault is converted to a permanent fault and result in long system interruption.

- When the feeder in which the DG is connected has been isolated from the power system, the probabilities of the ferro-resonance phenomenon to occur are high. The consequences of this phenomenon results in extreme overvoltages, which can damage expensive power system equipment and the possibility of the DG islanding is high.

- If the incorrect vector group of the interface transformer is selected, the protection operation is affected. The local protective devices can operate for unbalanced faults on the DG LV side. It is shown in Chapter 4 that any vector group with the delta winding connection is the preferred option due to the fact that during unbalanced power system faults, the zero-sequence current ($3I_0$) are trapped in the delta winding of the DG's interface transformer. Therefore, this prevents nuisance tripping in the power system during unbalanced faults on the DG side of the transformer.

8.1.3 Summary of DG responses to fault conditions

Different technologies of DGs operate and respond differently to power system faults. However, the fault current in the active distribution network is still dominated by the synchronous generators of large conventional power stations.

The impacts of different technologies are summarized below in Table 8-2. The details and simulation results are provided in Chapter 3. The contribution of the inverter-coupled DGs is between 0 A to full-load current. Therefore, this current is not significant, since the pick-up currents are set above full-load currents or maximum of the thermal rating of the conductor used.

Table 8-2: Summary of DG technology's response to fault conditions

DG technologies	
Inverter coupled DGs	**Non-inverter coupled DGs**
Due to the fast control of power electronics interface in wind and photovoltaic power plants, inverter-coupled DGs have the capability to control the fault current injection during power system faults.	The fault current contribution of a CSP is known and can be approximated to be at least 3 to 6 times the steady state fault current during the first cycle.
Doubly-fed (DFIG) and fully rated induction generators (FRIG) have a controlled fault current contribution due to the fast response of the control strategy implemented in power electronic inverters. During the sub-transient period, the contribution from these two induction generators can rise up to twice the steady state fault current.	The squirrel cage (SCIG) and wound rotor induction generator with variable rotor resistance (without control) contributes 3 to 6 times the steady state fault current in the first cycle. During the steady state cycle, the fault current contribution is at least twice the steady state fault current.

8.2 Recommendations

From the conclusions drawn in this research, the following recommendations are made.

- In the active distribution network, DGs with power electronics control strategies will not contribute more than the plant maximum current rating. It is important to check the sub-transient, transient and steady state current contributions of all types of DGs especially for equipment rating and for optimal protective relaying coordination where instantaneous protection is used.
- For networks where selectivity is more important than fast operation (*speed*), it is recommended that the conventional method be used as it has been shown in this research that the conventional coordination method has the capability of maintaining selectivity. However, this is more applicable to small networks.

- As PSO algorithm has proven to optimize the coordination results presented in this research, it is strongly recommended that PSO algorithm be used in the industry to optimize overcurrent relay's operating times.

8.3 Future work

PSO algorithm can be applied to calculate relay settings for protective devices and can be improved by adding a constraint which takes into account the ratio of the fault and pick-up currents since this factor has a major impact on the operating time of the relay.

9 References

[1] A. Eberhard, J. Kolker and J. Leigland, "South Africa's renewable energy IPP procurement program: success and lessons," 2014.

[2] T.S. Basso and R. DeBlasio, "IEEE standard 1457 series of standards: interconnection issues," 2004, pp. 1159 -1162.

[3] Urban Earth, South African carbon snapshot, Durban, 2012.

[4] I. Dincer, "Renewable energy and sustainabledevelopment: a crucial review," *Renewable and sustainable energy reviews,* vol. 4, no. 2, 2000, pp. 157-175.

[5] V.S.S.S. Sarma and K. Vijeta, "Protection of distributed generation connected distribution system," India, 2012.

[6] H. Yang, F. Wen and G.Ledwich, "Optimal coordination of overcurrent relays in distribution systems with distributed generation based on differential evolution algorithm," *International transactions on electrical energy systems,* vol. 23, no. 1, 2013, pp. 1-12.

[7] M.M. Mansour, S.F. Mekhamer and N.E.S El-Kharbawe, "A modified particle swarm optimizer for the coordination of directional overcurrent relays," *IEEE transactions on Power delivery,* vol. 22, no. 3, 2007, pp. 1400-1410.

[8] D. Birla, R.P. Maheshwari and H.O. Gupta, "Time-overcurrent relay coordination: a review," *International journal of emerging electric power system,* vol. 2, no. 2, 2005.

[9] M. Maleknia and H.K. Keragar, "Optimal coordination of overcurrent relay with distributed generation consideration.," *Advanced power system automation and protection (APAP),* 2011, pp. 1354-1358.

[10] M. Hussain, S. Rahim and I. Musirin, "Optimal overcurrent relay coordination: a review," *Procedia engineering,* vol. 53, 2013, pp. 332-336.

[11] S. A. Razar, T. Mahmood and S.B.A. Bukhari, "Application of optimization techniques in overcurrent relay coordination: a review," *World applied sciences journal,* vol. 28, no. 2, 2013, pp. 259-265.

[12] M. Bashir, M. Taghizadeh, J. Sadeh and H.R. Mashhadi, "A new hybrid particle swarm optimization for optimal coordination of overcurrent relay.," in *Power system technology IEEE POWERCON,* 2010, *pp.1-6*.

[13] L. Yinhong, S. Dongyaun and D. Xianzhong, "A study on optimal coordination of definite-time relay based on genetic algorithm," *In transmission and distribution conference and exposition, IEEE PES,* 2003, pp. 279 - 284.

[14] C.H. Lee and C.R. Chen, "Using genetic algorithm for overcurrent relay coordination in industrial power system," in International conference on intelligent systems applications to power systems, 2007.

[15] S.S. Rao, in *Engineering optimization: theory and practice*, John wiley and sons., 2009, pp. 1-21.

[16] S. Halpin and L. Grigsby, "The electric power engineering handbook," CRC Press LLc., 2001, pp. 264-265.

[17] P.M. Anderson, in *Power system protection* , Wiley, 1998. pp. 201-235.

[18] J.L. Blackburn and T.J. Domin, "Protective relaying: principles and applications," CRC Press, 2015, pp. 32-36.

[19] S. van Zyl and A. Lubbe, "Characterization of MV overhead feeder faults using auto-recloser event data.," in *Eskom power system protection conference*, Johannesburg, 2014.

[20] J.L. Blackburn and T.J. Donmin, in *Protective relaying: principles and applications*, CRC Press., 2015, pp. 200 - 204.

[21] J.D. Glover, M. Sarma and T. Overbye, in *Power system analysis and design*, United States of America, SI version: Cengage learning, 2011, pp. 492-527.

[22] J.M. Holmes and E.J. Gers, in *Protection of electricity distribution networks.*, vol. 47, IET, 2004, pp. 107-110.

[23] Institute of electrical engineers, Power system protection, London: Institute of electrical engineers, 1995, pp. 1 -5.

[24] Schweitzer engineering laboratories, “SEL 551 Overcurrent relay instruction manual,” Schweitzer engineering laboratories, Inc, Pullman, WA, 2010. pp. 17-23.

[25] J. Horak, "Directional overcurrent relaying (67) concepts.," in *Protective relay engineers 59th annual conference for IEEE*, 2006. pp. 13-18.

[26] Alstom Grid, "Network protection and automation guide," Alstom grid, 2011. pp. 5-126..

[27] D. Elliot, "Renewables, a review of sustainable energy supply options," IOP Publishing, 2013.

[28] Eskom, "Eskom holdings integrated report," Eskom , Johannesburg, 2011.

[29] T. Saksornchai and B. Eua-arporn, "determination of allowable capacity of distributed gneration with protection coordination consideration.," *Engineering journal,* vol. 13, no. 3, 2009, pp. 29-44.

[30] M. Bollen and F. Hassan, Integration of distributed generation in the power system, 1st ed., vol. 80, John wiley and sons., 2011, pp. 229-326.

[31] L.K. Kumpulainen and K.T. Kauhaniemi, "Analysis of the impact of distributed generation on automatic reclosing.," *Power systems conference and exposition,* pp. 603-608, 2004.

[32] Resource dynamics cooperation, "Application guide for distributed generation interconnection: March update," The NRECA guide to IEEE 1547, 2006.

[33] South African renewable grid code committee, "Grid connection fpr renewable power plants connected to the electricity transmission system or distribution system in South Africa.," Johannesburg, 2014. pp. 6-28.

[34] IEEE, "IEEE recommended practice for grounding of industrial and commercial power systems," IEEE, New York, 2007. pp. 1-20.

[35] Eskom, "Distribution standard for the interconnection of embedded generation.," Eskom, Johannesburg, 2008. pp. 14-15.

[36] S. Zhu, L. Geng, X. Wang, D. Choi and Y. Li, "Selection method for transformer interconnecting distributed generation and distribution networks.," in *Transmission and distribution conference and exposition: Asia and Pacific*, 2009. pp. 1-4.

[37] IEEE power engineering society, "Impact of distributed generation resources on distribution relay protection," IEEE, 2014.

[38] R. Arritt and R. Dugan, "Distributed generation interconnection tranformer and grounding selection.," in *Power and energy society general meeting-conversion and delivery of electrical energy in 21st century*, 2008. pp. 1-7.

[39] M.R. Patel, Wind and solar power systems: design, analysis, and operation: CRC press, 2005, pp. 138-158.

[40] T. Neumann and I. Erlich, "Short circuit current contribution of photovoltaic power plant," *Power plants and power systems control,* 2012, pp. 343-348.

[41] M.R. Patel, "Solar thermal systems," in *Wind and solar power systems: design, analysis and operation.*, CRC Press, 1999. pp. 159-168.

[42] J. Barsch, G. Bartok, G. Benmouyal, O. Bolado, B. Boysen, S. Brahma, S. Brettschneider, Z. Bukhala and J. Burnworth, "Fault current contributions from wind plants: a report to the T & D committee," in Electric machinery committee and power system relaying committee of the IEEE PES, 2012. pp. 7-49.

[43] V. Gevorgian and E. Muljadi, "Wind power plants short circuit current contribution for different fault and wind turbine topologies.," in *The 9th annual international workshop on large-scale integration of wind powet into power systems as well as transmission networks for offshore wind power plants*, 2010.

[44] E. Muljadi, N. Samaan, V. Li andS. Pasupulati., "short circuit current contribution for different wind turbines generator types.," in *Power and energy society general meeting.*, 2010. pp. 1-8.

[45] V. Gevrgian and E. Muljadi, "Wind power plant short circuit current contribution for different fault and wind turbine topologies.," In *9th International Workshop on Large Scale of Wind Power into Power Systems*, 2010.

[46] ABB Group, "Technical application papers No 13 wind power plants," ABB, Italy, 2011.

[47] M.H. Bollen and F. Hassan, "Integration of distibuted gneration in the power system," vol. 80, John wiley and sons., 2011, pp. 300-303.

[48] S. S. Rao, "Engineering optimization theory and practice," New Jersey, John wiley and sons., 2009, pp. 693-709.

[49] S. Boyd and L. Vandenberghe, in *Convex optimization*, Cambridge unviversity press., 2004, pp. 1-8.

[50] D.P. Rini, S.M. Shamsuddin and S.S. Yahunoz, "Particle swarm optimization: technique, system and challenges," *International journal of computer applications,* vol. 14, no. 1, 2011, pp. 19-26.

[51] Y. Fukuyama, "Modern heuristic optimization techniques, theory and application to power system.," in *Fundamentals of particle swarm optimization.*, New Jersey, John wileyand sons., 2008, pp. 71-77.

[52] R.L. Haupt and S.E. Haupt, in *Practical genetic algorithms*, John wiley and sons., 2004, pp. 28-47.

[53] M. Mitchell, An introcution to genetic algorithms, MIT Press, 1996, pp. 1-27.

[54] S. H. Horowitz and A.G. Phakde, in *Power system relaying*, John wiley and sons., 2008, p. 93.

[55] C.A. Ceollo, "Theoretical nad numerical constraint-handling techniques used with evolutionary algorithms: a surveyof the state of the art.," *Computer methods in applied mechanics and engineering,* vol. 191, no. 11, 2002, pp. 1245-1287.

[56] D. Uthitssunthorn, P. Pao-La-Or and T. Kulwarawnichpong, "Optimal coordination using artifical bees colony algorithm," in *The 8th electrical engineering, electronics, telecommunications and information technology conference*, Thailand, 2011, pp. 901-904.

[57] IEEE standard 142, “Recommended practice for grounding of industrial and commercial power systems,” IEEE, 2007. pp. 1-20.

[58] P. Venkataraman, Applied optimization with Matlab programming, New York City: John wiley and sons., 2002. pp. 357-366.

[59] A. Sieminski, "International energy outlook.," Energy information administration (EIA), 2014.

[60] T. Ackermann, Wind power in power systems, vol. 140, Chichester: UK: John Wiley and sons, 2005. pp. 13-23.

[61] E.J. Coster, "Distribution grid operation including distributed generation," Eindhoven University of Technology, The Netherlands, 2010.

[62] J. Keller and B.D. Kroposki, "Understanding fault characteristics of inverter-based distributed energy resources," National renewable energy laboratories, 2010.

[63] N. Nimpitiwanm G.T. Heydt, R. Ayyanar and S. Surynarayanan, "Fault current contribution from synchronous machine and inverter-based distributed generators," *The IEEE transactions on power delivery,* vol. 22, no. 1, 2007, pp. 634-641.

[64] T. Ackermann, G. Andersson and L. Soder, "Electricity market regulations and their impact on distributed generation.," in *In Electric utility deregulation and restructuring and power technologies*, 2000. pp. 608-613.

[65] M. Ezzeddine, R. Kaczmarek nad M.U. Iftikhar, "Coordination of directional overcurrent relays using novel method to select their settings.," *IET generation, transmission nad distribution.,* vol. 5, no. 7, pp. 743-750.

[66] K. Corfee, D. Korinek, W. Cassel, C. Hewicker, J. Zillmer,M.P. Morgado, H. Zeigler, N. Tong, D. Hawekins and J. Cernadas, "Distributed generation in Europe- Phyiscal infrastructure and distributed generation connection.," Berlin, 2011. pp. 5-23.

[67] South African renewable grid code committee, "Grid connection fpr renewable power plants connected to the electricity transmission system or distribution system in South Africa.," Johannesburg, 2014. pp. 6-8.

[68] A. Dexters, T. Loix, J. Driesen and R. Belmans., "A comparison of grounding techniques for distributed generators implemented in four-wire distribution grids, UPS systems and microgrids," *In preceedings of CIRED,* 2007, p. 4.

Appendix A

Data presented below in Table A-1 is for the induction machines used in chapter 3. The base quantities used for calculations are calculated as follows:

$$Z_B = \frac{(KV_B)^2}{VA_B} \tag{A-1}$$

$$Z_B = 0.216\ \Omega$$

and,

$$I_B = \frac{VA_B}{\sqrt{3}\times V_B} \tag{A-2}$$

$$I_B = 1840.83\ A$$

The base quantities are presented in Table A-1 below and machine data in given in the next Table A-2 below.

Table A-1: Base quantities for Type I induction machine

Base quantity	Value	Unit
Power rating (VA_B)	2.2	MVA
Voltage (V_{B1})	0.69	kV
Impedance (Z_{B1})	0.216	Ω
Current (I_{B2})	1840.83	A

Table A-2: Induction machine data

Parameter Name	Type I	Type II	Type III
Power rating (Srated)	2.2 MVA	0.69 MVA	2 MVA
Voltage (Vrated)	0.69 kV	0.69 kV	0.69 kV
Number of pole pairs (N)	2	2	2
Magnetizing reactance (X_m)	3.5 pu	3.5 pu	3.5 pu
Stator leakage reactance (X_s)	0.1 pu	0.1 pu	0.1 pu
Rotor leakage reactance (X_r)	0.1 pu	0.1 pu	0.1 pu
Stator resistance (R_s)	0.01 pu	0.01 pu	0.01 pu
Rotor resistance (R_r)	0.01 pu	0.01 pu	0.01 pu
Inertia (J)	75 kg m^2	75.38 kg m^2	175 kg m^2

Table A-3: Data of a Bosch a-Si 80 PV system

Name	Value	Symbol
Rated power	80	W
Rated voltage	95	V
Rated current	0.9	A
Mateial	Amorphous Silicon	a-Si
Open circuit voltage	137	V
Short circuit current	1.11	A

Above data is used to simulate the EMT studies of the distributed generation. The results presented in Chapter 3 shows the sub-transient fault currents obtained when an EMT study is simulated for at least 400 milli-seconds in PowerFactory.

Appendix B

The following transformer impedances are the standard impedances of the transformers at different MVA ratings.

Nominal Voltage			Impedance Type	Standard MVA Rating								HV/MV Impedance (%) referred to primary power rating		HV/Ter Impedance (%) Referred to tertiary power rating		Vector Group
Primary	Secondary	Tertiary		160	80	40	20	10	5	2.5	1.25	Nom @ tap 5	Min @ tap 17	Nom @ tap 5	Min @ tap 17	
88	11		STD			X	X					11	10			YNd1
88	11		STD					X	X			10	9			YNd1
88	6,6		STD				X					11	10			YNd1
88	6,6		STD					X	X			10	9			YNd1
66	22		STD			X	X					11	10			YNd1
66	22		STD					X	X			10	9			YNd1
66	11		STD				X					11	10			YNd1
66	11		STD					X	X	X		10	9			YNd1
66	6,6		STD				X					11	10			YNd1
66	6,6		STD					X	X			10	9			YNd1
44	22		STD				X					11	10			YNd1
44	22		STD					X	X			10	9			YNd1
44	11		STD				X					11	10			YNd1
44	11		STD					X	X	X		10	9			YNd1
44	6,6		STD					X	X	X		10	9			YNd1

Figure B-1: Standard transformer's impedances

Appendix C

The following data presented below in Table C-1 and C-2 is the load flow study results of the IEEE 8-bus and the modified IEEE 8-bus test case.

Table C-1: 8-bus test case load flow results

Relay ID	**Load Currents (A)**	**Pick-up currents (A)**	**CTR**	**Secondary currents (A)**	**P (MW)**	**Q (MVAr)**	**S (MVA)**
R 1	456	547	600/1	0.912	77.6	54.4	94.8
R 2	102	122	200/1	0.612	17.4	11.2	20.7
R 3	297	356	400/1	0.891	-52.7	-28.9	60.1
R 4	715	858	1000/1	0.858	-122.8	-80.1	146.6
R 5	365	438	600/1	0.73	63.6	43.4	77.0
R 6	304	365	400/1	0.912	54.3	34.3	64.2
R 7	93	112	200/1	0.558	14.2	13.1	19.3
R 8	456	547	600/1	0.912	-77.4	-51.2	92.8
R 9	102	122	200/1	0.612	-17.3	-11.1	20.6
R 10	297	356	400/1	0.891	52.8	30.1	60.8
R 11	715	858	1000/1	0.858	123	87	150.7
R 12	304	365	400/1	0.912	-54.2	-33.1	63.5
R 13	93	112	200/1	0.558	-14.2	-12.9	19.2
R 14	365	438	600/1	0.73	-63.4	-41.4	75.7

Observing the load currents in the second and third column, the load current has increased causing the selected CTR in Table C-1 to be changed in order to ensure that the secondary currents are less than 1 A.

Table C-2: Load flow results of a modified 8-bus test case

Relay ID	Load currents (A)	Pick-up currents (A)	CTR	Secondary current (A)	P (MW)	Q (MVAr)	S(MVA)
R 1	663	796	600/1	1.326	114.1	81.4	140.2
R 2	312	374	200/1	1.872	53.6	34.8	63.9
R 3	88	106	400/1	0.264	-16.6	-6.5	17.8
R 4	510	612	1000/1	0.612	-86.6	-56.6	103.5
R 5	405	486	600/1	0.81	-71.1	-45.1	84.2
R 6	103	124	400/1	0.309	-16	14.1	21.3
R 7	315	378	200/1	1.89	-56	-34.2	65.6
R 8	663	796	600/1	1.326	-113.6	-74.8	136.0
R 9	312	374	200/1	1.872	-53.4	-33.5	63.0
R 10	88	106	400/1	0.264	16.6	6.6	17.9
R 11	510	612	1000/1	0.612	86.9	60.1	105.7
R 12	103	124	400/1	0.309	16	14.2	21.4
R 13	315	378	200/1	1.89	56.1	35.7	66.5
R 14	405	486	600/1	0.81	71.2	47.6	85.6